

Historical Analysis of the Relationship of Streamflow Flashiness with Population Density, Imperviousness, and Percent Urban Land Cover in the Mid-Atlantic Region

INTERNAL REPORT
APM 408

Historical Analysis of the Relationship of Streamflow Flashiness with Population Density, Imperviousness, and Percent Urban Land Cover in the Mid-Atlantic Region

Internal Report
APM 408

by

S. Taylor Jarnagin
U.S. Environmental Protection Agency
Office of Research and Development
National Exposure Research Laboratory
Environmental Sciences Division
Landscape Ecology Branch
Environmental Photographic Interpretation Center (EPIC)
Reston, VA 20192-0002

Notice: The U.S. Environmental Protection Agency (EPA), through its Office of Research and Development (ORD), partially funded, performed, and collaborated in the research described here. It is intended for internal EPA use. Mention of trade names or commercial products does not constitute endorsement or recommendation for use.

U.S. Environmental Protection Agency
Office of Research and Development
Washington, DC 20460

235leb07

Paper Title: Historical analysis of the relationship of streamflow flashiness with population density, imperviousness, and percent urban land cover in the Mid-Atlantic region.

Author: S. Taylor Jarnagin, US EPA EPIC, Reston VA

Table of Contents:	i
Figures and Tables:	iii
Executive Summary:	1
<i>Research Topic:</i>	1
<i>Abstract:</i>	1
<i>Results:</i>	2
<i>Implications of this Research:</i>	3
<i>Audience and Potential Users of this Research and Directions for Future Research:</i>	4
Acknowledgements:	4
Introduction:	5
<i>Background Research</i>	5
<i>Our Background Research</i>	5
<i>Measures of Imperviousness and/or Degree of Development</i>	14
<i>Measure of Hydrologic Alteration: Stream Flashiness</i>	15
Data and Methodology for the current study:	19
<i>Population Density Data</i>	19
<i>Streamflow Data</i>	20
<i>Land Use/Land Cover Data</i>	21
<i>Imperviousness Data</i>	23
<i>Software and Hardware</i>	24

Results:	24
<i>Streamflow Data</i>	24
<i>Streamflow Flashiness and Population Density</i>	26
<i>Streamflow Flashiness and Degree of Urban Development</i>	32
<i>Streamflow Flashiness and Imperviousness</i>	37
Discussion:	46
References:	53
Appendices: Historical analysis of the relationship of streamflow flashiness with population density, imperviousness, and percent urban land cover in the Mid-Atlantic region.	
Appendix 1: County-Level Decadal Population Density for EPA Region 3.	I
Appendix 2 - Station Table	XI
Appendix 3: NLCD1992 and NLCD2001 Land Cover Class Definitions	XX
Appendix 4 - Flashiness Results table	XXVIII

Figures and Tables: Historical analysis of the relationship of streamflow flashiness with population density, imperviousness, and percent urban land cover in the Mid-Atlantic region.

	Page
Figure 1: Location of the upper Accotink Creek subwatershed.	7
Table 1: Aerial Photographic Data.	7
Figure 2: Median streamflow for VDEQ/USGS stream gage 01654000 for October 1947 through September 1998.	8
Figure 3: Frequency of high-flow events for VDEQ/USGS stream gage 01654000 for October 1947 through September 1998.	9
Figure 4: Frequency of low-flow events for VDEQ/USGS stream gage 01654000 for October 1947 through September 1998.	10
Figure 5: Streamflow per unit precipitation for VDEQ/USGS stream gage 01654000 and mean daily precipitation for days where total precipitation was equal to or greater than 6 mm for October 1947 through September 1998.	11
Figure 6: Median streamflow per unit precipitation ≥ 6 mm for VDEQ/USGS stream gage 01654000 for October 1947 through September 1998.	12
Figure 7: 1947–1998 Streamflow vs. Precipitation by Decade for days of measurable precipitation.	13
Figure 8: Percent Imperviousness (TIA%) from ground truth vs. Percent Urban (%Urban) per watershed from the NLCD1992 land cover dataset.	14
Equation 1: The R-B Index (Baker <i>et al.</i> , 2004).	15
Figure 9: Annual Richards-Baker Flashiness Index (R-B Index) values plotted for the Upper Accotink stream gage 01654000 for 1948 through 2000.	16
Figure 10: Plot of both the TIA% and Flashiness for the Upper Accotink stream gage 01654000 for 1948 through 2000.	17
Figure 11: Plot of both the TIA% and Flashiness for the Upper Accotink stream gage 01654000 for 1948 through 2000 with 5-year moving average of annual flashiness.	18
Figure 12: Mean flashiness per TIA% estimate date in the Upper Accotink.	19
Table 2: The seven NALC70s land cover classes from Edmonds <i>et al.</i> (2002).	22

Table 3: Urban Gradient used for imperviousness accuracy assessment in Jones <i>et al.</i> (2003) and Jarnagin <i>et al.</i> (2006).	22
Table 4: 1970s NALC - NLCD1992 - NLCD2001 crosswalks of land cover classes used for ATtILA PCT_LC computation.	23
Table 5: Flashiness Summary Table showing the overall increase or decrease over time of the monotonic trend revealed by the linear (parametric) or Mann-Kendall Tau (nonparametric) tests.	24
Table 6: Streamflow Station Flashiness Significance Categories.	25
Figure 13: Streamflow flashiness results.	25
Figure 14: Population density change (\pm people \cdot -mi ²) from 1930 to 2000 mapped at the watershed spatial scale.	26
Table 7: Mean population density change per category for stations showing significant vs. no significant change in monotonic flashiness trend over the station period of record.	27
Figure 15: Mean watershed flashiness per census population density level.	28
Figure 16: Mean watershed flashiness per 1990 census at the tract population density level.	29
Figure 17: Mean watershed flashiness per 2000 census at the block-group population density level.	30
Figure 18: Mean watershed flashiness per 1998 LandScan population density level.	31
Table 8: Watershed Mean Stream Flashiness by County-Level Population Density Group.	31
Figure 19: Watershed Mean Stream Flashiness by County-Level Population Density Group.	32
Figure 20: Mean Stream Flashiness as a function of Watershed Urban Development Percent.	33
Figure 21: Mean Stream Flashiness as a function of Watershed Urban Development Percent.	34
Figure 22: Mean Stream Flashiness as a function of Watershed Slope.	35
Figure 23: Mean Stream Flashiness as a function of Watershed Elevation.	36

Table 9: Mean Stream Flashiness of stations grouped by Urban Development Gradient class based on the percentage of 'Urban' NALC/NLCD pixels in the area to be analyzed (Table 3).	36
Figure 24: Mean Stream Flashiness of stations grouped by Urban Development Gradient based on the percentage of 'Urban' NALC/NLCD pixels in the area to be analyzed (Table 3).	37
Figure 25: Comparison of 1992 'Percent Imperviousness' (TIA%) estimators.	38
Figure 26: A comparison of the NLCD2001 Imperviousness data layer and the ATtILA ArcView extension 2001 estimator of watershed TIA% based on the NLCD2001 land cover data.	39
Figure 27: A comparison of the NLCD2001 Imperviousness data layer and the ATtILA ArcView extension 1992 estimator of watershed TIA% based on the NLCD1992 land cover data.	40
Figure 28: A comparison of the ATtILA ArcView extension 2001 estimator of watershed TIA% based on the NLCD2001 land cover data and the ATtILA ArcView extension 1992 estimator of watershed TIA% based on the NLCD1992 land cover data.	41
Figure 29: Mean Stream Flashiness as a function of Watershed 'Percent Imperviousness' (TIA%).	42
Figure 30: Mean Stream Flashiness as a function of Watershed 'Percent Imperviousness' (TIA%) for those watersheds with TIA% less than 10% (n = 149).	43
Table 10: Mean Stream Flashiness by Percent Impervious Group (n = 3).	43
Figure 31: Mean Stream Flashiness by Percent Impervious Group (n = 3).	44
Table 11: Mean Stream Flashiness by Percent Impervious Group (n = 9).	45
Figure 32: Mean Stream Flashiness by Percent Impervious Group (n = 9).	45
Table 12: Streamflow stations that exhibit less mean flashiness than would be expected given their level of urban development and the dates of the development/flashiness pairs.	46
Figure 33: Mean Stream Flashiness as a function of Watershed Urban Development Percent (% Urban) showing the 'positive outliers' listed in Table 12.	47

Figure 34: The 'Percent Urban' (% Urban) parameter compared between the NALC1973 and NLCD1992 land cover datasets for the 150 watersheds that had both those parameters computed.	48
Figure 35: The 'Percent Urban' (% Urban) parameter compared between the NLCD1992 and NLCD2001 land cover datasets for the 143 watersheds that had both those parameters computed.	49
Figure 36: The 'Percent Urban' (% Urban) parameter compared between the NALC1973 and NLCD2001 land cover datasets for the 143 watersheds that had both those parameters computed.	50
Figure 37: Watershed percent imperviousness (TIA%) from Jennings and Jarnagin (2002) for the Upper Accotink are plotted in red along with the Coefficient-based estimation derived from the NLCD1992 (Jennings <i>et al.</i> , 2004).	51
Figure 38: A plot of the number of USGS National Water Information System (NWIS) historical daily mean streamflow stations per year meeting my 'long-term' requirements for this study.	52

Paper Title:

Historical analysis of the relationship of streamflow flashiness with population density, imperviousness, and percent urban land cover in the Mid-Atlantic region.

Author:

S. Taylor Jarnagin
EPA Landscape Ecology Branch
Environmental Photographic Interpretation Center (EPIC)
2D115 USGS National Center, MS-555
12201 Sunrise Valley Drive
Reston VA 20192-0002
E-mail: jarnagin.taylor@epa.gov

Executive Summary:*Research Topic:*

This research is an examination of the relationship between stream flashiness and watershed-scale estimates of percent imperviousness, degree of urban development, and population density. The relationship between anthropogenic land uses and hydrologic change has previously been demonstrated by Schueler (1994), Arnold and Gibbons (1996), Jennings and Jarnagin (2002), and many others at the watershed scale, using locality-based datasets. My research goal is to determine if regional-scale, publicly-available datasets can be used in an historic landscape analysis to detect hydrologic change due to population density/urban development/imperviousness change as the spatial scale of the individual watershed scale.

Abstract:

I used historical US Census population data (from decades 1930-2000) and satellite imagery from circa 1973, 1992, and 2001 to estimate population density, the degree of urban development, and the percent imperviousness (for 1992 and 2001) for a set of 150 small (< 130 km²) watersheds with long-term (> 20 years) USGS National Water Information System (NWIS) historical daily mean streamflow datasets in EPA Region 3 (R3, Mid-Atlantic USA). Watershed boundaries for the study watersheds were generated from USGS gage locations using smoothed USGS National Elevation Dataset 30-meter resolution digital elevation model data. 'Population Density', 'Percent Imperviousness', and 'Percent Urban' Land Use/Land Cover (LULC) parameters were estimated for each watershed. I used decadal Census population data from 1930-2000, proportionally allocated into 2000-era county boundaries, to estimate 'Population Density' for each decade from 1930 through 2000 as well as at the dates of satellite imagery acquisition (1973, 1992, and 2001). For decades after 1960, higher spatial resolution census data were used along with the LandScan 1998 dasymetric estimation of population density at a 450 m grid cell spatial resolution. Temporal land use/land cover (LULC) data: 1973 North American Landscape Characterization (NALC) data, 1992 National Land Cover Data (NLCD1992), and

NLCD2001 were used to estimate a 'Percent Urban' LULC parameter for each watershed at the dates of satellite imagery acquisition (1973, 1992, and 2001). The NLCD2001 Imperviousness data layer and the ArcView ATtILA extension (Wade and Ebert, 2004) was used for a 2001 estimator of watershed 'Percent Imperviousness' and both the coefficient technique of Jennings *et al.* (2004) and ATtILA were used to estimate 1992 watershed 'Percent Imperviousness'.

I used the Richards-Baker Flashiness Index (R-B Index, Baker *et al.*, 2004), applied to historical NWIS streamflow, to calculate annual flashiness values for the long-term USGS stream gage stations for the period of record for each station. A seven-year-window mean stream flashiness value was calculated for each population/LULC estimation date.

Results:

Historical changes in mean stream flashiness were correlated with county-scale based changes in watershed population density estimates. Streamflow stations that showed significant changes in historical flashiness had a higher mean population density than those that showed no change. The strength of the population-flashiness correlation increased (more of the observed variability in flashiness was explained by population density) as the spatial scale of the population estimator was reduced, with dasymetric LandScan data giving the best relationship. LULC and imperviousness estimators were equally effective at exploring the relationship between stream flashiness and watershed development. Urban development classes 'None' and 'Rural' were statistically the same while increasing levels of development were associated with statistically significant increases in stream flashiness. Watersheds with less than 20% 'urban' development displayed background levels of stream flashiness and mean flashiness increase with urban development density thereafter (Figure E-1).

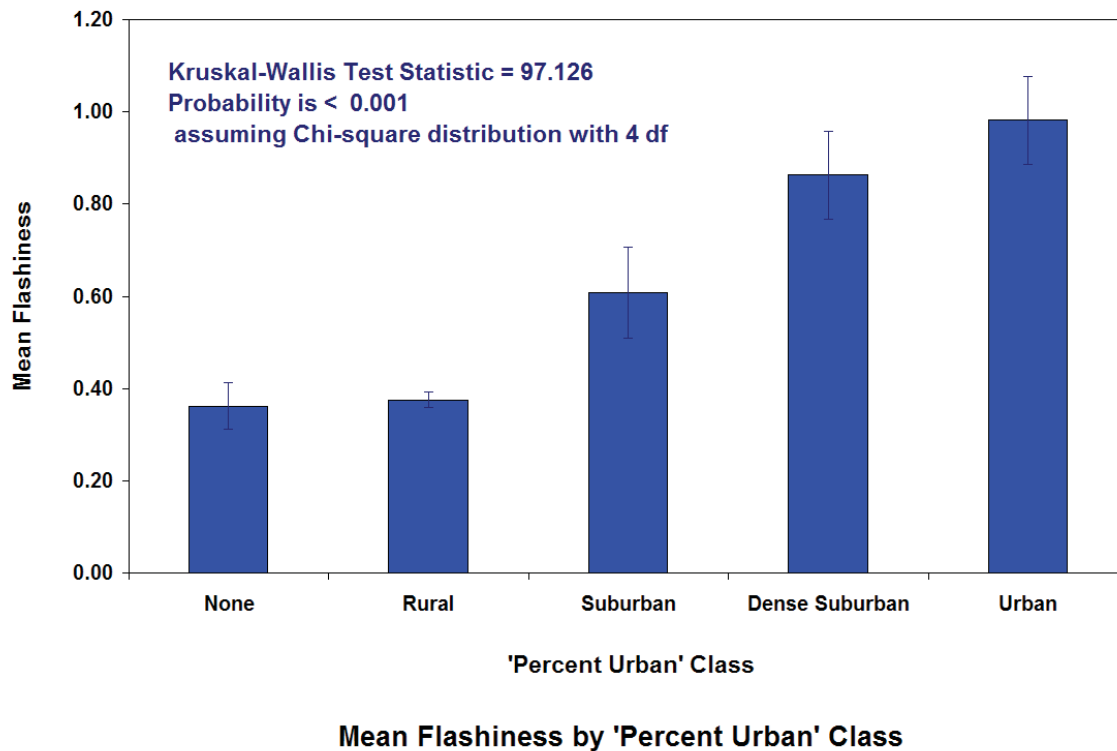


Figure E-1: The relationship between 'Percent Urban Development' and mean stream flashiness per watershed based on a seven-year window centered on the date of imagery acquisition. N = 317.

Implications of this Research:

My results support previous research that suggests low intensity development does not substantially alter streamflow. My empirical data provide support for a historic development pattern 'hard limit' of approximately 10% imperviousness and/or 20% 'percent urban' development without significant changes in stream hydrology as measured by the R-B Flashiness Index. The historical data suggest that increasing degrees of development intensity beyond this point do significantly alter streamflow.

Audience and Potential Users of this Research and Directions for Future Research:

The Federal-level people and groups that will find these results to be the most useful and interesting are: EPA ORD ReVA, EPA/USGS Chesapeake Bay Program, and EPA Program Offices such as the Office of Water and the Smart Growth Initiative. These units are actively engaged with using regional-scale analyses of the impact of urban development on freshwater resources. Local stakeholders such as County Departments of Planning and Environmental Protection and non-governmental groups such as The Center for Watershed Protection will also find this empirical study of historical relationships both interesting and informative. While this

research cannot predict the success of 'Phase 2' Best Management Practices (BMPs) on mitigating the effect of future development on streams, knowing what past practices have wrought can inform future decisions. One use of this dataset is to search for 'positive outliers' - where predicted stream flashiness is less than anticipated by the level of urban development. Detailed examination of these watersheds may yield examples where BMPs or patterns of development have been successful at mitigating the impact of urban development on stream hydrology.

Acknowledgements:

I wish to thank Tim Wade (EPA LEB-RTP) for his assistance in delineating watershed boundaries from DEM data and Don Ebert (EPA LEB-LV) for his advice and assistance in running the ATtILA tool. Terry Slonecker (EPA LEB-EPIC) and John Jones (USGS EGSC) reviewed this paper and provided valuable advice and recommendations both during the review and the research. Rachel Laughrige (EPA LEB-EPIC) kept my travel, leave, and every other administrative aspect of my life in order. Dave Jennings (now NOAA, formerly EPA LEB-EPIC) was my research partner and 'Mr. GIS' (I was 'Mr. Spreadsheet') during the initial phase of this research and this project could not have happened without his input and effort over many years. In addition to Terry, Dave, and Rachel, I also would like to acknowledge Don Garofalo, Joan Bozik, Pete Stokely, Mary Benger, and Dave Williams; all former members of the EPA LEB-EPIC staff in Reston during the period this research occurred. We made a great team, greater than the sum of our parts, and you will all be missed.

Taylor Jarnagin
September 2007
EPA EPIC
Reston VA

Introduction:

Background Research

In recent decades, the environmental protection of water quality has begun to shift in focus on point sources of water pollution, such as industrial waste and municipal sewage discharges, towards a watershed management approach based primarily on non-point-source (NPS) pollution (USEPA, 1994). NPS pollution is related to anthropogenic changes in land use and land cover (LULC) such as agriculture, forestry, and urban development and the associated increase in impervious surfaces on the landscape. The amount of impervious surface in a watershed is a landscape indicator integrating a number of concurrent interactions that influence a watershed's hydrology (Schueler, 1994). The direct hydrologic effect of impervious surfaces occurs as a change in the magnitude and variability of velocity and volume of surface flow. When the landscape is covered with impervious surfaces, precipitation that would normally infiltrate to ground water instead flows over impervious surfaces to receiving waters via storm sewers directly into the receiving stream. This alteration of the natural hydrologic process reduces runoff lag time (the amount of time it takes precipitation to reach the stream), increases the peak rate of streamflow discharge, increases stream flashiness (the difference between day-to-day streamflow, increases both the number of bankfull/sub-bankfull events (high-water streamflow) and low-water streamflow, and brings about subsequent increases in the scouring and incision of the stream channel (Leopold, 1973; Booth, 1990). The channeled and increased runoff from anthropogenic impervious surfaces influences the morphological structure of the stream and thereby alters the in-stream and riparian ecology.

As human population and associated anthropogenic activities have increased over time, land use and land cover change (LULCC) has become a major factor in changes in ecological processes at local to global scales (see Jarnagin, 2004, for a review). While global climate change has the potential to become the dominant driver affecting regional- to global-scale ecosystem change in the future, for the historical record, LULCC has been the dominant driver, particularly at local spatial scales (Sala *et al.*, 2000; Wilson, 2002).

Our Background Research

The US Environmental Protection Agency (EPA) Landscape Ecology Branch (LEB) has been conducting research on the effect of LULCC on ecosystem parameters and functions for more than a decade (see the URLs: < <http://www.epa.gov/esd/land-sci/projects.htm> > and < <http://www.epa.gov/nerlesd1/land-sci/epic/research.htm> > for a partial list of recent projects). One of those projects, "The Detection and Mapping of Impervious Surfaces: a Multi-date, Multi-scale, Multi-sensor Approach in a Mid-Atlantic Sub-Watershed" (URL: < <http://www.epa.gov/nerlesd1/land-sci/epic/rsmidatlantic.htm> >), began as an investigation of the historical relationship between the response of streamflow to precipitation in a watershed that had undergone extensive urban development.

Our basic research during this project has focused on the development of impervious surface estimators from land use/land cover (LULC) data (Jennings *et al.*, 2004) and the accuracy assessment of preexisting impervious surface estimators (Jones *et al.*, 2003; Jarnagin *et al.*, 2004; Jarnagin *et al.*, 2006). Our applied research has focused on the application of estimates of Total Impervious Area Percentage (TIA%) to historical records of streamflow and precipitation (Jennings and Jarnagin, 2002) in an attempt to derive empirical relationships between human development and its impact upon lotic (flowing water) aquatic ecosystems.

We have been focused on the environmental parameter of impervious surfaces and the landscape metric of TIA% of catchments for several reasons. First, and perhaps most importantly for a user of remote sensing, impervious surfaces can be readily identified and quantified using data and methods as diverse as manually-compiled enumeration from historical aerial photography and computer-derived, sub-pixel estimators based upon satellite imagery. Second, impervious surfaces not only directly alter the hydrology of the area they cover (through reduced infiltration to groundwater) and increase runoff to neighboring aquatic systems (via increased overland flow) but also act as surrogate measures for the hidden anthropogenic infrastructure - curbs, storm sewers, etc. - that defines the artificial 'sewershed' of an aquatic system. Third, the amount of impervious surface in a watershed is a landscape indicator integrating a number of concurrent interactions that influence a watershed's hydrology, ecosystem habitat, and changes in water quality, quantity, and biota (Schueler, 1994; CWP, 2003; for a review, again see Jarnagin, 2004).

In our studies, these impervious features specifically include roads, rooftops, parking lots, driveways, sidewalks, and other visually identifiable anthropogenic sources of imperviousness and exclude any calculation of naturally occurring imperviousness (such as rock outcroppings). The reason for this single-minded focus upon human activities is that in historical studies, naturally occurring imperviousness is assumed to remain constant and the changes observed in hydrology, if any, are assumed to be the result of observed changes in anthropogenic activity or other external drivers (such as changes in precipitation). We make no attempt to quantify or separate the effects of 'connected' vs. 'unconnected' imperviousness but rather attempt to accurately compile and estimate the TIA% for a given study area.

Our initial study site was the upper Accotink Creek subwatershed in Fairfax County, Virginia, USA (Figure 1, Jennings and Jarnagin, 2002). Anthropogenic impervious surface area was mapped from six dates of rectified historical aerial photography ranging from 1949 to 1994 (Table 1). Over that period, anthropogenic impervious surface area increased from approximately 3% in 1949 to 33% in 1994.

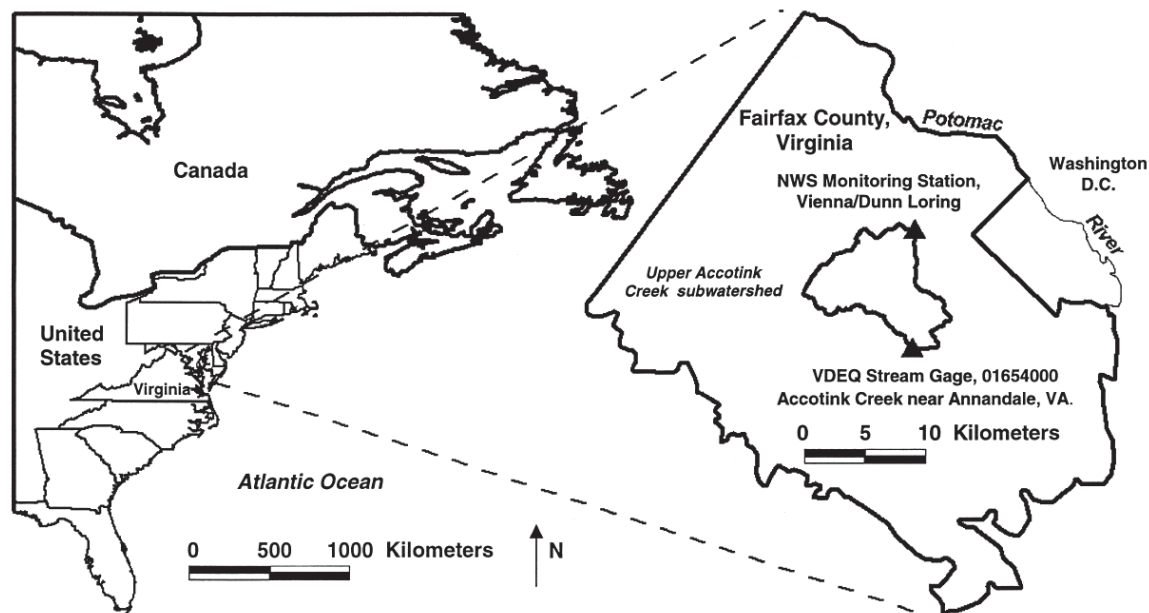


Figure 1: Location of the upper Accotink Creek subwatershed.

Date	Photo Scale	Film Type	Source
3/94 ##	1:40,000	Color Infra-Red	USGS
4/88 ##	1:40,000	Color Infra-Red	USGS
10/79	1:40,000	Black + White	ASCS
4/71	1:24,000	Black + White	VDOT
4/63	1:24,000	Black + White	USGS
4/49	1:24,000	Black + White	USGS

Table 1: Aerial Photographic Data.

USGS = United States Geological Survey, ASCS = Agricultural Soil Conservation Service, VDOT = Virginia Department of Transportation. ## = Also acquired in USGS DOQQ format.

We acquired the mean daily streamflow from the United States Geological Survey (USGS) National Water Information System (NWIS) Web Interface (USGS, 2006) for the period of record for the stream gage that formed the 'pour-point' for our study watershed. The streamflow analysis for the Virginia Department of Environmental Quality (VDEQ)/USGS stream gage 01654000 showed that, for the 51-year period studied (October 1947 through September 1998), median streamflow decreased (Figure 2) while the frequency of both high-flow (Figure 3) and low-flow (Figure 4) events increased. 'High-flow' was considered to be daily streamflow discharge at a volume of above the historical daily mean plus two standard deviations. 'Low-flow' was considered to be flow less than one-half the historical daily mean.

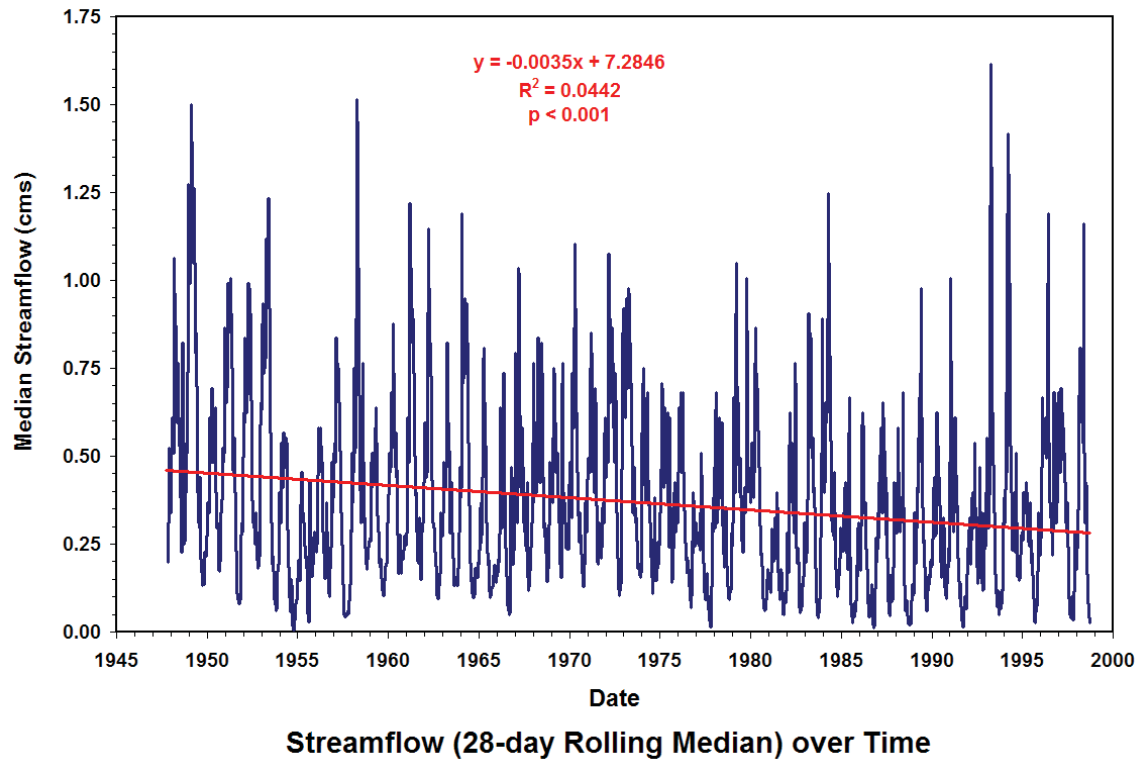


Figure 2: Median streamflow for VDEQ/USGS stream gage 01654000 for October 1947 through September 1998. Median streamflow was calculated as a rolling 28-day median. P-value is on the t-test of the linear regression line slope = 0 (no change).

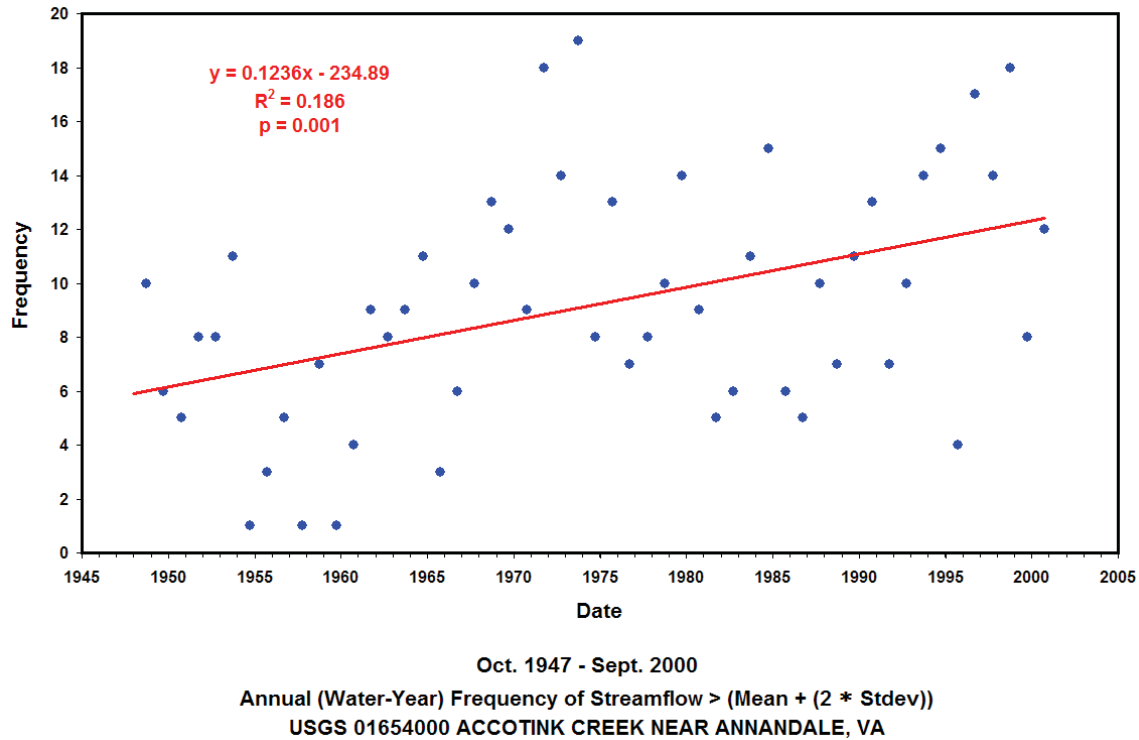


Figure 3: Frequency of high-flow events for VDEQ/USGS stream gage 01654000 for October 1947 through September 1998. 'High-flow' is here defined as the flow equal to or greater than the mean streamflow for the period plus two standard deviations. P-value is on the t-test of the linear regression line slope = 0 (no change).

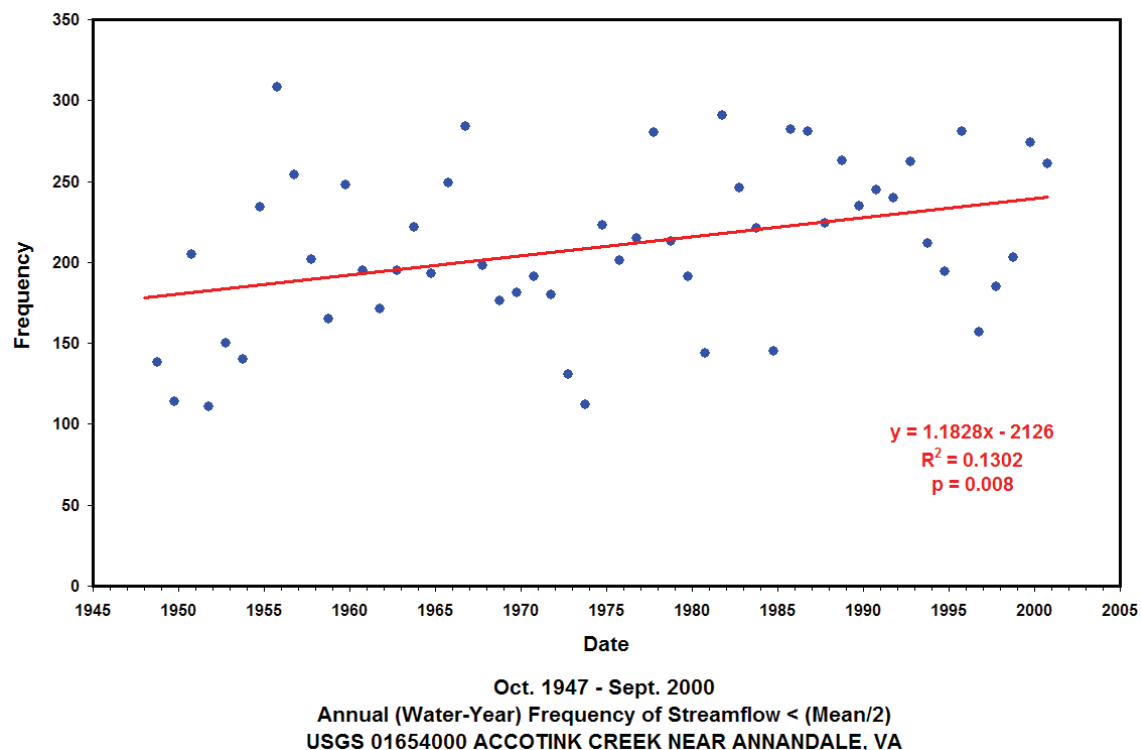


Figure 4: Frequency of low-flow events for VDEQ/USGS stream gage 01654000 for October 1947 through September 1998. 'Low-flow' is here defined as the flow less than or equal to one-half of the mean streamflow for the period. P-value is on the t-test of the linear regression line slope = 0 (no change).

We acquired historical daily precipitation records coincident with the streamflow records from the National Weather Service (NWS) monitoring station 448737, Vienna/Dunn Loring (NCDC, 1998). We computed the daily streamflow (mean daily streamflow, $\text{m}^3\cdot\text{s}^{-1}$) per unit precipitation (total daily precipitation, $\text{m}\cdot\text{d}^{-1}$) for the VDEQ/USGS stream gage 01654000 for days where total precipitation was equal to or greater than 6 mm for October 1947 through September 1998. We aggregated the data by decade and compared decadal means to see if the amount of streamflow per unit precipitation and mean daily precipitation had changed over time as the watershed became increasingly impervious. Our analysis showed a statistically significant increase (Kruskal-Wallis One-Way Analysis of Variance test statistic = 176.07, 4 df, $p < 0.001$) in the streamflow discharge response per meter of precipitation associated with "normal" (> 6 mm) daily precipitation amounts while the mean daily precipitation didn't change (Figure 5). Similar results were found for streamflows associated with "extreme" (> 35 mm) daily precipitation amounts. The historical magnitude, frequency and pattern of daily precipitation values ≥ 0 mm, ≥ 6.0 mm and ≥ 35.0 mm showed no statistically significant change.

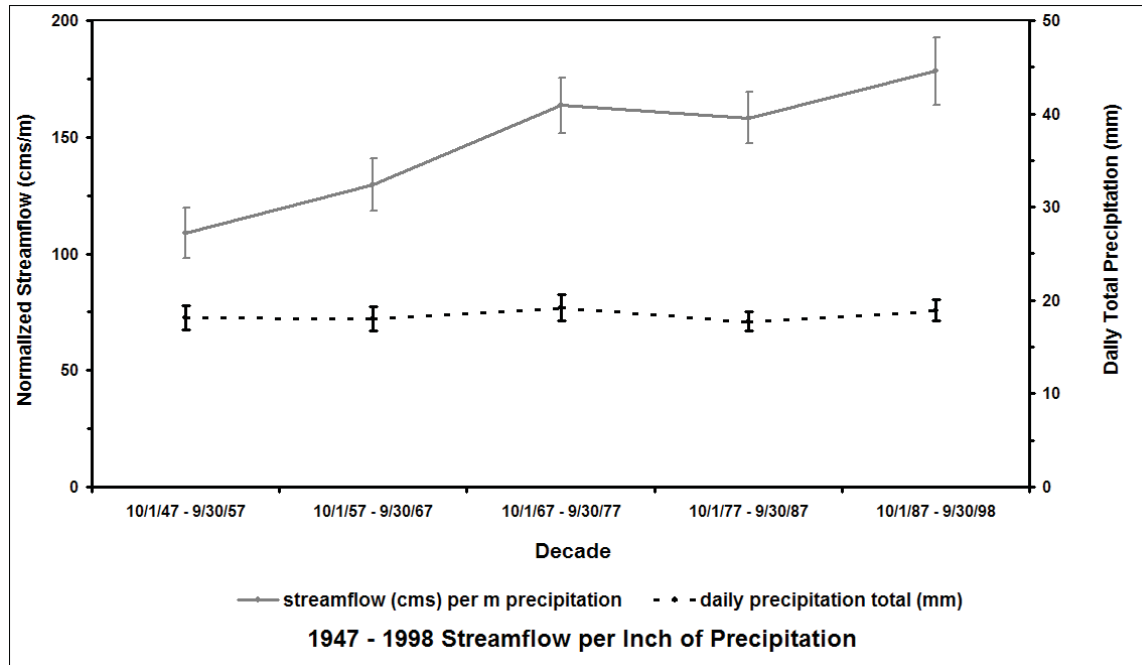


Figure 5: Streamflow (mean daily streamflow, $\text{m}^3 \cdot \text{s}^{-1}$) per unit precipitation (total daily precipitation, $\text{m} \cdot \text{d}^{-1}$) for VDEQ/USGS stream gage 01654000 and mean daily precipitation for days where total precipitation was equal to or greater than 6 mm for October 1947 through September 1998. Data are binned by decade and decadal means displayed. Error bars = $\pm 95\%$ confidence interval. Two trends emerge from the data: 1) mean precipitation volume show no significant variation over time, while 2) the streamflow response value shows a significant change over the same period.

Historical changes in streamflow response to precipitation in this basin (Figure 6) appear to be related to increases in anthropogenic impervious surface cover and not to changes in precipitation. Changes in streamflow response to precipitation were larger in magnitude than changes in streamflow alone and are therefore thought to be an indicator variable related to increases in anthropogenic impervious surface cover or other anthropogenic activities such as installation of impoundments or other best management practices (BMPs) that result in hydrological alteration.

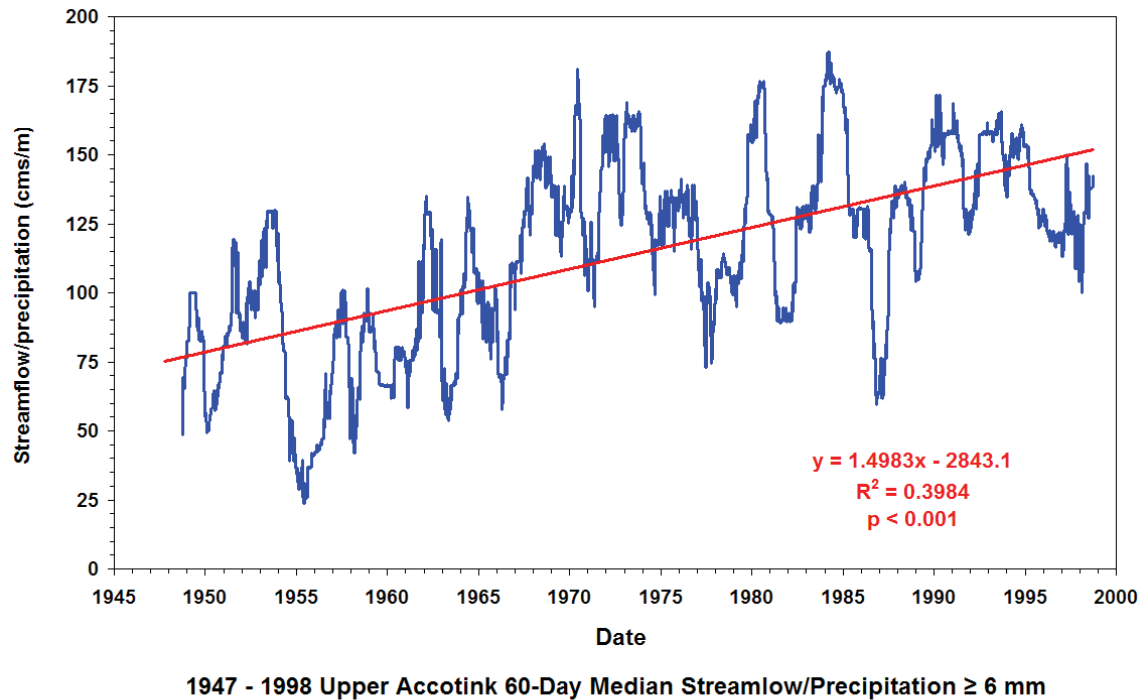
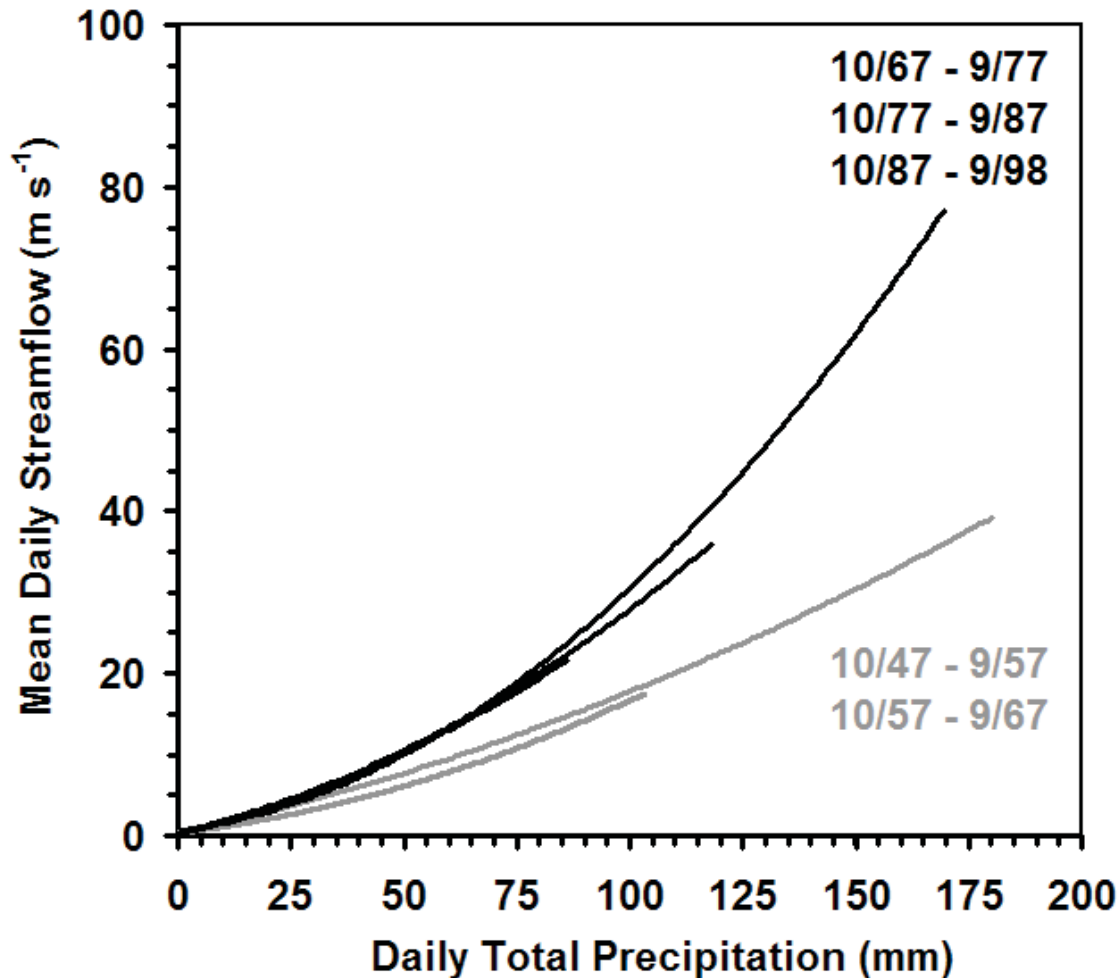


Figure 6: Median streamflow per unit precipitation ≥ 6 mm for VDEQ/USGS stream gage 01654000 for October 1947 through September 1998. Median streamflow was calculated as a rolling 60-day median of days where total daily precipitation was at least 6 mm. P-value is on the t-test of the linear regression line slope = 0 (no change).

Changes in stream hydrology change more than the physical morphology of the stream. Changes in flow regime also have an effect upon aquatic ecosystem health and the ecosystem services provided. From the perspective of a benthic macroinvertebrate or a fish, the annual frequency of extreme flow events, both high and low, are critical factors in assessing the suitability of the stream ecosystem for aquatic life. From the perspective of a watershed manager or stakeholder, the relationship between the amount of development and the corresponding amount of impervious surfaces is a critical factor in predicting the impact of a given level of development on stream ecosystem health. Figure 7 is a graph of the regression lines from all streamflow-precipitation data pairs (precipitation values > 0 mm), grouped in 10-year bins. The graph represents a generalized historical characterization of the decadal streamflow-precipitation relationships. An increased slope over time is observed indicating an increasingly direct relationship between precipitation and runoff. The data appear to form two distinct groupings of slopes over time, with the precipitation/streamflow response curves for the first two decades showing a lower streamflow response to increasing precipitation than the last three decades. These data support the hypothesis that there may be a level of imperviousness at which a 'phase-change' in streamflow response/precipitation amount occurs, as suggested by the Schueler's 1994 paper (Schueler suggested a limit of around 10% imperviousness, beyond which stream degradation occurs). Figure 7 also graphically illustrates how the same amount of precipitation

received in one of the three later decades results in much higher streamflow than if received in the first two decades of the study. This increase in streamflow response to precipitation over time is a major determinant in streambank erosion, stream habitat alteration, and many other negative consequences to streams associated with urban development.

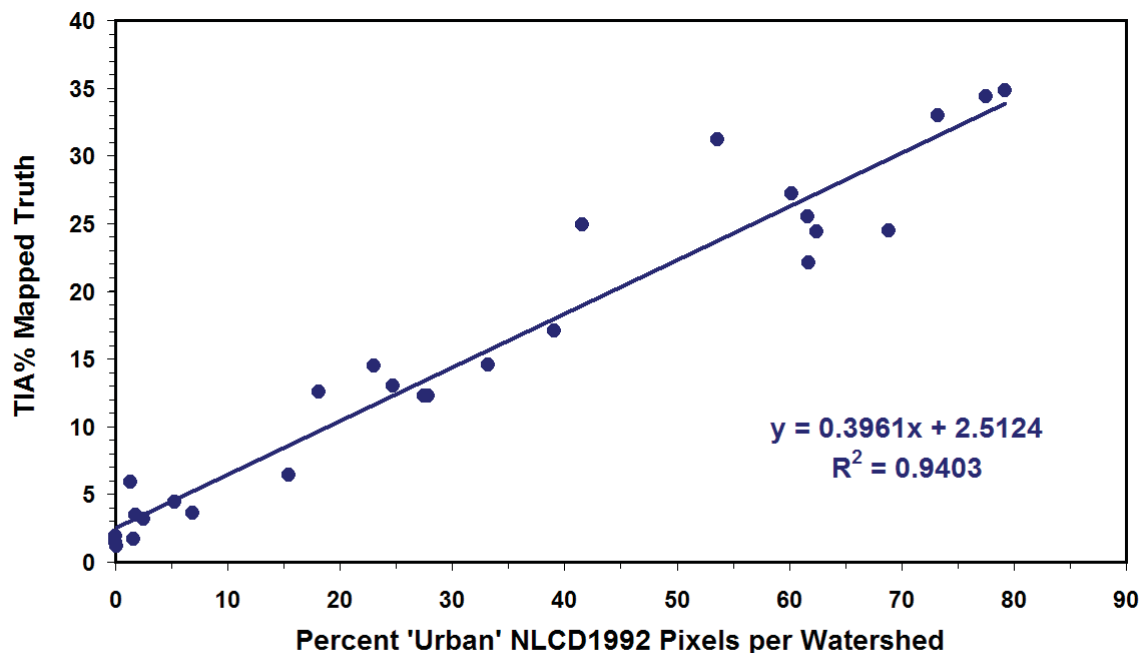


1947 - 1998 Streamflow vs. Precipitation for days of measurable precipitation

Figure 7: 1947–1998 Streamflow vs. Precipitation by Decade for days of measurable precipitation. This decade-by-decade series of regressions illustrates the general historical curvilinear relationships of daily precipitation and streamflow. Figure includes all streamflow-precipitation data pairs where precipitation values > 0 , $N = 5865$. The regression lines for the first two decades follow a similar path while the curves for the last three decades form a second group.

Measures of Imperviousness and/or Degree of Development

While the results of the extensive historical study of streamflow and precipitation in the Upper Accotink were exciting and highly informative, they also were very data-intensive and time-consuming to assemble. I wanted to explore a metric that could be used to conduct an analysis on a large number of streamflow stations at a regional scale. My goal in this regional-scale analysis was to try to relate patterns of streamflow change to regional-scale measures of development. Since mapping impervious surfaces directly for a large number of study watersheds is unfeasible without the input of huge effort (and expenditure), the surrogate measure of population was used for decades prior to regional-scale land use/land cover (LULC) landscape mapping and temporal LULC data were acquired for circa 1973, 1992, and 2001 (see further discussion in Methodology below).



**TIA% Mapped Truth per Percent 'Urban' NLCD Pixels
for 1992 NLCD Coefficients paper (n = 27 watersheds)**

Figure 8: Percent Imperviousness (TIA%) from ground truth vs. Percent Urban (%Urban) per watershed from the NLCD1992 land cover dataset. NLCD1992 percent 'urban' pixels are the sum of categories 21, 22, 23, & 85 divided by the total number of pixels in the watershed's NLCD coverage. The TIA% truth was mapped from aerial photography using the methods described in Jarnagin *et al.* (2004) and Jennings and Jarnagin (2002). The percent 'urban' pixels in the NLCD1992 land cover dataset is a good estimator of the Total Impervious Area % (TIA%) for the watersheds (n = 27) mapped by Jennings and Jarnagin in their NLCD1992 coefficients paper (Jennings *et al.*, 2004).

There is a good relationship between the 'percent urban' metric for a watershed and the TIA% for that watershed (Figure 8). Therefore, 'percent urban' will also be used as a metric for measuring the extent of anthropogenic impact upon the watershed for the temporal LULC data. There are two coefficient-based techniques for estimating impervious surfaces from National Land Cover Data (NLCD) data (USEPA, 2006): the NLCD1992 coefficient method of Jennings and Jarnagin (Jennings *et al.*, 2004) and the Analytical Tools Interface for Landscape Assessments (ATtILA) for ArcView 3.x (Ebert and Wade, 2000; Wade and Ebert, 2004). The ATtILA coefficients were derived from land use coefficients compiled by the Center for Watershed Protection (Caraco *et al.*, 1998) and can be applied to both the NLCD1992 and the cross-walked NLCD2001. Finally, the NLCD2001 has a separately downloadable imperviousness layer that is an input to the LULC data. Thus, both the NLCD1992 and the NLCD2001 have two independently derived estimators of TIA% for the study watersheds.

Measure of Hydrologic Alteration: Stream Flashiness

There are many measures of hydrologic alteration, all of which are intended to provide a metric by which changes in streamflow over time can be assessed. Olden and Poff (2003) reviewed 171 hydrologic indices using long-term flow records from across the continental USA (and found many of them to be redundant). For this study, I chose the Richards-Baker Flashiness Index (R-B Index, Baker *et al.*, 2004) to calculate annual flashiness values for study streams.

$$\text{R-B Index} = \frac{\sum_{t=1}^n |q_{t-1} - q_t|}{\sum_{t=1}^n q_t} \quad (\text{Baker } et al., 2004)$$

Equation 1: The R-B Index (Baker *et al.*, 2004).

The R-B Index is the sum of the absolute values of the day-to-day changes in mean daily streamflow, normalized for total flow per station by dividing by the total annual flow. The advantages of the R-B Index, compared to the numerous other methods of calculating streamflow variability, are: 1) the R-B Index has low year-to-year variability and therefore is sensitive to long-term trends; 2) the R-B Index integrates the entire range of hydrological response over an annual time step; and 3) the R-B Index is easily calculated from NWIS historical daily mean streamflow.

Prior to the analysis of the regional set of watersheds, the R-B Index was applied to the streamflow history of the Upper Accotink watershed previously studied. The annual R-B Index stream flashiness over time for the Upper Accotink shows a significant increase (Figure 9). Both the flashiness and the TIA% are increasing for the Upper Accotink watershed (Figure 10) for the period 1947-2000. When flashiness over time is plotted as a 5-year moving average (Figure 11), the period of greatest increase in the flashiness of the system occurs as the TIA% increases from roughly 10% to 20%. This again implies a 'hard limit' of around 10% for imperviousness effects, at least for this system.

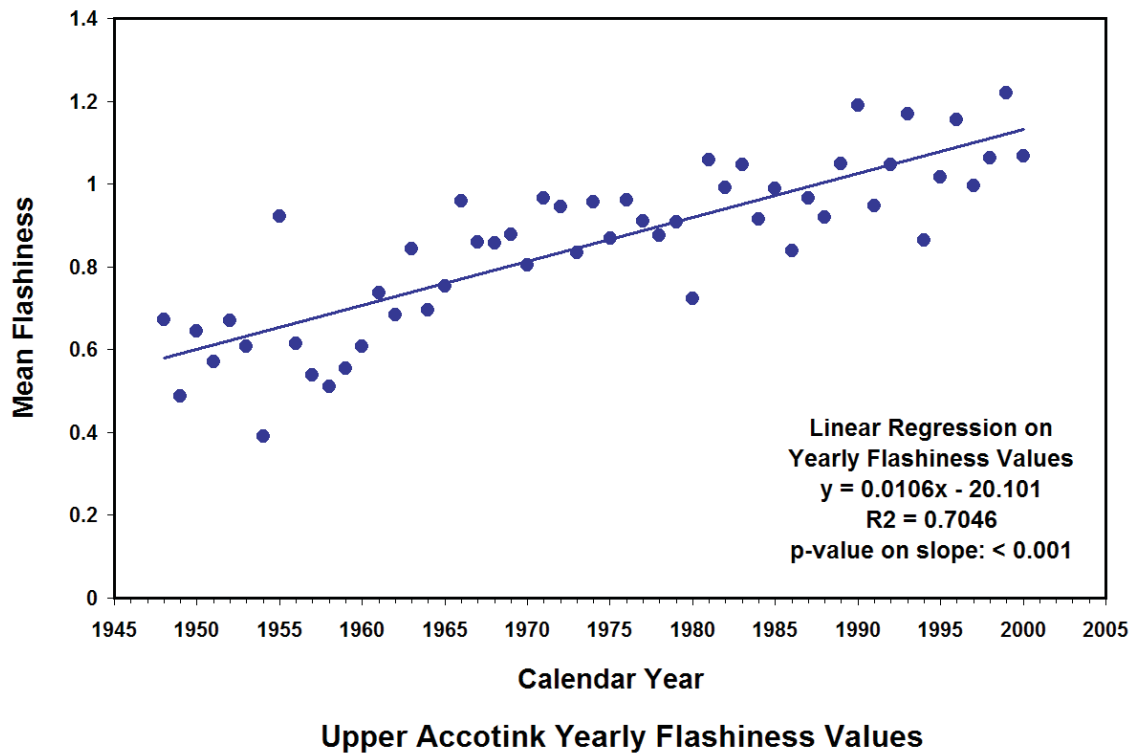


Figure 9: Annual Richards-Baker Flashiness Index (R-B Index) values plotted for the Upper Accotink stream gage 01654000 for 1948 through 2000. Flashiness in this system increased significantly over time. P-value is on the t-test of the linear regression line slope = 0 (no change).

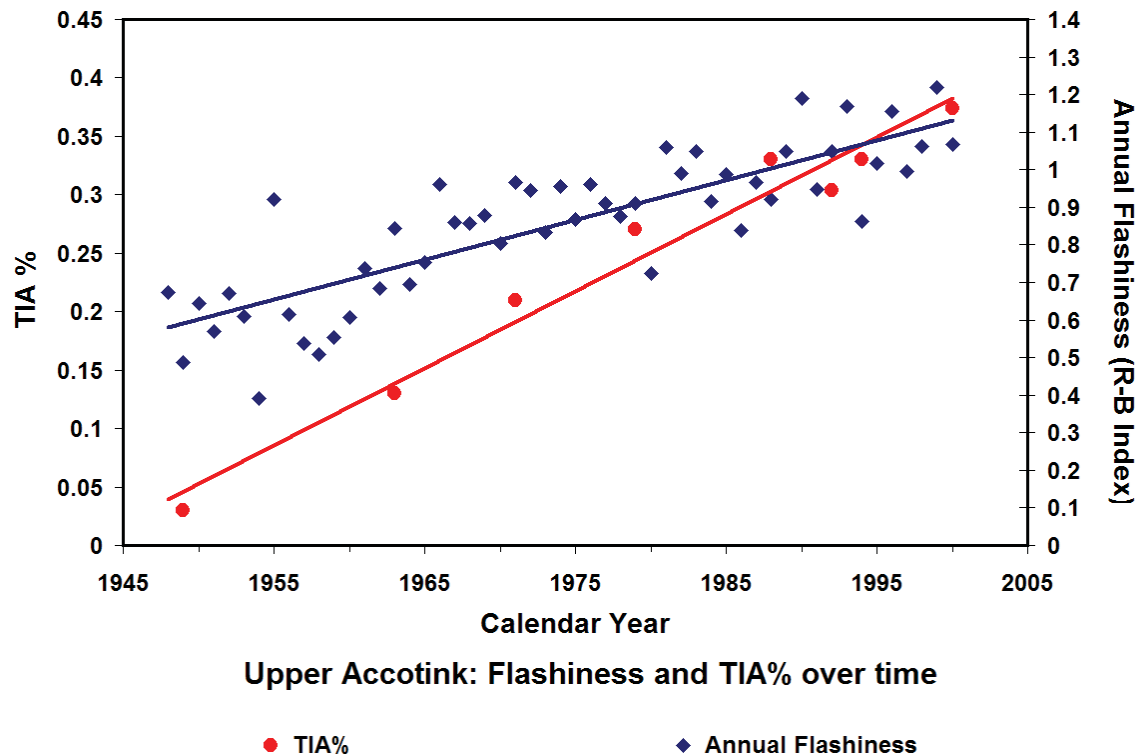


Figure 10: Plot of both the TIA% and Flashiness for the Upper Accotink stream gage 01654000 for 1948 through 2000. TIA% was directly compiled through 1994 and estimated via coefficient methods from the circa 1992 and 2001 land use/land cover data. The flashiness of the system is increasing as the TIA% increases.

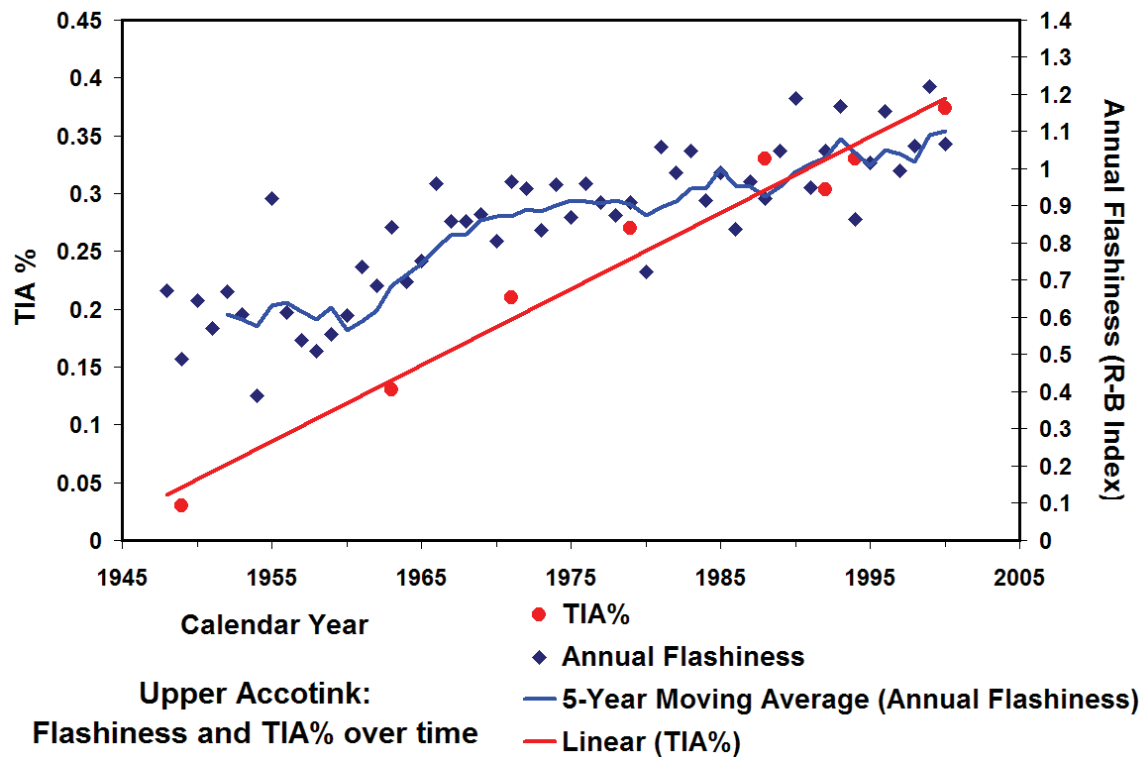


Figure 11: Plot of both the TIA% and Flashiness for the Upper Accotink stream gage 01654000 for 1948 through 2000 with 5-year moving average of annual flashiness. The period of greatest increase in the flashiness of the system as revealed by a 5-year moving average occurs as the TIA% increases from roughly 10% to 20%.

The Upper Accotink study is unique in the large number of estimations of TIA% made. For the larger, regional-scale study, there were roughly decadal estimates of 'percent urban' and imperviousness based upon the temporal LULC data and decadal population data. In order to draw inferences about flashiness associated with any measure of anthropogenic effect, it will be necessary to bin the flashiness data in the same manner that decadal bins and photo date bins were used to study historic changes in streamflow/precipitation response in the Upper Accotink. I used 7-year flashiness bins centered on the six photo dates used to estimate TIA% and the two coefficient-based TIA% estimates (NLCD1992 and NLCD2001) for the Upper Accotink to test the efficacy of this analysis technique (Figure 12). The mean flashiness increased over time as measured by the flashiness bins (ANOVA on Upper Accotink Flashiness Groups by Photo Date: $F = 13.78$, $df = 7$, $p\text{-value} < 0.001$). The same analysis technique was used in the large-scale, regional study.

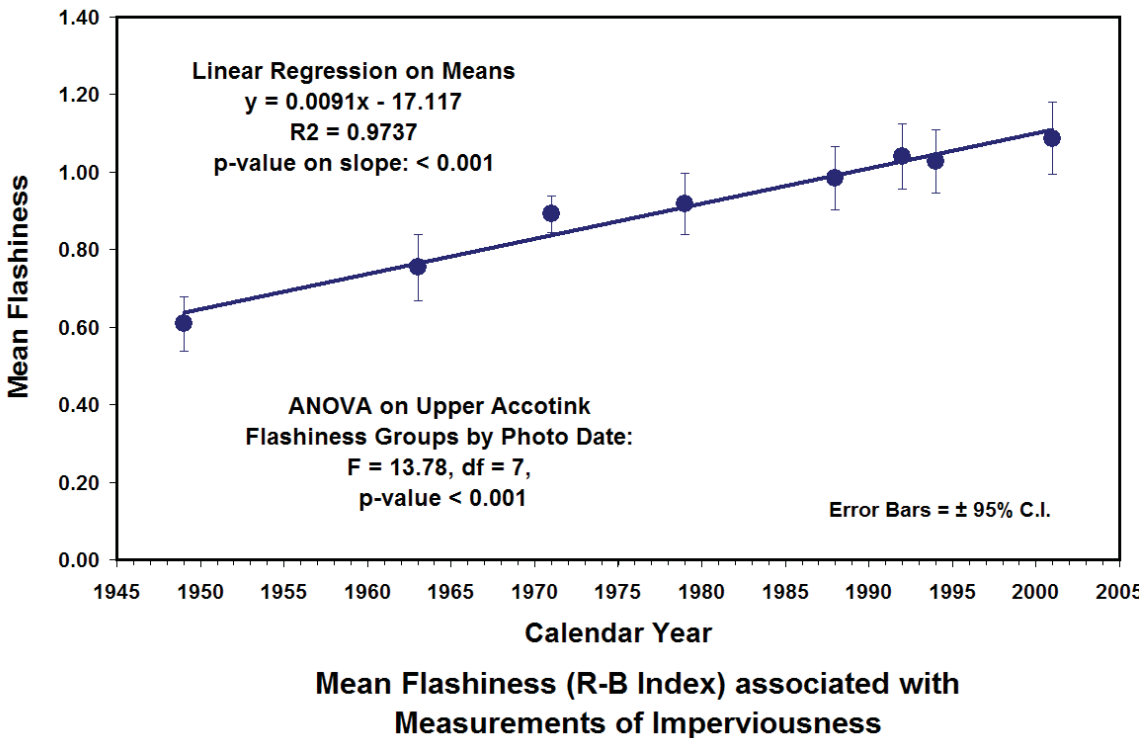


Figure 12: Mean flashiness per TIA% estimate date in the Upper Accotink. Mean flashiness is computed from a 7-year interval centered on the six photo dates used to estimate TIA% and the two coefficient-based TIA% estimates (NLCD1992 and NLCD2001) for the Upper Accotink. The mean flashiness increased significantly over time (ANOVA on Upper Accotink Flashiness Groups by Photo Date: $F = 13.78$, $df = 7$, $p\text{-value} < 0.001$).

Data and Methodology for the current study:

Population Density Data

Decadal census data were obtained and proportionally allocated into 2000-era county boundaries (Jennings and Jarnagin, 2004). Census data from a variety of sources was used to construct the county level population density databases at for 1930-2000 for EPA Region 3 (Delaware, District of Columbia, Maryland, Pennsylvania, Virginia, and West Virginia). Historic census data for 1930-1960 were obtained from the University of Virginia Library Historical Census Browser < <http://fisher.lib.virginia.edu/collections/stats/histcensus/index.html> > (UVA, 2004). Identical county-level decadal census data were obtained from the U.S. Census Bureau (U.S. Census, 2004) accessed via their State and County QuickFacts browser < <http://quickfacts.census.gov/qfd/> > as accuracy cross check (see < <http://www.census.gov/population/cencounts/dc190090.txt> > for an example file). County-scale census data for all of Region 3 for 1970 and 1980 were obtained from GeoLytics, Inc (GeoLytics, 2003). County-scale census data for all of Region 3 for 1990 and 2000 was obtained from the Environmental Systems Research Institute, Inc. (ESRI) Data 2003 disks: ESRI Data - 2000 data (ESRI, 2003) < http://www.esri.com/data/community_data/census/index.html >. All

population density data were mapped to the ESRI 2002 county boundaries using proportional allocation for those areas (particularly in the state of Virginia) where political reporting jurisdictions had merged or otherwise altered their boundaries during the 1930-2000 time period. Appendix 1 contains a series of figures showing the 1930 and 2000 population densities, decadal changes in density, and the net change in population density from 1930 through 2000; mapped to a uniform numerical scale at the county spatial scale.

For decades after 1960, higher spatial resolution census data were also acquired. 1970-1990 data were obtained from GeoLytics, Inc (GeoLytics, 2003). For 1970, census data were available at the Census tract scale; for 1980, block-group data; and for 1990, block data. I also used the LandScan 1998 dasymetric estimation of population density and areal interpolation of census data at a 450 m grid cell spatial resolution (LandScan, 2003). 2000 population densities were based on the ESRI Data 2003 data at the Census block scale (ESRI, 2003).

Census population densities were calculated for watershed at the tract-scale for 1990 and 2000 and block-group data were used for 2000. LandScan population density was calculated only for 1998 at the watershed spatial scale. Decadal population density was calculated at both the county and watershed spatial scale for 1930-2000. Changes in overall (period-of-record) population density were calculated at both the county and watershed spatial scale for 1930-2000 as a set of Population Density Change Metrics: 1) net population density change from 1930 to 2000 (Figure A10); 2) net positive change in population density only from 1930 to 2000; 3) sum of the positive changes in decadal population density from 1930 through 2000; and 4) sum of the absolute values of both positive and negative decadal changes in population density from 1930 through 2000.

Streamflow Data

I selected 151 long-term gage stations in EPA Region 3 (EPA R3, mid-Atlantic: DC, DE, MD, PA, VA, and WV) from the USGS National Water Information System (NWIS) historical daily mean streamflow dataset for analysis. The initial data set consisted of the thirty-six watersheds, ranging in size from 2 km² to 150 km², used to derive impervious surface coefficients per NLCD92 class (Jennings *et al.*, 2004). An additional 115 streamflow stations were selected from a search of the surface water stations listed on the NWIS in EPA R3. Streamflow stations were sorted by length of record, completeness of record, and watershed size. I wanted to find long-term, continuous records where the watersheds were small enough to assume a unitary response to precipitation, *i.e.*: the precipitation that would fall on a watershed during a day would be reflected in a change in streamflow at the recording station on that same day. The additional streamflow station selection criteria were: 1) more than 20 total years of data, 2) watershed size less than 130 km², and 3) continuous periods of data (more than 75% of available daily records per decade of data).

Streamflow station information and daily flow data for the period of record for each station selected were downloaded from the USGS National Water Information System (NWIS) Web Interface - Surface-Water Daily Data for the Nation web site: < http://waterdata.usgs.gov/nwis/dv/?referred_module=sw >. Station ID codes, names, locations,

etc. are shown in Appendix 2. Streamflow data were analyzed by computing their annual flashiness values, both by water year (as defined by the USGS: from October first of one year to September 30th of the following) and by calendar year. For simplicity of discussion, for this report only calendar year values will be discussed, as there was no difference between results obtained when considering water year vs. calendar year data. In order for a flashiness value to be computed for a calendar year, at least 75% of all the available daily records had to be present for that year. Seven-year windows of flashiness data around each decadal census date from 1930 through 2000 and the imagery acquisition dates of 1973 and 1992 were used to calculate mean flashiness values for each station for each analysis date. The flashiness data bin used for the 2000 Census date was used also for the 2001 imagery (1997-2001, since the dataset analyzed ended in 2001). At least four years of data out of the seven-year period had to be present in order for a mean flashiness value to be computed for an analysis date.

Tim Wade, EPA/LEB RTP NC, using a smoothed version of the USGS National Elevation Dataset (NED) 30-meter resolution digital elevation model (DEM) data clipped to the EPA R3 boundaries, created watershed boundaries for each streamflow station in ArcInfo. These watershed boundaries were used to extract population, 'percent urban' LULC, and 'percent imperviousness' data for comparison with the streamflow records. One of the 151 watersheds (01585095, North Fork Whitemarsh Run near White Marsh, one of the original thirty-six NLCD1992 coefficient paper watersheds) was determined to have too short a record and was not mapped. Nine of the 150 watersheds in R3 used in the NLCD1992 land cover analysis lay outside of the area of completed NLCD2001 coverage at the time of the analysis so the 2001 land cover analysis was done for that era using the 141 watersheds within the NLCD2001 completed extent.

Land Use/Land Cover Data

Temporal land use/land cover (LULC) data were acquired for circa 1973, 1992, and 2001. The 1970s land-cover data were created from Landsat Multispectral Scanner (MSS) data that were acquired as part of the North American Landscape Characterization (NALC) program. The NALC program distributed the MSS data at a resampled pixel size of 60 meters. The 1990s (NLCD1992) and 2000s (NLCD2001) National Land Cover Data were acquired from the Multi-Resolution Land Characteristics (MRLC) program using Landsat TM imagery at 30-meter spatial resolution (Vogelmann *et al.*, 2000 and Homer *et al.*, 2004).

No attempt to align pixels or reassign values among datasets was made. Watershed-scale assessment of land cover for each era was done using the 'Tabulate Areas' command in ArcView 3.3. Tables created were exported from ArcView as tab-delimited ASCII text files and imported in MS Excel for analysis. The MRLC NLCD Classification Schemes (Level II) land cover classes for the NLCD1992 and NLCD2001 are found at < <http://www.epa.gov/mrlc/classification.html> > and are listed in Appendix 3 of this report. Unlike the MRLC coverages for 1992 and 2001, there was no pre-existing land-cover data from the NALC program for the 1970s. The NALC Landsat MSS data were classified into seven land-cover classes using Euclidean minimum-distance-to-mean clustering and ancillary data. The

primary ancillary data sets were USGS Land Use Data Analysis (LUDA) land-cover and National Wetlands Inventory (NWI) data (Table 2; Edmonds *et al.*, 2002).

ID	NALC Land Cover Class
1	Water
2	Forest
3	Agriculture (herbaceous)
4	Wooded Wetland
5	Emergent Wetland
6	Urban (developed)
7	Bare Ground (bare rock, sand, mines)

Table 2: The seven NALC70s land cover classes from Edmonds *et al.* (2002).

The 'percent urban developed' (%Urban) parameter was estimated for each watershed using the protocol set forth by Jones *et al.* (2003) and Jarnagin *et al.* (2006). The NALC70s %Urban decimal percent is the sum of pixels in land cover class 6 divided by the total number of pixels in the coverage. The NLCD1992 %Urban decimal percent is the sum of pixels in land cover classes 21, 22, 23, & 85 divided by the total number of pixels in the coverage. The NLCD2001 %Urban decimal percent is the sum of pixels in land cover classes 21, 22, 23, & 24 divided by the total number of pixels in the coverage.

Jennings *et al.* (2004) found that the imperviousness coefficients derived from NLCD1992 land cover data changed depending on the degree of development seen in the watershed. Jones *et al.* (2003) and Jarnagin *et al.* (2006) used a set of '%Urban' categories to bin data for areal analysis, where an Urban Gradient is established based on the percentage of 'Urban' NLCD pixels in the area to be analyzed (Table 3). The same %Urban categories were used to look at stream flashiness.

Urban Gradient Category	%Urban
None	No 'Urban' pixels in the area to be analyzed
Rural	0 to <20% 'Urban' pixels
Suburban	20 to <50% 'Urban' pixels
Dense Suburban	50 to <80% 'Urban' pixels
Urban	80 to 100% 'Urban' pixels

Table 3: Urban Gradient used for imperviousness accuracy assessment in Jones *et al.* (2003) and Jarnagin *et al.* (2006).

Imperviousness Data

The NLCD1992 Coefficient technique (Jennings et al., 2004) and the ATtILA ArcView extension 'Human Stressors' computation 'PCTIA_LC' (Wade and Ebert, 2004) were applied to the NLCD1992 coverages clipped by the watershed boundaries. This provided two independent estimates of TIA% for 1992 for the 150 watersheds mapped. The NLCD2001 Imperviousness data layer was used for a circa 2001 estimator of watershed imperviousness and the ATtILA technique was applied to the 2001 land cover categories cross-walked to approximate the NLCD1992 watershed categories (Table 4).

1970s NALC Class	NLCD1992 Class	NLCD2000 Class
1 - Water	11 - Open Water	11 - Open Water
2 - Forest	41 - Deciduous Forest, 42 - Evergreen Forest, 43 - Mixed Forest, 51 - Shrubland, 61 - Orchards/ Vineyards/ Other, 71 - Grasslands/ Herbaceous	41 - Deciduous Forest, 42 - Evergreen Forest, 43 - Mixed Forest, 52 - Shrub\Scrub, 71 - Grasslands/ Herbaceous
3 - Agricultural Land	81 - Pasture/ Hay, 82 - Row Crops, 83 - Small Grains, 84 - Fallow	81 - Pasture/ Hay, 82 - Cultivated Crops
4 - Woody Wetland	91 - Woody Wetlands	91 - Woody Wetlands
5 - Emergent Wetland	92 - Emergent Herbaceous Wetlands	92 - Emergent Herbaceous Wetlands
6 - Urban	21 - Low Intensity Residential, 22 - High Intensity Residential, 23 - Commercial/ Industrial/ Transportation, 85 - Urban/ Recreational Grasses	21 - Developed Open Space, 22 - Developed, Low Intensity, 23 - Developed, Medium Intensity, 24 - Developed, High Intensity
7 - Bare	31 - Bare Rock/ Sand/ Clay, 32 - Quarries/ Strip Mines/ Gravel Pits, 33 - Transitional	31 - Barren Land (Rock/Sand/Clay)

Table 4: 1970s NALC - NLCD1992 - NLCD2001 crosswalks of land cover classes used for ATtILA PCT_LC computation. Note: NLCD land cover classes do not include 'perennial ice and snow' or Coastal or Alaska only classes.

No attempt to assign a TIA% to the 1970s NALC data was made since this technique has not been validated via comparison to ground-truth impervious measurements. Both the

NLCD1992 and the NLCD2001 have two independently derived estimators of TIA% for the study watersheds. See the Discussion area of this report for a comparison of these estimators.

Software and Hardware

Disclaimer: Mention of a product name in this report does not constitute an endorsement of that product by either the author or EPA and should not be construed as such. All computations for this project were performed on IBM-compatible PCs running Microsoft XP Service Pack 2 OS using either Pentium or AMD processors. GIS computations were done using ESRI ArcGIS 9.1 or ArcView 3.3 plus applicable extensions (Spatial Analyst, ATtILA, etc.) All statistical analyses were performed using either SAS 9 or SYSTAT 10. Spreadsheet, graphing, and word processing were done with MS Office 2000 and 2003 products.

Results:

Streamflow Data

Of the 151 streamflow stations analyzed, roughly three-fifths showed an increasing flashiness trend (Table 5) with the parametric and/or nonparametric test finding a significant increase at thirty-five stations (23.2%) and a significant decrease in flashiness seen at thirteen stations (8.6%). Table 6 and Figure 13 display the streamflow station flashiness results grouped by Significance Category using the p-value of the linear (parametric) statistical test and the positive or negative slope of the monotonic trend to sort the results.

n = 151	
n increasing (linear) =	92
% increasing (linear) =	60.9%
n decreasing (linear) =	59
% decreasing (linear) =	39.1%

n = 151	
n increasing (Kendall) =	94
% increasing (Kendall) =	62.3%
n decreasing (Kendall) =	57
% decreasing (Kendall) =	37.7%

Table 5: Flashiness Summary Table showing the overall increase or decrease over time of the monotonic trend revealed by the linear (parametric) or Mann-Kendall Tau (nonparametric) tests.

Significance Categories	p-values	n	percent
No Change	$-0.2 > p\text{-values} > 0.2$	82	54.3%
Not Significant Increase	$0.2 \geq p\text{-value} \geq 0.05$	16	10.6%
Not Significant Decrease	$-0.2 \leq p\text{-value} \leq -0.05$	10	6.6%
Significant Increase	$0 < p\text{-value} < 0.05$	33	21.9%
Significant Decrease	$0 > p\text{-value} > -0.05$	10	6.6%

Table 6: Streamflow Station Flashiness Significance Categories. Results for the linear (parametric) tests are shown with the number and percentage of the total for each significance category. The slope of the monotonic trend ('+' is increasing over time, '-' is decreasing over time) is used in front of the p-value to indicate in a single measure the direction and strength of the relationship.

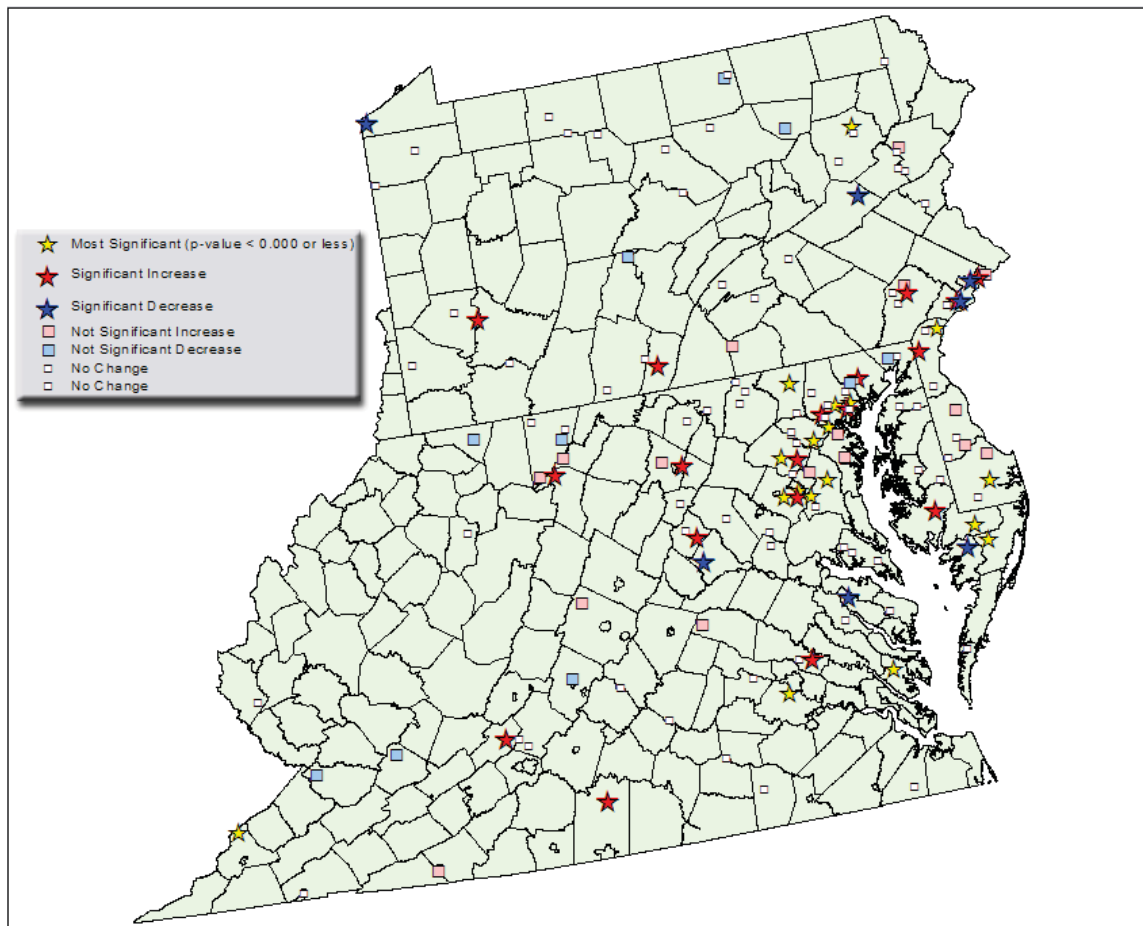


Figure 13: Streamflow flashiness results. The p-value of the linear (parametric) statistical test and the positive or negative slope of the monotonic trend are used to sort the results. Significance Categories: 'No Change' stations are those with p-values greater than .2 or less than -.2; 'Not Significant Increase': $0.2 \geq p\text{-value} \geq 0.05$; 'Not Significant Decrease': $-0.2 \leq p\text{-value} \leq$

-0.05; 'Significant Increase': p-value < 0.05; 'Significant Decrease': p-value > -0.05; and 'Most Significant': p-value = 0.000.

The full results of the R-B Flashiness analysis are given in Appendix 4: Flashiness Results Table. Both linear regression (parametric) and Mann-Kendall Tau (nonparametric) tests were used to check for the significance of monotonic change in the flashiness trend over time. The results of both tests are shown in Appendix 4, using the p-value of the respective test to show the relative strength of the trend and the positive or negative sign indicating the direction of the trend over time. The Appendix 4 table is ranked in ascending order of the direction and strength of the linear p-value. Station IDs and the test p-value are highlighted in light green for those stations with a significant ($\alpha = 0.05$) relationship with either or both of the statistical analysis methods.

Streamflow Flashiness and Population Density

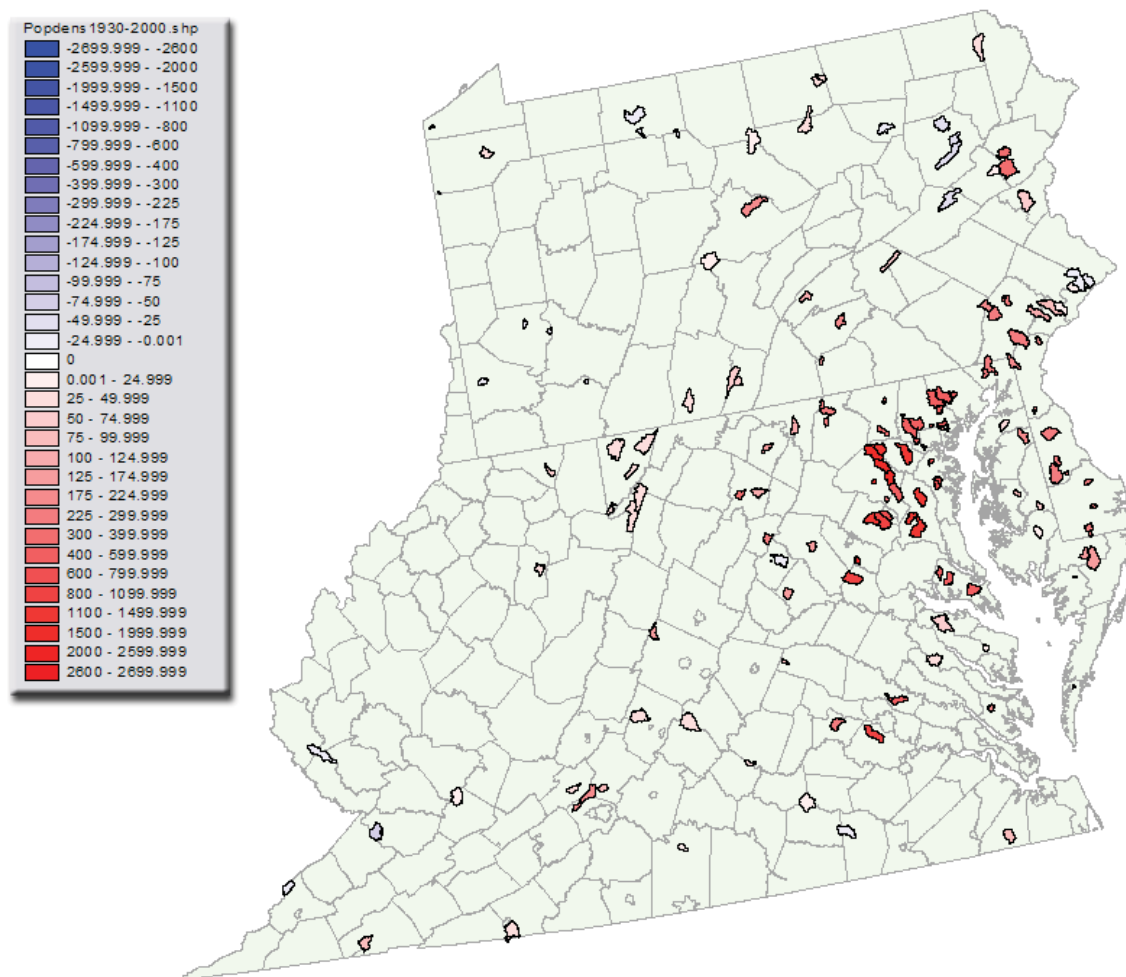


Figure 14: Population density change (\pm people \cdot mi²) from 1930 to 2000 mapped at the watershed spatial scale. County-level Census data (Appendix 1: Figure A10) were mapped to the watershed boundaries using proportional allocation.

Decadal population density was calculated at both the county and watershed spatial scale for 1930 to 2000. Changes in overall (period-of-record) population density were calculated at both the county and watershed spatial scale for 1930 through 2000. Figure 14 displays the population density change from 1930 to 2000 at the watershed spatial scale.

One method of viewing the effects of population on stream flashiness is to look at county-level population change over time and see if there is a relationship between those changes and streamflow stations showing significant changes over time or not. I compared stations showing significant change in their flashiness at $\alpha = 0.05$ in either linear and/or Kendall tests ($n = 48$) with those that were not significant at that level ($n = 103$) using the Population Density Change Metrics: 1) absolute value of the overall net population density change from 1930 to 2000 ('Net_Abs'); 2) net positive change only in population density from 1930 to 2000 ('Net_Pos'); 3) sum of the positive changes in decadal population density from 1930 through 2000 ('Sum_Pos'); and 4) sum of the absolute values of both positive and negative decadal changes in population density from 1930 through 2000 ('Sum_Abs'). Table 7 shows the means and $\pm 95\%$ Confidence Intervals (C.I.s) for the groups.

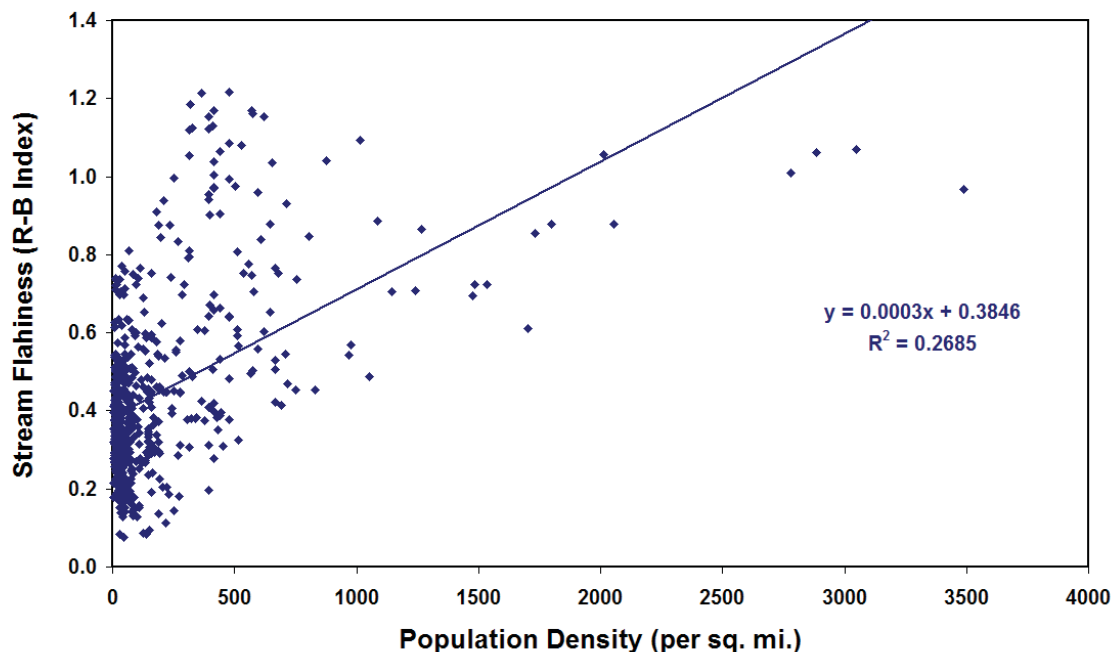
	Mean 'Net_Abs '	$\pm 95\%$ C.I. 'Net_Abs '	Mean 'Net_Pos '	$\pm 95\%$ C.I. 'Net_Pos '	Mean 'Sum_Pos '	$\pm 95\%$ C.I. 'Sum_Pos '	Mean 'Sum_Abs'	$\pm 95\%$ C.I. 'Sum_Abs'
Significant Flashiness Change ($n = 48$)	247.7	108.4	276.78	148.18	317.51	159.86	420.59	200.63
No Significant Flashiness Change ($n = 103$)	111.8	32.6	109.59	31.81	117.50	32.82	133.47	46.27
Kruskal- Wallis p- value	0.041		0.272		0.019		0.007	

Table 7: Mean population density change per category for stations showing significant vs. no significant change in monotonic flashiness trend over the station period of record. The Kruskal-Wallis p-value reports the results of the nonparametric test of equivalency of the station group means.

The mean population density change per category for stations showing no significant change in monotonic flashiness trend were similar for all categories but those stations that had a significant change in stream flashiness over their period of record displayed an increased mean with greater differences seen with the sums of decadal density changes. Due to unequal sample size, a nonparametric Kruskal-Wallis test of equivalency of the station group means was used for the four population density change metrics. The absolute value of the overall net change in population density from 1930-2000 and both the sum of positive density changes and the sum of the absolute value of both positive and negative changes were significant at $\alpha = 0.05$ (respectively: Mann-Whitney U test statistics =2955.0, 1883.5, and 1794.5; Chi-square

approximations with 1 df = 40173, 5.534, and 7.335; p-values = 0.041, 0.019, and 0.007). The net positive change only in population density from 1930 to 2000 was not significantly different between the stations that showed a significant change in mean stream flashiness with those that did not.

Using the seven-year flashiness means, centered at each census date, I constructed a dataset of 621 independent estimates of mean watershed flashiness per population density (Figure 15). Streamflow flashiness was weakly correlated with increasing population density ($R^2 = 0.269$), with population densities above roughly 700 people \cdot -mi² visually showing what appears to be an increasing trend.



Watershed Flashiness per Census Population Density

Figure 15: Mean watershed flashiness per census population density level. Mean watershed flashiness is calculated as a seven-year mean centered at the decadal census. Census population density level (people \cdot -mi²) is calculated at the county level, proportionally allocated to watersheds, for 1930-2000. N = 621.

Increasing the spatial resolution of the population density estimate improved the correlation between population density and streamflow flashiness. 1990 census tract data were used to calculate population density for the 93 watersheds with 1990 flashiness values. The 1990 results are shown in Figure 16 ($R^2 = 0.455$).

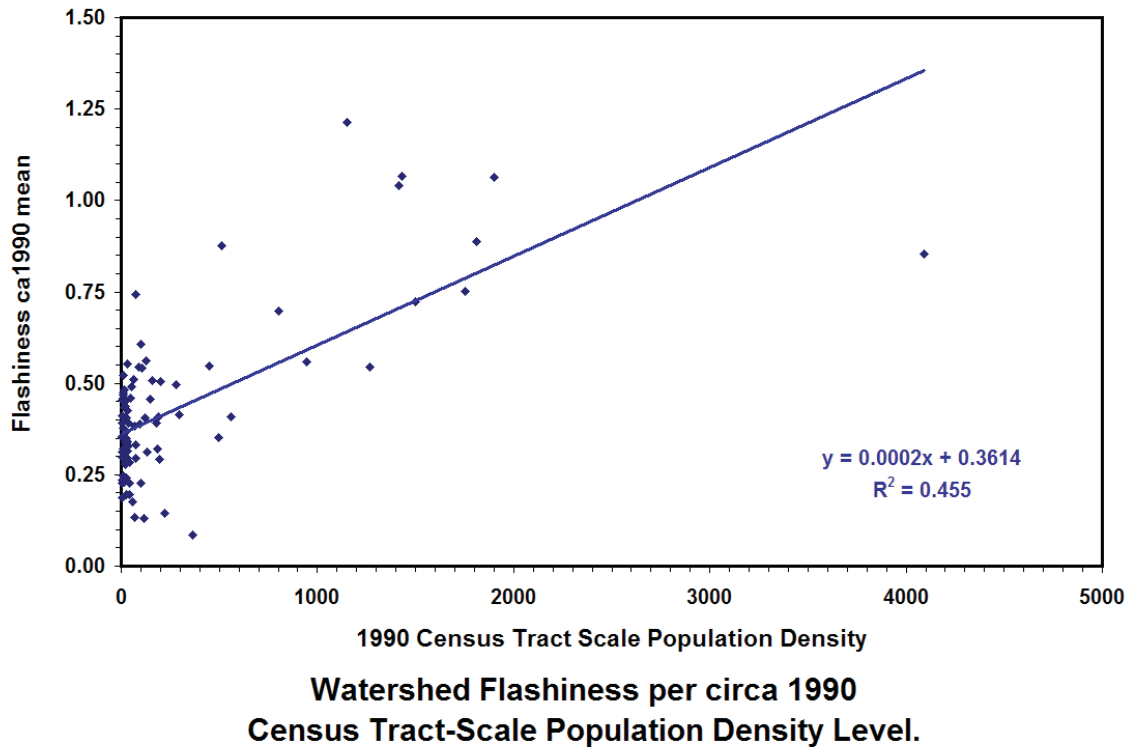


Figure 16: Mean watershed flashiness per 1990 census at the tract population density level. Mean watershed flashiness is calculated as a seven-year mean centered at the decadal census. Census population density level (people \cdot mi^2) is calculated at the census tract level, proportionally allocated to watersheds, for 1990. $N = 93$.

2000 census tract and block-group data were used to calculate population density for the 89 watersheds with 2000 flashiness values. The 2000 results are shown in Figure 17 ($R^2 = 0.634$). The relationship was essentially the same at the census tract level ($R^2 = 0.636$). Using the dasymetric LandScan data (Figure 18) only marginally improved the relationship ($R^2 = 0.647$). As was seen in Jennings and Jarnagin (2004), increasing the spatial resolution of census data does not improve correlations beyond a certain point.

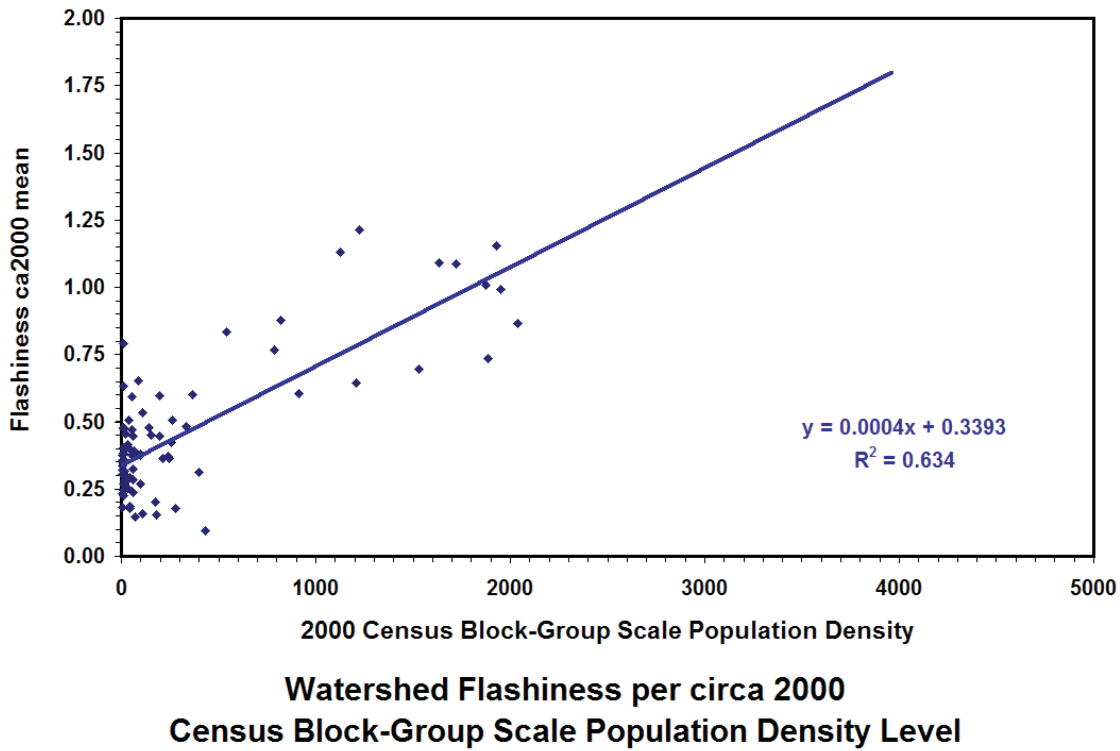
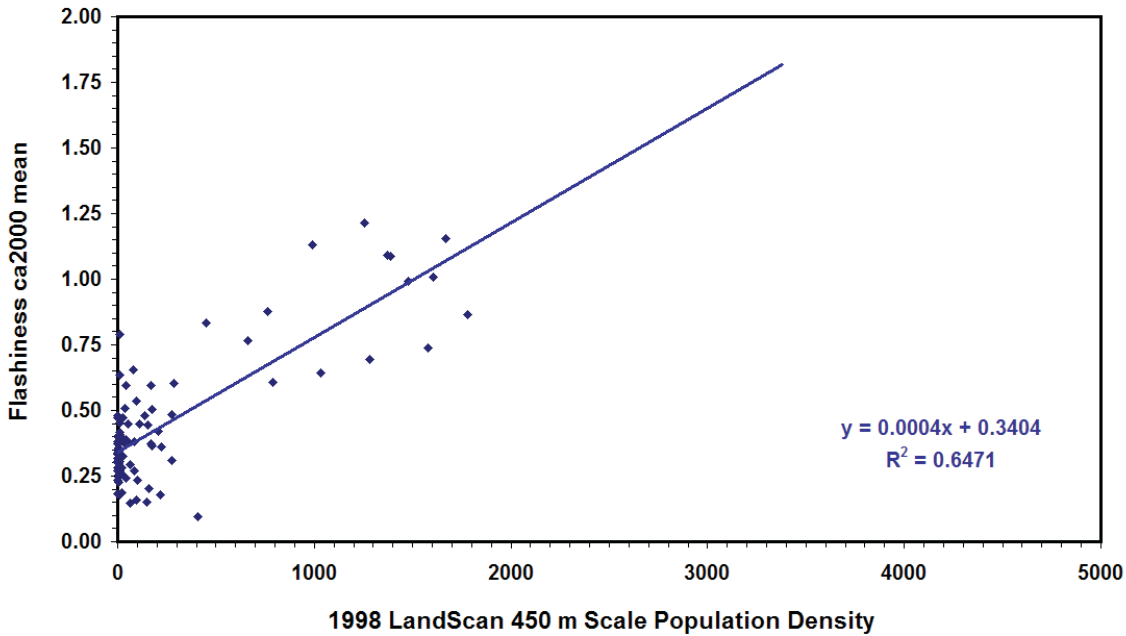


Figure 17: Mean watershed flashiness per 2000 census at the block-group population density level. Mean watershed flashiness is calculated as a seven-year mean centered at the decadal census. Census population density level (people \cdot -mi²) is calculated at the census block-group level, proportionally allocated to watersheds, for 2000. N = 89.



**Watershed Flashiness circa 2000 per
1998 LandScan 450m Scale Population Density Level.**

Figure 18: Mean watershed flashiness per 1998 LandScan population density level. Mean watershed flashiness is calculated as a seven-year mean centered at 2000. LandScan population density level (people · -mi²) is calculated at a 450 m grid cell spatial resolution, proportionally allocated to watersheds, for 2000. N = 89.

In a similar manner to the Urban Gradient based on the percentage of 'Urban' NLCD pixels in the area to be analyzed (Table 3), population density categories based on near-equal numbers and natural breaks in the data were used to look at all flashiness/density pairs based upon County-level population density estimates (n = 621). Table 8 lists these data and Figure 19 graphically presents the results of this analysis.

PopDens Group	n	Mean Flashiness	± 95% C.I.
0 - 16	99	0.386	0.024
16.001 - 30	113	0.354	0.019
30.001 - 60	110	0.361	0.029
60.001 - 150	118	0.376	0.029
150.001 - 400	96	0.533	0.054
400.001 - 3500	85	0.740	0.054

Table 8: Watershed Mean Stream Flashiness by County-Level Population Density Group. Mean watershed flashiness is calculated as a seven-year mean centered at the decadal census 1930-2000. Population density categories were based on a combination of attempting to achieve near-

equal numbers per group and utilized natural breaks in the ranked data. N = 621 flashiness/density pairs.

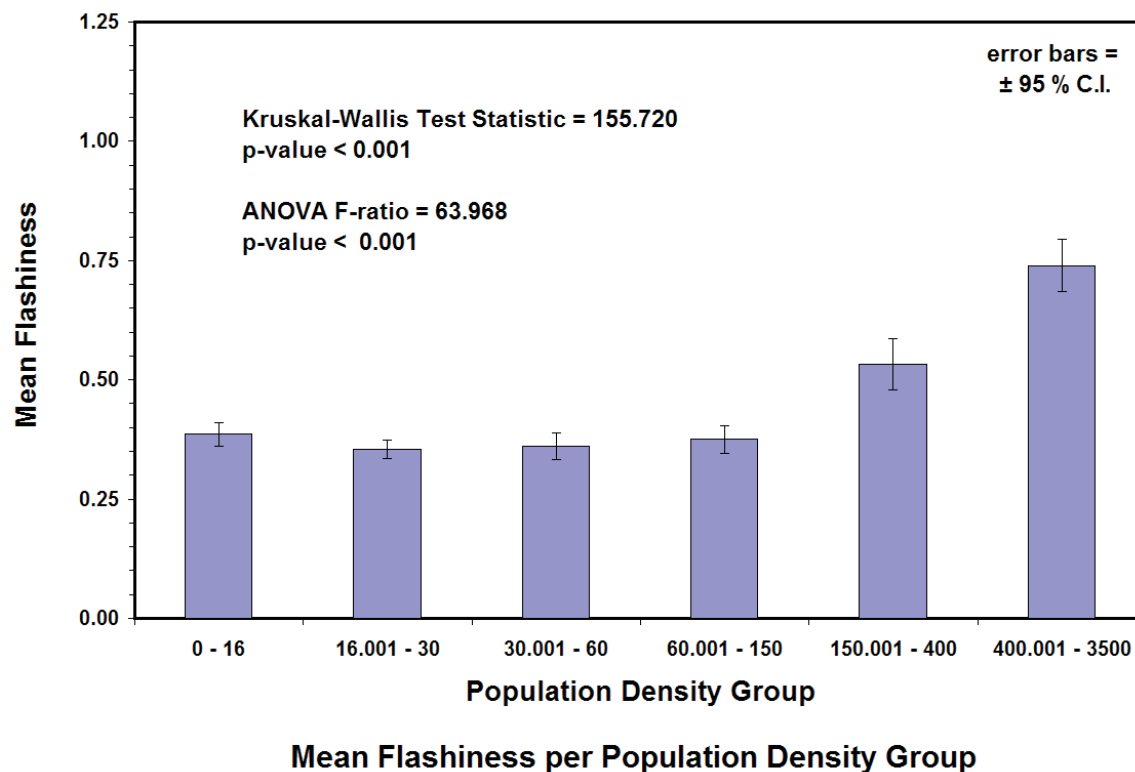


Figure 19: Watershed Mean Stream Flashiness by County-Level Population Density Group. Mean watershed flashiness is calculated as a seven-year mean centered at the decadal census 1930-2000. Population density categories were based on a combination of attempting to achieve near-equal numbers per group and utilized natural breaks in the ranked data. N = 621 flashiness/density pairs.

Both parametric (ANOVA: $F = 63.97$, $df = 5$, $p\text{-value} < 0.001$, Bonferroni Post Hoc test of flashiness) and nonparametric (Kruskal-Wallis: Test Statistic = 155.72, $p\text{-value} < 0.001$ 0.000 assuming Chi-square distribution with 5 df) statistical tests found mean stream flashiness to be significantly different among population density groups. There were no statistical differences among the population density groups until the population density exceeded 150 people \cdot mi^2 . Mean flashiness increased significantly beyond that population density.

Streamflow Flashiness and Degree of Urban Development

Mean stream flashiness values (from the seven-year data bins) for the NALC and NLCD imagery acquisition dates of 1973, 1992 and 2001 were compared to the %Urban metric derived from the satellite-based LULC data. A total of 317 independent data pairs met the data requirements and they are displayed in Figure 20 along with a linear regression through the points. The variable 'Decimal Percent Urban Watershed' accounted for more than half of the

variability in stream flashiness ($R^2 = 0.543$). The t-test on the slope of the regression line was significant (p-value < 0.001). Visually, this data set suggests that once the %Urban parameter of a watershed exceeds 20% - 25%, the stream flashiness of the system increases.

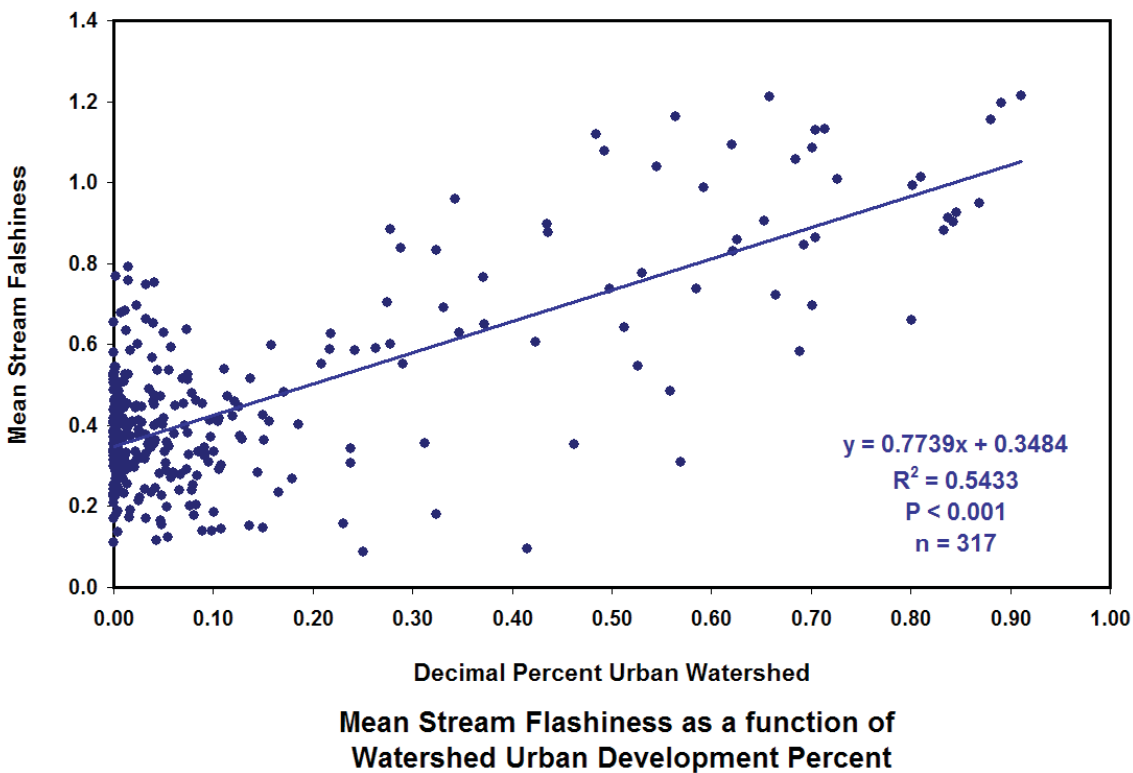
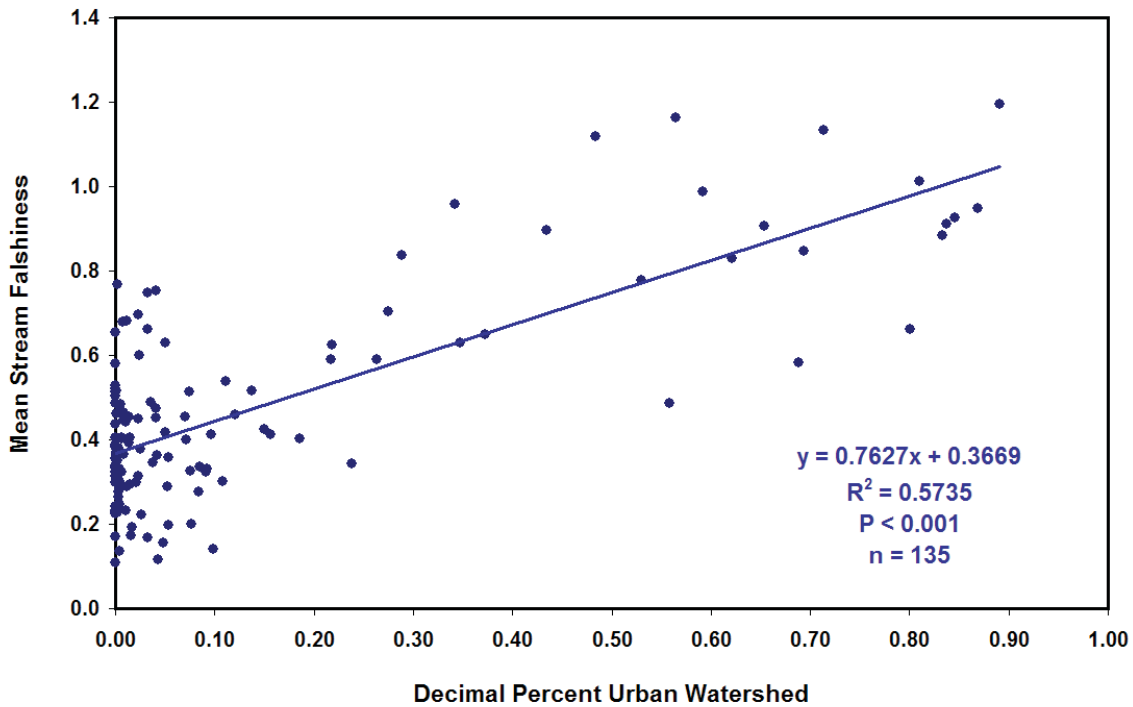


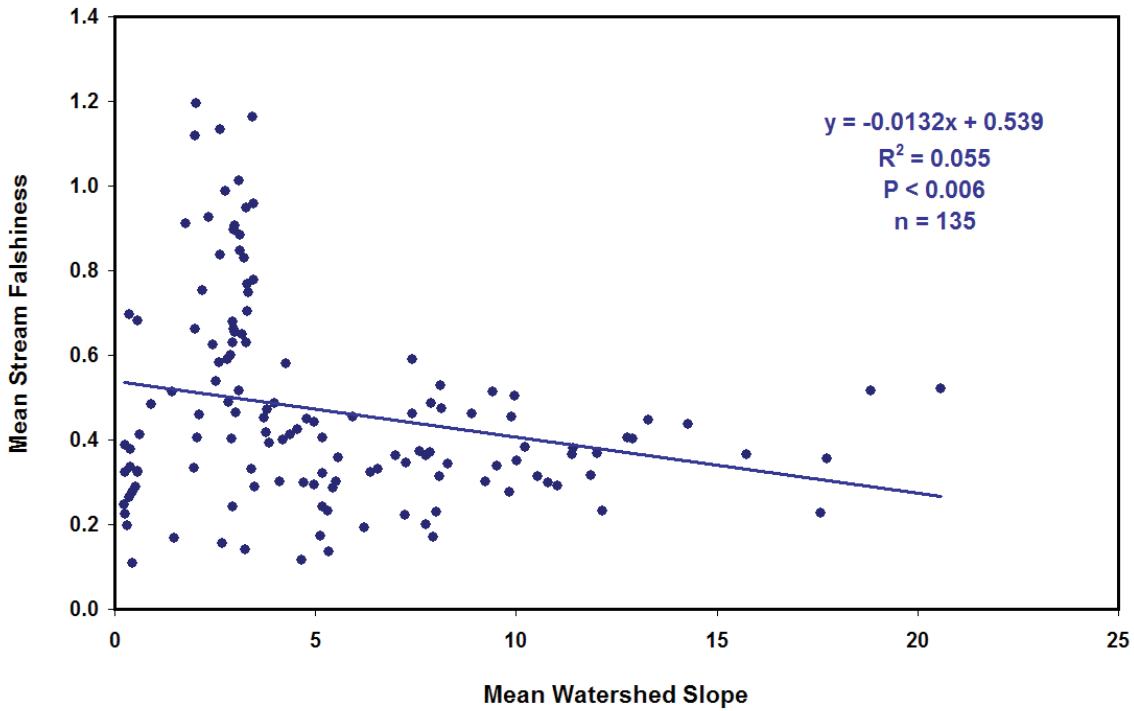
Figure 20: Mean Stream Flashiness as a function of Watershed Urban Development Percent. Stream flashiness is based on the mean of a seven-year data bin centered at the imagery acquisition dates of 1973, 1992, and 2001. The urban development percent is calculated as a decimal percent of the number of 'urban' land cover pixels in the watershed coverage divided by the total number of pixels in each watershed. $N = 317$.

Figures 21, 22, and 23 show the effect of the 1973 %Urban parameter, watershed slope, and watershed elevation (the last two parameters measured using the ATtILA ArcView extension) on the 1973 stream flashiness mean ($n = 135$). The %Urban parameter clearly is positively associated with increasing flashiness while the topographic variables of slope and elevation are not.



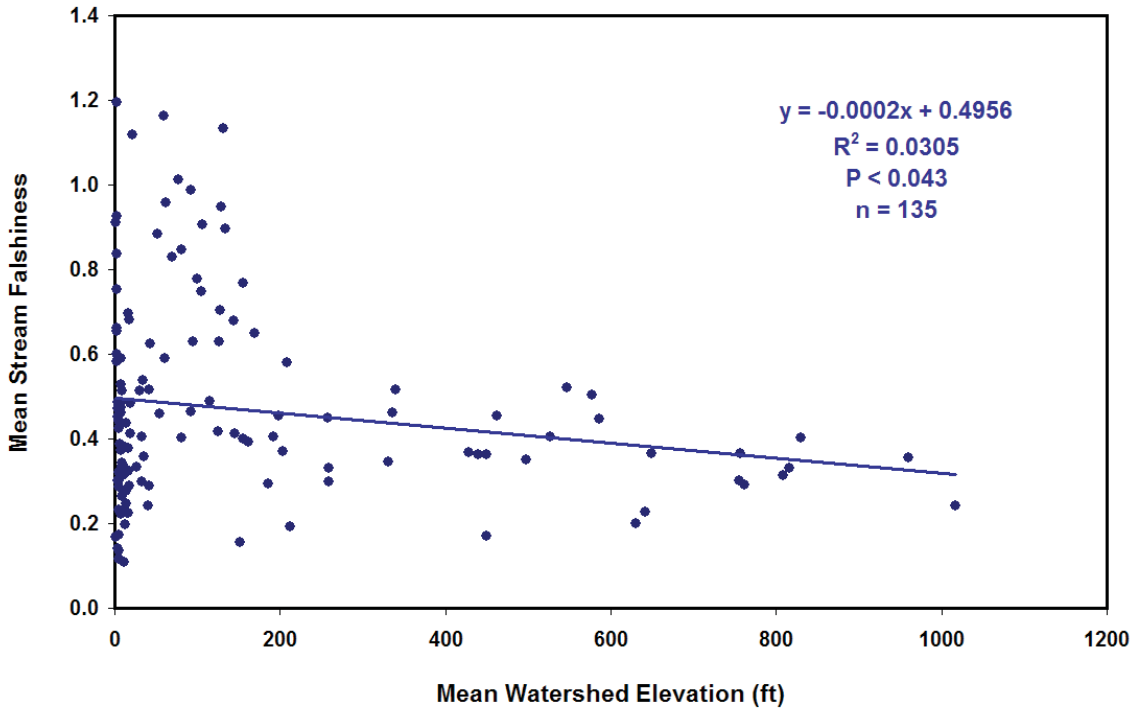
Circa 1973: Stream Flashiness vs. Percent Urban Watershed

Figure 21: Mean Stream Flashiness as a function of Watershed Urban Development Percent. Stream flashiness is based on the mean of a seven-year data bin centered at the 1973 NALC imagery acquisition date. The urban development percent is calculated as a decimal percent of the number of NALC 'urban' land cover pixels divided by the total number of pixels in each watershed. $N = 135$.



Circa 1973: Stream Flashiness vs. Mean Watershed Slope

Figure 22: Mean Stream Flashiness as a function of Watershed Slope. Stream flashiness is based on the mean of a seven-year data bin centered at the 1973 NALC imagery acquisition date. The watershed slope parameter is calculated from the 30-meter National Elevation Dataset Digital Elevation Model (NED DEM). $N = 135$.



Circa 1973: Stream Flashiness vs. Mean Watershed Elevation

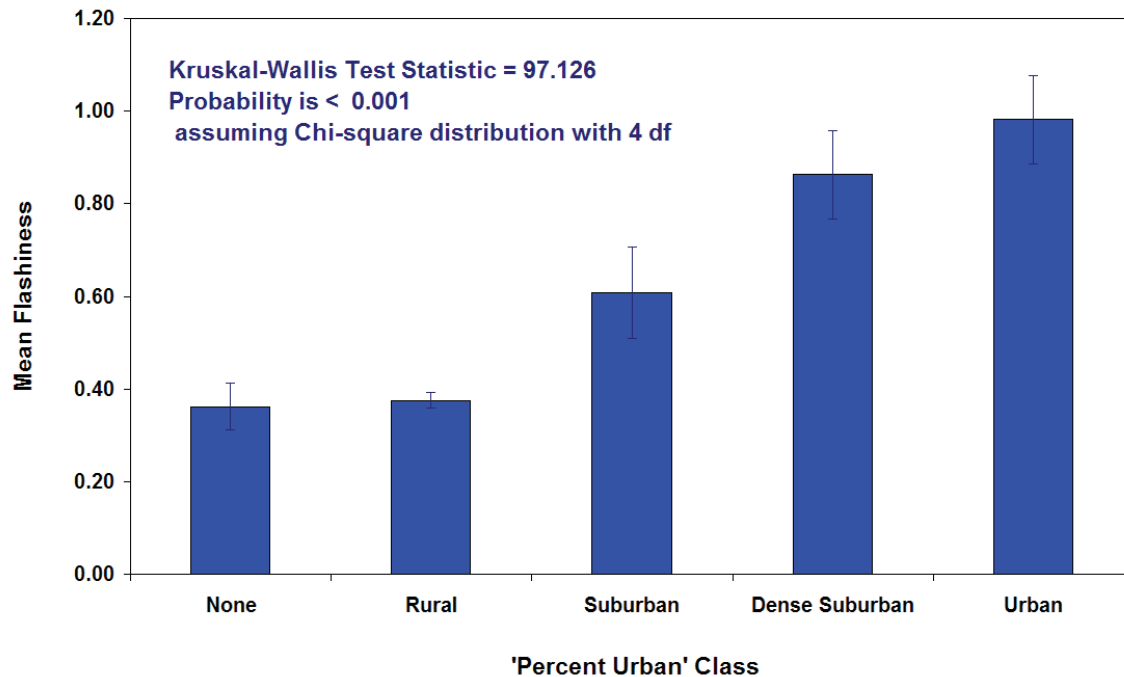
Figure 23: Mean Stream Flashiness as a function of Watershed Elevation. Stream flashiness is based on the mean of a seven-year data bin centered at the 1973 NALC imagery acquisition date. The watershed elevation parameter is calculated from the 30-meter National Elevation Dataset Digital Elevation Model (NED DEM). N = 135.

Table 9 shows the results and Figure 21 displays the same data set grouped by Urban Development Gradient based on the percentage of 'Urban' NALC/NLCD pixels in the area to be analyzed (Table 3). Due to unequal group numbers, a nonparametric Kruskal-Wallis One-Way Analysis of Variance was used to test for differences among groups.

Urban Class	Mean Flashiness	± 95 % C.I.	Definition (% 'Urban' Pixels)	n
None	0.36	0.05	none	25
Rural	0.38	0.02	0 < to < 20 %	227
Suburban	0.61	0.10	20 < to < 50 %	30
Dense Suburban	0.86	0.10	50 < to < 80 %	24
Urban	0.98	0.10	80 < to 100 %	11

Table 9: Mean Stream Flashiness of stations grouped by Urban Development Gradient class based on the percentage of 'Urban' NALC/NLCD pixels in the area to be analyzed (Table 3).

There was no difference between the mean flashiness of stations characterized by watershed %Urban less than 20% ('None' and 'Rural') while those above 20% %Urban ('Suburban', 'Dense Suburban', and 'Urban') had significantly higher mean flashiness (Kruskal-Wallis Test Statistic = 97.126; p-value < 0.001 assuming Chi-square distribution with 4 df).



Mean Flashiness by 'Percent Urban' Class

Figure 24: Mean Stream Flashiness of stations grouped by Urban Development Gradient based on the percentage of 'Urban' NALC/NLCD pixels in the area to be analyzed (Table 3). Stream flashiness is based on the mean of a seven-year data bin centered at the imagery acquisition dates of 1973, 1992, and 2001. The urban development percent is calculated as a decimal percent of the number of 'urban' land cover pixels in the watershed coverage divided by the total number of pixels in each watershed. N = 317.

Streamflow Flashiness and Imperviousness

The results for the analyses of stream flashiness compared to the 'Percent Imperviousness' (TIA%) parameter were much the same as seen with the 'Percent Urban' (&Urban) parameter. However, there were some differences seen in my various TIA% estimators that should be discussed first before we proceed to the flashiness relationships. For 1992, both the empirical coefficient-based technique of Jennings *et al.* (2004) and the ATtILA ArcView extension (Ebert and Wade, 2000; Wade and Ebert, 2004) were used to estimate 1992 watershed TIA% from the NLCD1992 land cover for the 150 study watersheds. Slonecker and Tilley (2004) found both techniques to be approximately equal in their accuracy but the empirical coefficient-based

technique tends to overestimate %TIA at very low values and underestimate TIA% at very high values (Figure 25). I feel that the ATtILA TIA% estimator is both easier to use and more robust across the entire range of potential urban development intensities and further discussion of the 1992 TIA% parameter will be limited to the ATtILA-derived estimator.

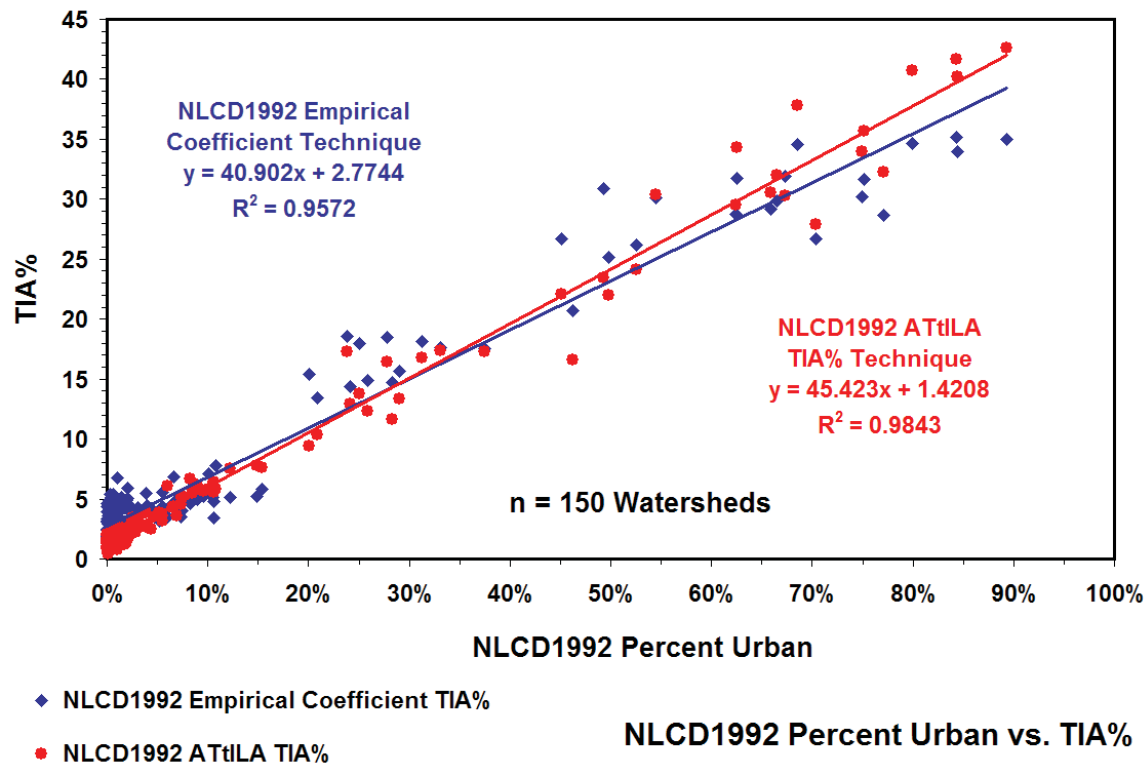
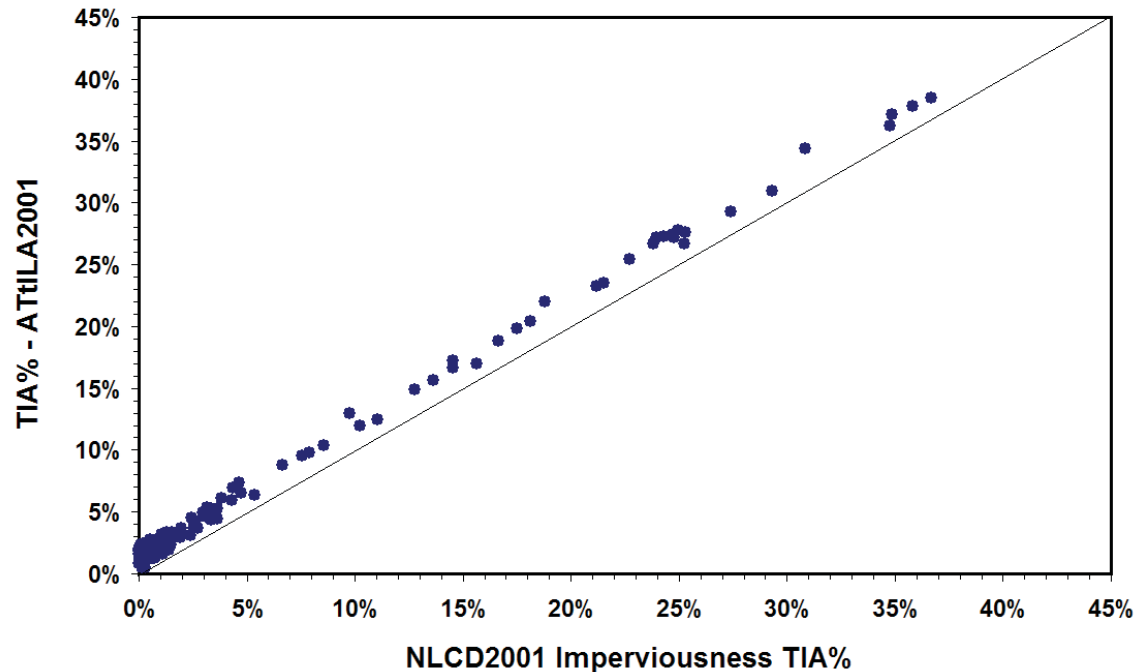


Figure 25: Comparison of 1992 'Percent Imperviousness' (TIA%) estimators. The empirical coefficient-based technique of Jennings *et al.* (2004) is compared with the ArcView ATtILA extension (Wade and Ebert, 2004) when both techniques are applied to the NLCD1992 land cover data for the 150 study watersheds. While both techniques agree well with the 'Percent Urban' (%Urban) parameter (also derived from the NLCD1992) The tendency of the empirical coefficient-based technique to overestimate %TIA at very low values and underestimate TIA% at very high values is clearly seen in this comparison.

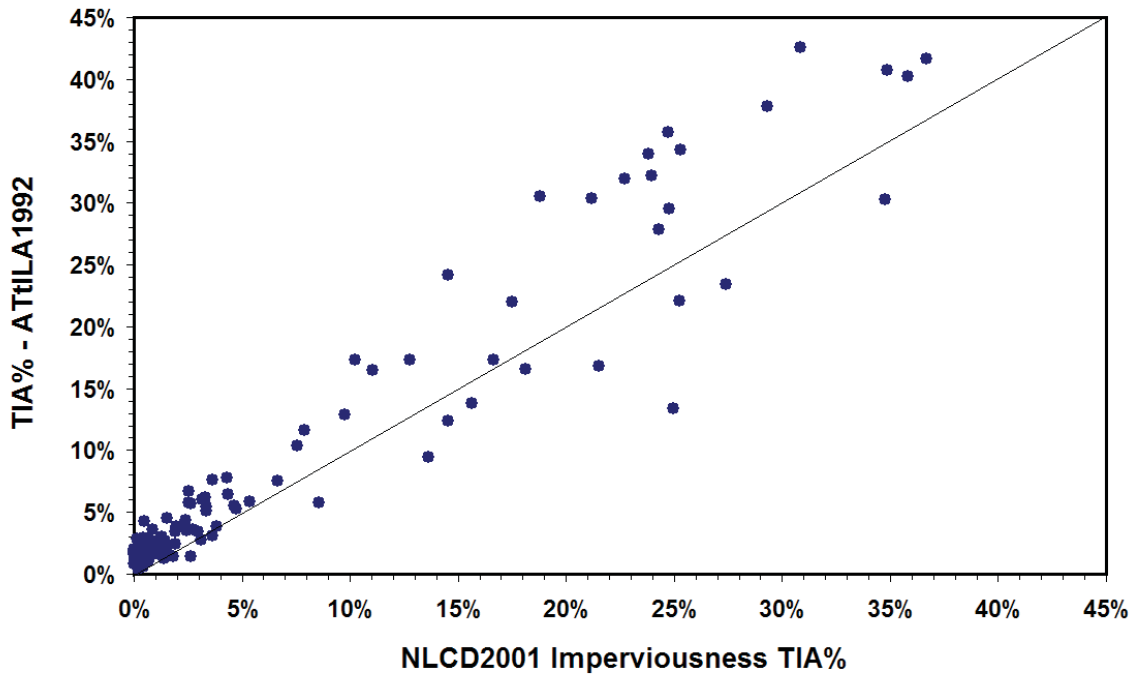
For 2001, the NLCD2001 Imperviousness data layer and the ArcView ATtILA extension were used for 2001 estimators of watershed TIA%. A detailed accuracy assessment of the NLCD2001 Imperviousness layer in the Chesapeake Bay watershed is in preparation for publication (Jones and Jarnagin, unpublished) but preliminary results (Jarnagin *et al.*, 2006) indicate that there is a systematic underestimation of TIA% by these data, at least in the Mapping Zone 60 area assessed in the Chesapeake Bay Watershed of EPA Region 3. A comparison of the ATtILA computation of TIA% based on the NLCD2001 land cover data and the TIA% derived from the NLCD2001 Imperviousness data shows a consistently higher TIA% with the ATtILA-derived TIA% parameter (Figure 26).



NLCD2001 Imperviousness TIA% vs. NLCD2001 ATtILA TIA%

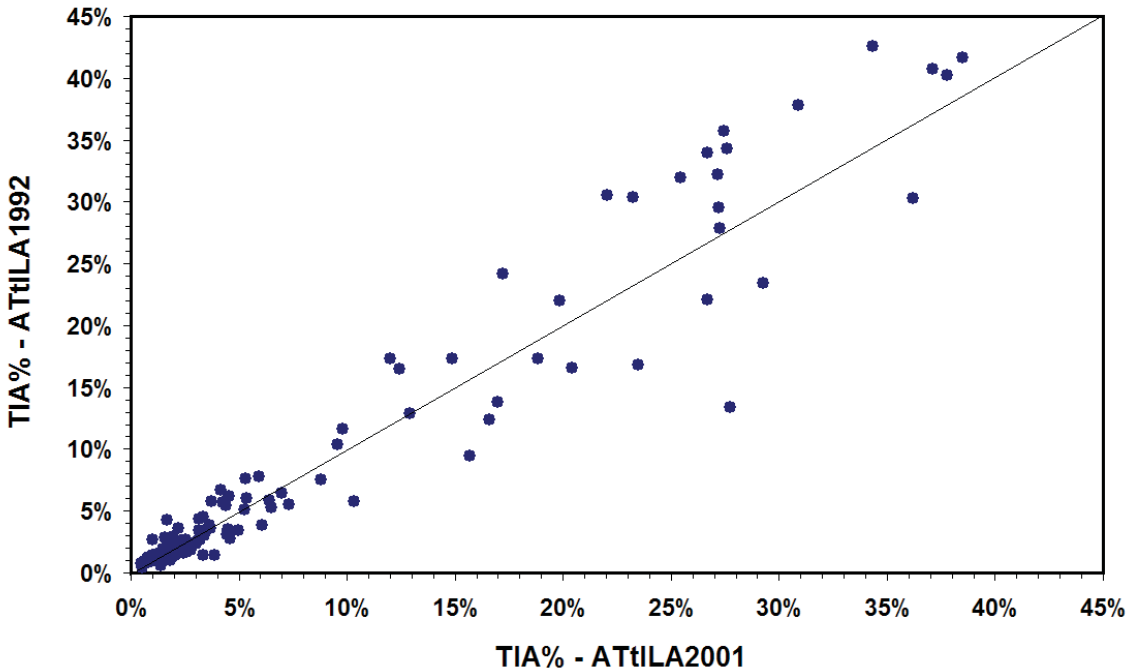
Figure 26: A comparison of the NLCD2001 Imperviousness data layer and the ATtILA ArcView extension 2001 estimator of watershed TIA% based on the NLCD2001 land cover data. The TIA% derived from the NLCD2001 Imperviousness data shows a consistently lower TIA% than the ATtILA-derived TIA% parameter. Every watershed showed a higher ATtILA estimator: mean difference = $1.67\% \pm 0.001\%$; range: 0.20% - 3.53%; $n = 150$ (absolute TIA%, not relative TIA%; confidence interval is $\pm 95\%$).

I also compared the TIA% estimated from the NLCD2001 Imperviousness data layer to the ATtILA-estimated TIA% using the NLCD1992 land cover data (Figure 27). One would expect that the TIA% estimated from the NLCD2001 Imperviousness data layer would be either equal to or greater than the 1992 TIA% based on the population growth and increase in urban development in the mid-Atlantic. However, only 10% of the study watersheds (15 out of 150) showed a higher TIA% estimate with the 2001 Imperviousness layer compared to the ATtILA-derived NLCD1992 TIA% estimate. Comparing the ATtILA-derived NLCD1992 TIA% estimate with the NLCD2001 TIA% estimate (Figure 28) showed a more believable distribution. 57.3% of the study watersheds (86 out of 150) showed higher TIA% with the ATtILA-derived estimator using the NLCD2001 compared to the NLCD1992 land cover data. I feel that the ATtILA TIA% estimator for 2001 is more accurate than the NLCD2001 Imperviousness layer for the EPA Region 3 area under consideration in this study and further discussion of the 2001 TIA% parameter with respect to watershed stream flashiness will be limited to the ATtILA-derived estimator. Further discussion of the NLCD2001 Imperviousness layer TIA% estimator and impervious surface truth data can be found in the Discussion section.



NLCD2001 Imperviousness TIA% vs. NLCD1992 ATtILA TIA%

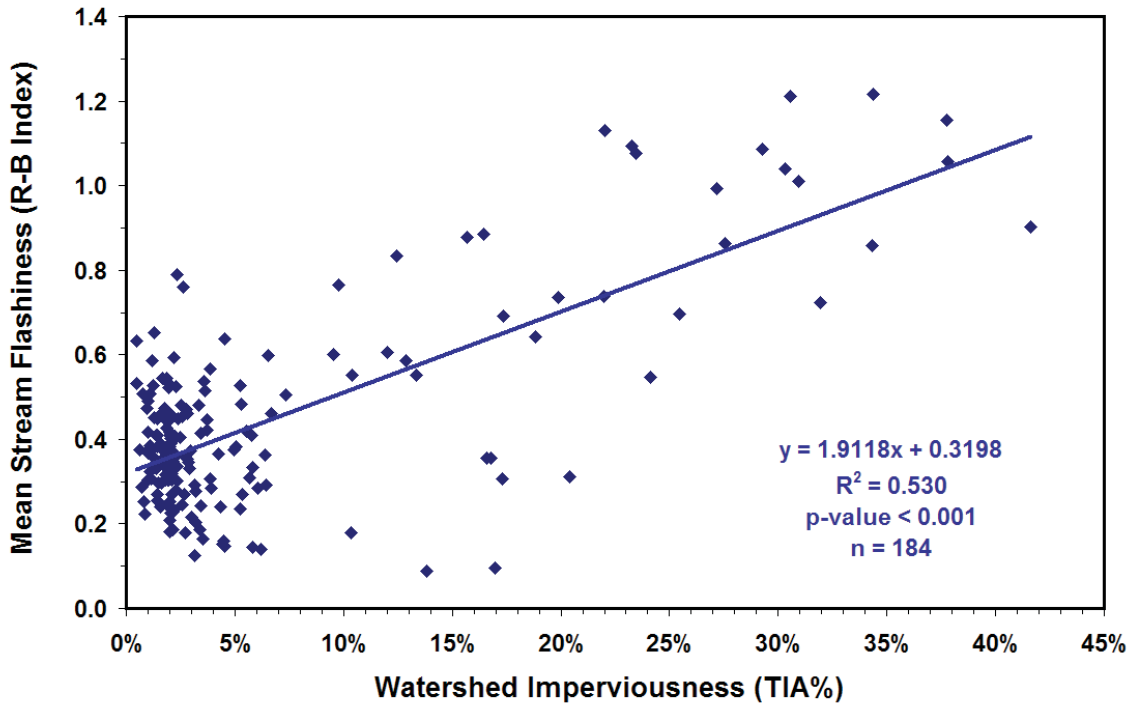
Figure 27: A comparison of the NLCD2001 Imperviousness data layer and the ATtILA ArcView extension 1992 estimator of watershed TIA% based on the NLCD1992 land cover data. The TIA% derived from the NLCD2001 Imperviousness data was higher than the ATtILA-derived TIA% parameter for 1992 in only 10% (15 out of 150 of the study watersheds).



NLCD2001 ATtILA TIA% vs. NLCD1992 ATtILA TIA%

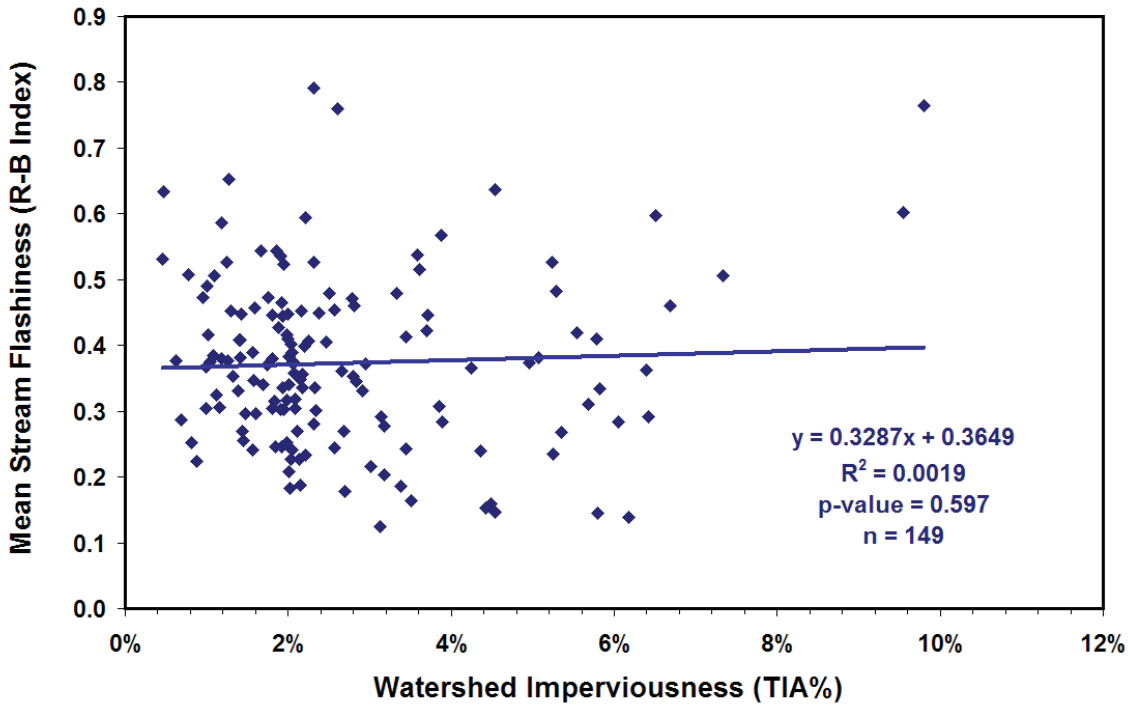
Figure 28: A comparison of the ATtILA ArcView extension 2001 estimator of watershed TIA% based on the NLCD2001 land cover data and the ATtILA ArcView extension 1992 estimator of watershed TIA% based on the NLCD1992 land cover data. The ATtILA-derived TIA% from the NLCD2001 land cover data was higher than the ATtILA-derived TIA% from the NLCD1992 land cover data in 57.3% of the study watersheds (86 out of 150 watersheds).

As in the analysis of watershed stream flashiness as a function of %Urban land cover, stream flashiness showed a clear increasing trend with increasing watershed TIA% (Figure 29, t-test on the slope: $t = 14.3$, $p\text{-value} < 0.001$, $n = 184$). Over half of the variability in stream flashiness is explained by the watershed TIA% ($R^2 = 0.530$). Support for the notion of a 10% level of TIA% without changes in hydrology is seen by the increasing data cloud above 10% TIA. Figure 30 shows the same regression on the portion of the data with TIA% less than 10%. Now, virtually none of the variability in flashiness is explained by TIA% and there is no significant monotonic trend in the data ($R^2 = 0.002$, t-test on the slope: $t = 0.53$, $p\text{-value} = 0.597$, $n = 149$).



Mean Stream Flashiness vs. Watershed Imperviousness

Figure 29: Mean Stream Flashiness as a function of Watershed 'Percent Imperviousness' (TIA%). Stream flashiness is based on the mean of a seven-year data bin centered at the NLCD 1992 imagery acquisition date and a four-year bin (1998-2001) at the NLCD 2001 imagery acquisition date. The TIA% is calculated using the ATtILA ArcView extension applied to the respective NLCD land cover data for each watershed. $N = 184$. Stream flashiness showed a clear increasing trend with increasing watershed TIA% (t-test on the slope: $t = 14.3$, $p\text{-value} < 0.001$, $n = 184$). Over half of the variability in stream flashiness ($R^2 = 0.530$) is explained by the watershed TIA%.



Mean Stream Flashiness vs. TIA% less than 10%

Figure 30: Mean Stream Flashiness as a function of Watershed 'Percent Imperviousness' (TIA%) for those watersheds with TIA% less than 10% (n = 149). Stream flashiness is based on the mean of a seven-year data bin centered at the NLCD 1992 imagery acquisition date and a four-year bin (1998-2001) at the NLCD 2001 imagery acquisition date. The TIA% is calculated using the ATtILA ArcView extension applied to the respective NLCD land cover data for each watershed. Stream flashiness shows no trend with increasing watershed TIA% (t-test on the slope: $t = 0.53$, $p\text{-value} = 0.597$). Virtually none of the variability in stream flashiness ($R^2 = 0.002$) is explained by the watershed TIA%.

My final analysis of the relationship between TIA% and stream flashiness is to sort the 184 data pairs by increasing order of TIA% and look for a combination of natural breaks and near-equality of dataset analysis bin size to see if there is a difference in mean stream flashiness based on TIA% groups. My first view is to look at watersheds with less than 10% TIA% to see if they have less mean stream flashiness than those with greater amounts of imperviousness. Table 10 shows the numbers and Figure 31 graphically displays the results of this analysis.

Percent Impervious Group	Mean Stream Flashiness	$\pm 95\%$ C.I.	n
0 < to < 10 %	0.37	0.02	149
10 to < 20%	0.52	0.12	16
20 to < 42%	0.93	0.11	19

Table 10: Mean Stream Flashiness by Percent Impervious Group (n = 3). Percent Impervious Groups formed by first sorting watersheds with TIA% less than 10% into an analysis bin and

sorting watersheds with TIA% greater than 10% into bins classified by natural breaks and an attempt to near-equalize the number of watersheds in each data bin. Flashiness means increase with increasing TIA% and are significantly different among groups: Kruskal-Wallis Test Statistic = 46.579, p-value > 0.001 assuming Chi-square distribution with 2 df.

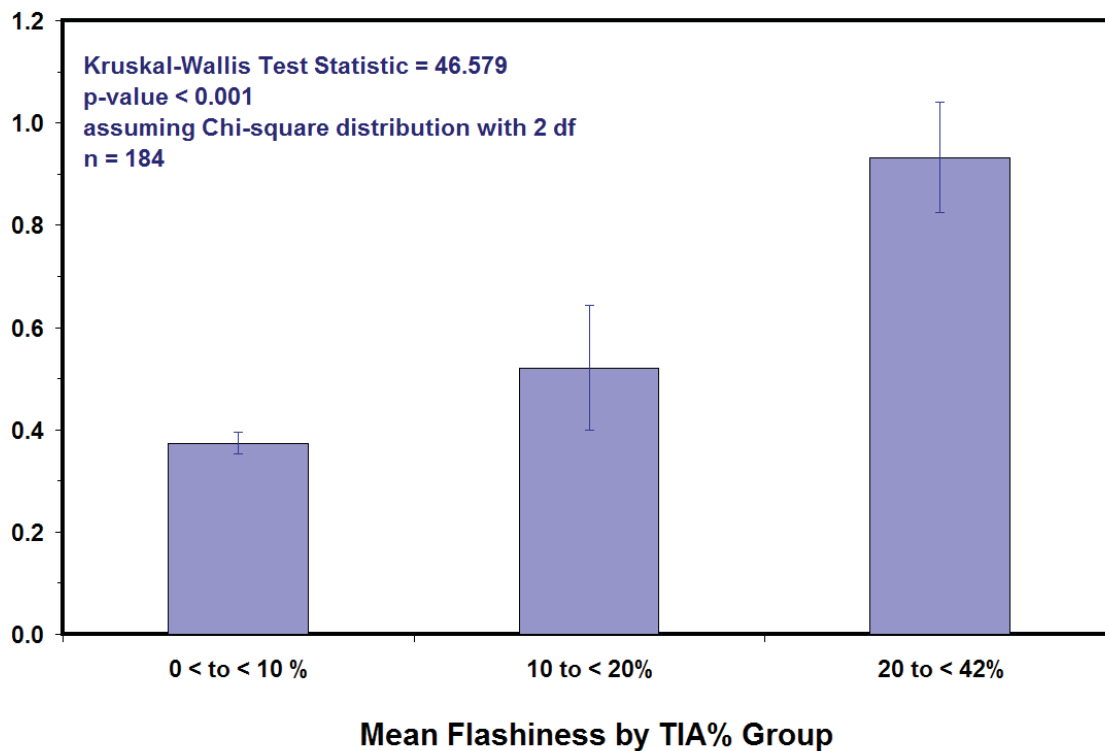


Figure 31: Mean Stream Flashiness by Percent Impervious Group (n = 3). Percent Impervious Groups formed by first sorting watersheds with TIA% less than 10% into an analysis bin and sorting watersheds with TIA% greater than 10% into bins classified by natural breaks and an attempt to near-equalize the number of watersheds in each data bin. Flashiness means increase with increasing TIA% and are significantly different among groups: Kruskal-Wallis Test Statistic = 46.579, p-value > 0.001 assuming Chi-square distribution with 2 df.

I sorted the 184 data pairs by increasing order of TIA% and used a combination of natural breaks and near-equality of dataset analysis bin size to form nine TIA% groups of near equal size. Table 11 shows the numbers and Figure 32 graphically displays the results of this analysis. Flashiness means increase with increasing TIA% beyond 10% imperviousness and are significantly different among groups: Kruskal-Wallis Test Statistic = 52.216, p-value > 0.001 assuming Chi-square distribution with 8 df. There was no significant difference between flashiness groups with TIA% less than 10%: Kruskal-Wallis Test Statistic = 7.808, p-value = 0.253 assuming Chi-square distribution with 6 df.

Percent Impervious Group	Mean Stream Flashiness	$\pm 95\%$ C.I.	n
0 < to < 1.25 %	0.41	0.05	19
1.25 < to < 1.75 %	0.39	0.05	20
1.75 < to < 2.0 %	0.38	0.04	20
2.0 < to < 2.2 %	0.33	0.03	23
2.2 < to < 2.9 %	0.41	0.06	22
2.9 < to < 4.5 %	0.32	0.05	23
4.5 < to < 10 %	0.39	0.07	22
10 to < 20%	0.52	0.12	16
20 to < 42%	0.93	0.11	19

Table 11: Mean Stream Flashiness by Percent Impervious Group (n = 9). Percent Impervious Groups formed by sorting all watersheds into TIA% group analysis bins classified by natural breaks and an attempt to near-equalize the number of watersheds in each data bin. Flashiness means increase with increasing TIA% beyond 10% imperviousness and are significantly different among groups: Kruskal-Wallis Test Statistic = 52.216, p-value > 0.001 assuming Chi-square distribution with 8 df. There was no significant difference between flashiness groups with TIA% less than 10%: Kruskal-Wallis Test Statistic = 7.808, p-value = 0.253 assuming Chi-square distribution with 6 df.

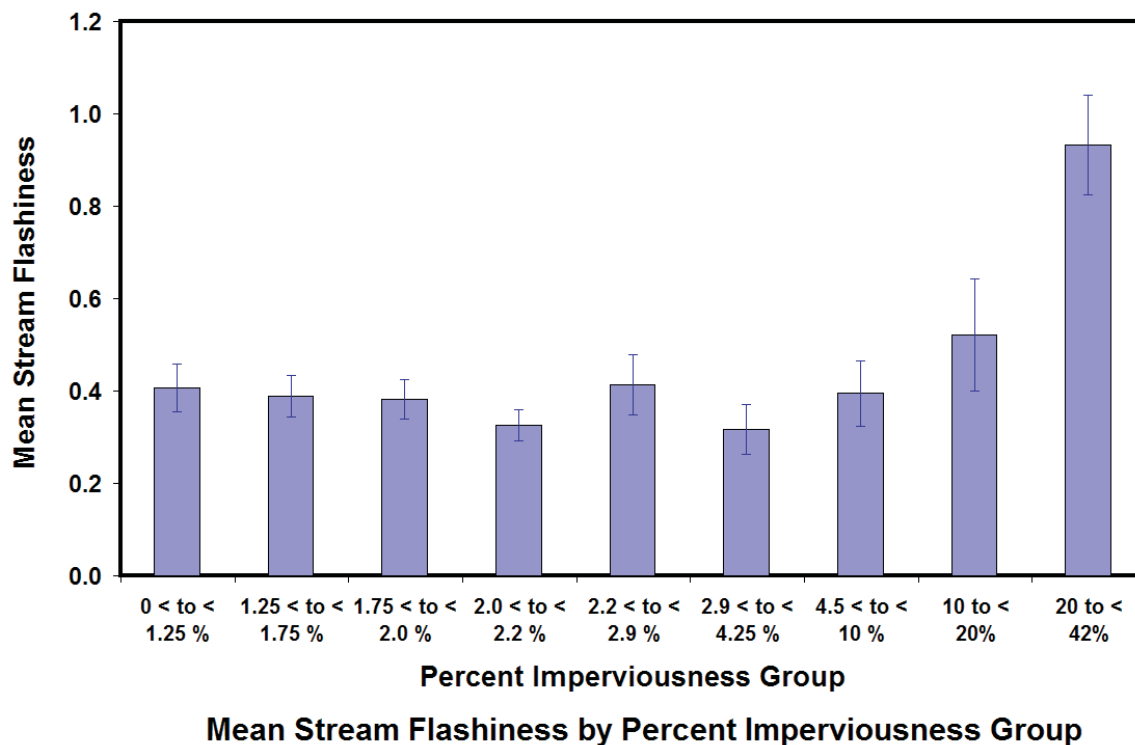


Figure 32: Mean Stream Flashiness by Percent Impervious Group (n = 9). Percent Impervious Groups formed by sorting all watersheds into TIA% group analysis bins classified by natural breaks and an attempt to near-equalize the number of watersheds in each data bin. Flashiness

means increase with increasing TIA% beyond 10% imperviousness and are significantly different among groups: Kruskal-Wallis Test Statistic = 52.216, p-value > 0.001 assuming Chi-square distribution with 8 df. There was no significant difference between flashiness groups with TIA% less than 10%: Kruskal-Wallis Test Statistic = 7.808, p-value = 0.253 assuming Chi-square distribution with 6 df.

Discussion:

My research shows that regional-scale historical analysis of the relationship between stream flashiness and the watershed parameters of population density, percent urban development, and percent imperviousness are a useful technique that yields information about the historical relationship among these variables. I have demonstrated that stream flashiness increases as a function of increasing population and development and that there historically has been a limit of around 10% watershed imperviousness or 20% watershed urban development where stream flashiness apparently has not been affected. Our results therefore support previous research that suggests low intensity development does not substantially alter streamflow. Increasing degrees of development intensity do significantly alter streamflow.

Stream Gage ID	Site Name	Analysis Year	Percent Urban	Mean Flashiness
01467048	Pennypack Creek at Lower Rhawn St Bridge, Phila.	1973	68.8%	0.5823
01467048	Pennypack Creek at Lower Rhawn St Bridge, Phila.	2000	70.1%	0.6956
01467086	Pennypack Creek at Lower Rhawn St Bridge, Phila.	1973	80.1%	0.6608
01475510	Darby Creek near Darby	1992	52.6%	0.5469
01475510	Darby Creek near Darby	1973	55.9%	0.4853
01569800	Letort Spring Run near Carlisle	2000	41.5%	0.0955
01589500	Sawmill Creek at Glen Burnie	1992	46.3%	0.3545
01589500	Sawmill Creek at Glen Burnie	2000	57.0%	0.3104

Table 12: Streamflow stations that exhibit less mean flashiness than would be expected given their level of urban development and the dates of the development/flashiness pairs.

One use of this dataset is to search for 'positive outliers' - where predicted stream flashiness is less than anticipated by the level of urban development. Detailed examination of these watersheds may yield examples where BMPs or patterns of development have been successful at mitigating the impact of urban development on stream hydrology.

Table 12 shows a listing of those stations that exhibit less mean flashiness than would be expected given their level of urban development and the dates of the development/flashiness pairs. The fact that several stations appear more than once gives credence to the notion that something different is happening in those watersheds that should be investigated. Figure 33 graphically displays these 'positive outlier' stream stations in relation to the rest of the dataset as displayed in Figure 20.

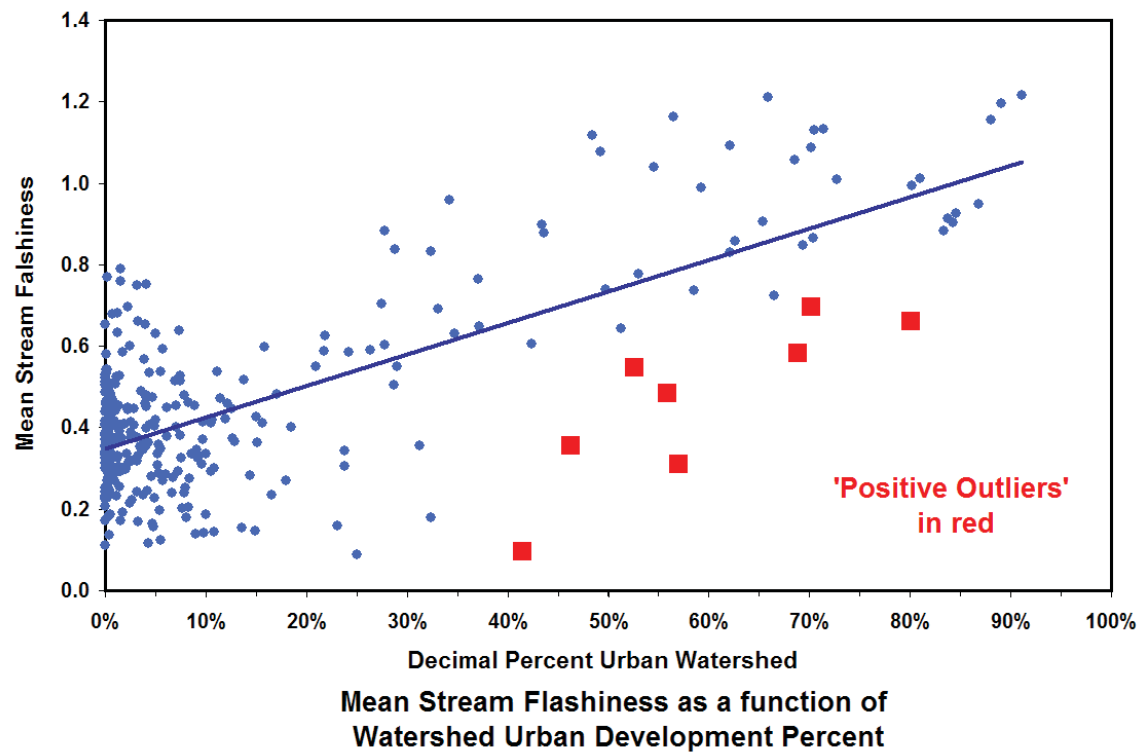
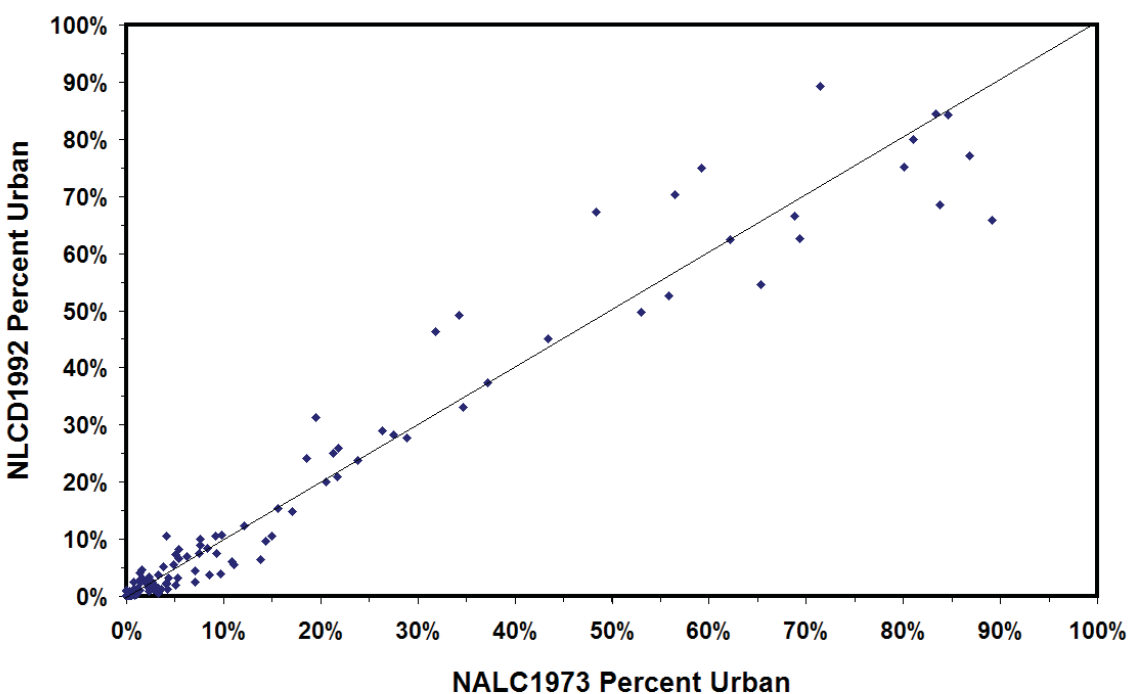


Figure 33: Mean Stream Flashiness as a function of Watershed Urban Development Percent (%Urban) showing the 'positive outliers' listed in Table 12. Stream flashiness is based on the mean of a seven-year data bin centered at the imagery acquisition dates of 1973, 1992, and 2001. The urban development percent is calculated as a decimal percent of the number of 'urban' land cover pixels in the watershed coverage divided by the total number of pixels in each watershed. Stations that are 'positive outliers' display less mean stream flashiness than would be expected given their watershed percent urban development. These flashiness/%Urban data pairs are marked in red in the lower right quadrant of the data cloud.

Identification of areas that have been able to develop without 'normal' increases in mean stream flashiness and analysis of the techniques mitigating the effects of urban development in those area is a future goal of my continuing research in the Water Quality and Ecosystem Services research areas. This study is an example of 'top-down' research where regional-scale analyses are used to identify areas for focused research. The ongoing research project "Collaborative Research: Streamflow, Urban Riparian Zones, BMPs, and Impervious Surfaces"

(Jarnagin, 2007) is an example of 'bottom-up' research aimed at the same question: how can the effects of urban development on freshwater resources be mitigated or avoided?

The NALC1973, NLCD1992, and NLCD2001 are independent products using different imagery and analysis techniques to produce their respective land cover data layers. This raises the question as to whether or not these independent estimates agree with each other. I expect that if the different land cover analyses are in fact measuring the same thing, then each watershed for a later year should show either an equal or increased amount of %Urban land cover. This assumes that once an area is 'urbanized', it does not become 'un-urbanized', at least during the time frame for this study. Figure 34 shows the 'Percent Urban' (%Urban) parameter compared between the NALC1973 and NLCD1992 land cover datasets for the 150 watersheds that had both those parameters computed. 70 out of the 150 watersheds (46.7%) showed a higher NALC1973 %Urban parameter estimate than %Urban from the NLCD1992. This is a higher percentage than what I would have expected given my above hypothesis. The NALC1973 %Urban increases over the NLCD1992 %Urban seems to be most pronounced at the highest levels of urban development.

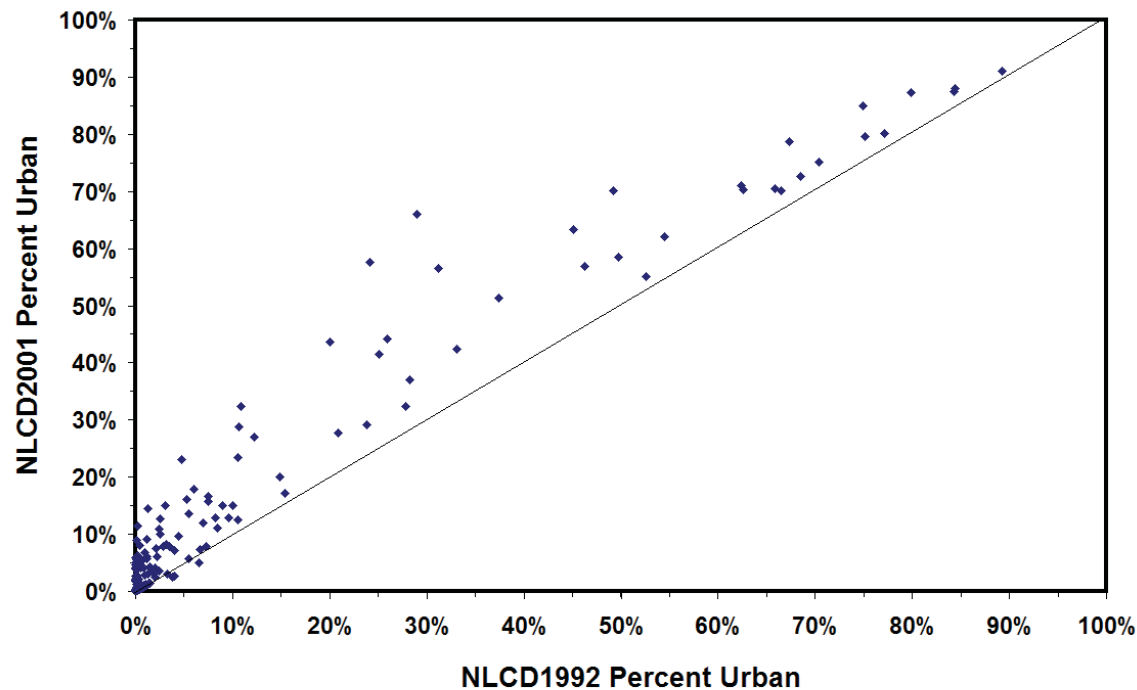


NALC 1973 vs. NLCD1992 Percent Urban

Figure 34: The 'Percent Urban' (%Urban) parameter compared between the NALC1973 and NLCD1992 land cover datasets for the 150 watersheds that had both those parameters computed. 70 out of the 150 watersheds (46.7%) showed a higher NALC1973 %Urban parameter estimate than %Urban from the NLCD1992.

In contrast, when I compared the NLCD1992 and NLCD2001 %Urban parameter estimates (Figure 35), only nine of the 143 watersheds where both parameters had been

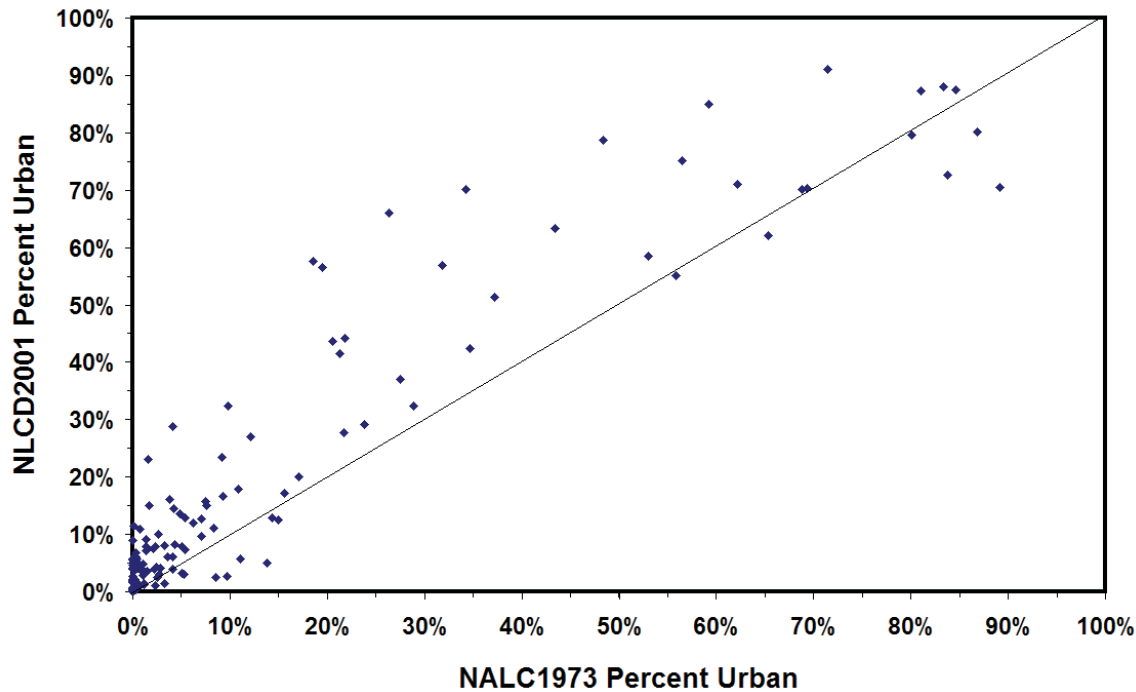
estimated showed more %Urban in 1992 than in 2001. This is comforting but the data cloud seems to reside well above the equality line in Figure 35, particularly in the middle range of the urban development scale where many watersheds are 20% or more higher in %Urban in 2001 than in 1992. This seems to me to indicate that the NLCD1992 is underestimating %Urban relative to the NLCD2001.



NLCD1992 vs. NLCD2001 Percent Urban

Figure 35: The 'Percent Urban' (%Urban) parameter compared between the NLCD1992 and NLCD2001 land cover datasets for the 143 watersheds that had both those parameters computed. Nine out of the 143 watersheds (6.3%) showed a higher NLCD1992 %Urban parameter estimate than %Urban from the NLCD2001.

Figure 36 shows the relationship between the %Urban estimators for the NALC1973 and NLCD2001. Eighteen out of the 143 watersheds where both parameters had been estimated (12.6%) showed a higher NALC1973 %Urban parameter estimate than %Urban from the NLCD2001. The pattern seen is similar to that between the NLCD1992 and NLCD2001 %Urban estimators with some watersheds in the 20% - 50% percent urban development range in 1973 showing a 40% increase in %Urban over the period.



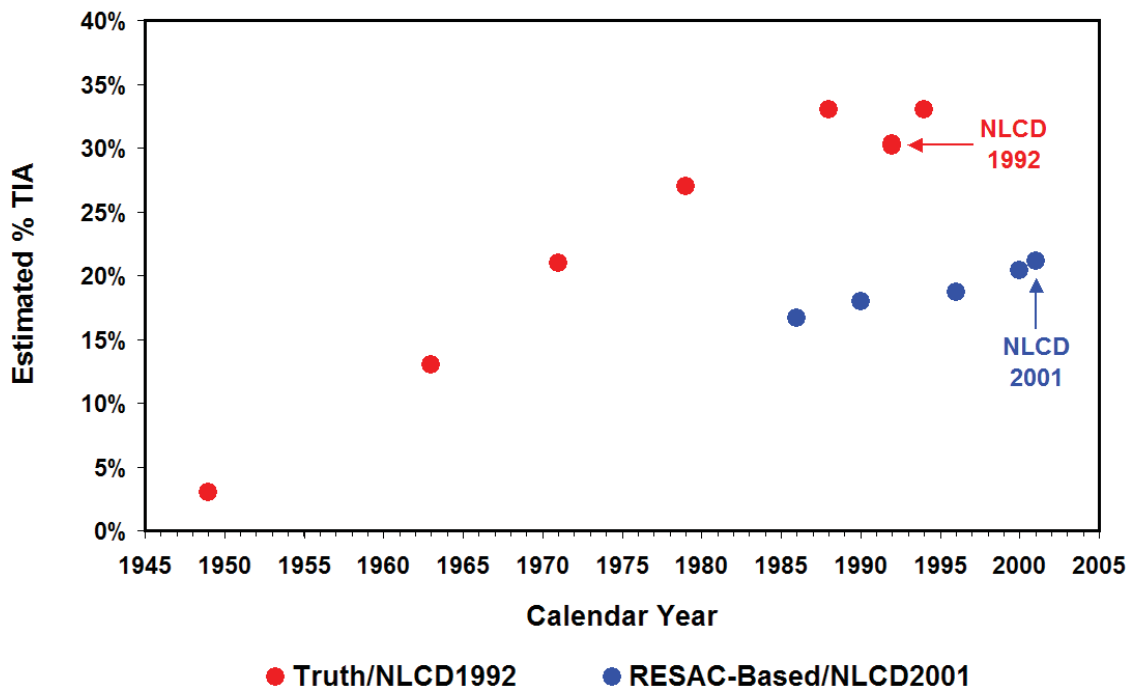
NALC1973 vs. NLCD2001 Percent Urban

Figure 36: The 'Percent Urban' (%Urban) parameter compared between the NALC1973 and NLCD2001 land cover datasets for the 143 watersheds that had both those parameters computed. Eighteen out of the 143 watersheds (12.6%) showed a higher NALC1973 %Urban parameter estimate than %Urban from the NLCD2001.

These comparisons indicate the possibility that the NLCD1992 %Urban is underestimating relative to both the NALC1973 and NLCD2001, particularly at higher degrees of urban development. These comparisons also highlight the lack of 'ground-truth'-based assessments of the accuracy of the %Urban and imperviousness parameters. The imperviousness measure is directly computed from the NLCD land cover classes for 1992 and since the imperviousness layer is used as an input into the regression tree computation of land cover class for the NLCD2001, both the NLCD land cover and imperviousness products are tightly interrelated.

More historical 'ground-truth' as developed by Jennings and Jarnagin (2002) would help to resolve these questions for prior periods and current accuracy assessment research on the NLCD2001 imperviousness layer by Jones and Jarnagin is ongoing for a portion of Mapping Zone 60 in the Chesapeake Bay watershed. I plotted the TIA% calculated for the Upper Accotink watershed used by Jennings and Jarnagin (2002). When the TIA% computed by the NLCD Coefficient Technique is added to the data series, that estimate seems to fit well with the truth dataset (Figure 37). The Regional Earth Science Applications Center (RESAC) at the University of Maryland, College Park developed an imperviousness estimation technique using sub-pixel classification techniques and decision tree algorithms to estimate imperviousness and land cover in the Chesapeake Bay. The RESAC methodology was adopted by the NLCD2001

(Goetz *et al.*, 2000; Mid-Atlantic RESAC, 2003). When the RESAC and the NLCD2001 %TIA estimates for the Upper Accotink watershed are added to Figure 37, they form an estimation trend line that is roughly 10-15% less than that formed by the ground-truth and NLCD1992.



Tia% Estimates for Upper Accotink Watershed

Figure 37: Watershed percent imperviousness (TIA%) from Jennings and Jarnagin (2002) for the Upper Accotink are plotted in red along with the Coefficient-based estimation derived from the NLCD1992 (Jennings *et al.*, 2004). The Mid-Atlantic RESAC TIA% values and the NLCD2001 Imperviousness Layer estimates for the Upper Accotink watershed are plotted in blue.

James Falcone, USGS Water Resources Discipline (WRD), has unpublished data for the Chesapeake Bay that showed a similar underestimation of imperviousness for a set of 60 sample blocks in Mapping Zone 60. His data showed a 'ground-truth' actual imperviousness of 48% over all blocks while the NLCD2001 imperviousness layer showed 28% (RMSE = 22.09). These results were also found to a lesser degree using the same technique in Mapping Zones 54 and 59 (Atlanta, GA and Raleigh, NC areas) with both sample block datasets being about 10-15% mean difference underestimated in those areas while the Portland OR area was less than 1% mean difference underestimated using the NLCD2001 imperviousness product (Falcone and Pearson, 2006). Jarnagin *et al.* (2006) preliminary results reported a systematic underestimation of impervious surfaces by the NLCD 2001 Imperviousness data across our entire range of urban development intensity categories. Clearly, accuracy assessment of the NLCD2001 Imperviousness and Land Cover data layers is a needed activity.

I look forward to a NLCD2010 product and the opportunity to expand this study using future data. Whether this study can be replicated at a regional-scale is an open question given the continuing disinvestment in basic scientific research and data collection occurring in the USA in recent years. Figure 38 is a plot of the number of USGS NWIS historical daily mean streamflow stations per year meeting my 'long-term' requirements for this study. The most stations per year was in the 1960s and 70s at about 125-130 gage stations operating per year. The number of USGS NWIS gage stations has been steadily declining in recent years and the USGS continues to close gage locations due to funding reductions.

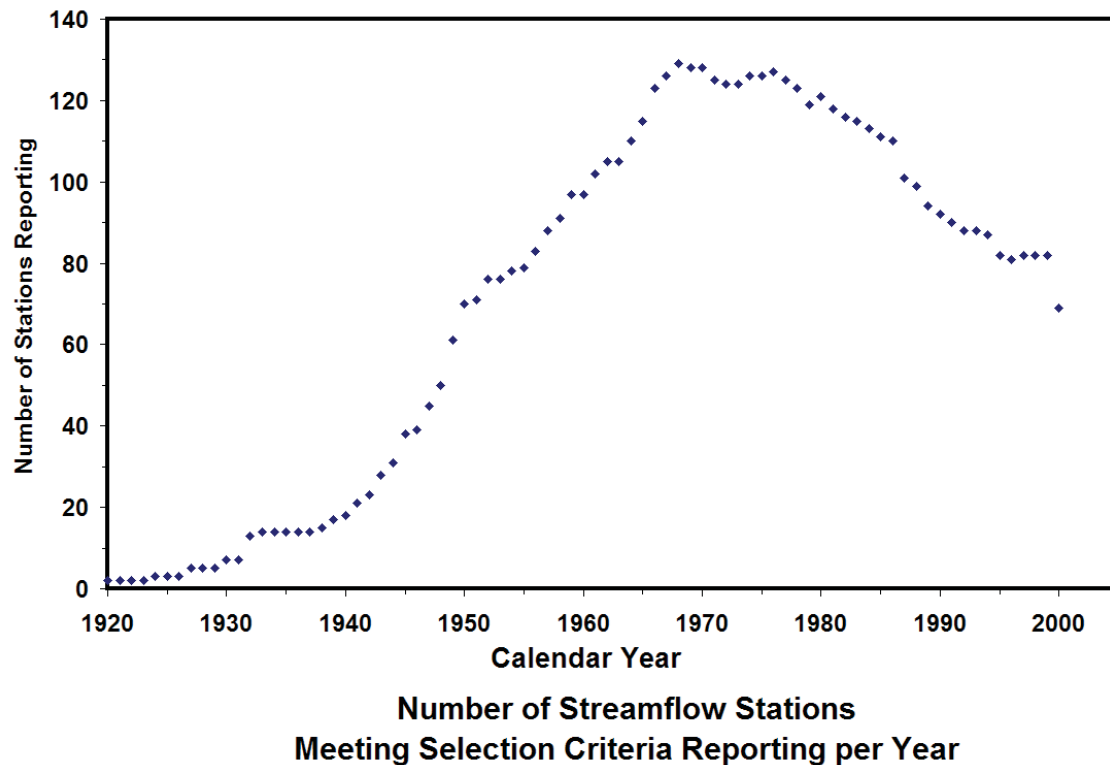


Figure 38: A plot of the number of USGS National Water Information System (NWIS) historical daily mean streamflow stations per year meeting my 'long-term' requirements for this study. The number has been steadily declining in recent years and the USGS continues to close gage locations due to funding reductions. Time will tell.

References:

- Arnold Jr., C. L. and C. J. Gibbons. 1996. Impervious surface coverage: The emergence of a key environmental indicator. *Journal of the American Planning Association* 62(2): 243-258.
- Baker, D. B., R. P. Richards, T. T. Loftus, and J. K. Kramer. 2004. A New Flashiness Index: Characteristics and Applications to Midwestern Rivers and Streams *Journal of the American Water Resources Association* 40(2): 503-522.
- Booth, D. B. 1990. Stream channel incision following drainage-basin urbanization. *Water Resources Bulletin*, 26(3): 407-417.
- Caraco, D., R. Claytor, P. Hinkel, H. Y. Kwon, T. Schueler, C. Swann, S. Vysotsky, and, J Zielinske. 1998. *Rapid Watershed Planning Handbook*. Center for Watershed Protection. Ellicott City, Maryland.
- CWP (Center for Watershed Protection). 2003. *Impacts of Impervious Cover on Aquatic Systems*, Center for Watershed Protection, Ellicott City, MD. 142 p.
- Ebert, D. W., and T. G. Wade. 2000. *Analytical Tools Interface for Landscape Assessments (ATtILA) User Guide: Version 2.0*. Office of Research and Development. U.S. Environmental Protection Agency. Las Vegas, NV. 23 p.
- Edmonds, C. M., D. T. Heggem, and K. B. Jones. 2002. *Mid-Atlantic Region Land Use/Land Cover Data Set 1970s to 1990s*. U.S. Environmental Protection Agency (EPA), Office of Research and Development (ORD), National Exposure Research Laboratory (NERL), Environmental Sciences Division (ESD), Landscape Ecology Branch (LEB), Las Vegas, NV. EPA/600/R-02/035.
- ESRI. 2003. *Data 2003 disks: ESRI Data - 2000 data*. Environmental Systems Research Institute, Inc., Redlands, CA. < http://www.esri.com/data/community_data/census/index.html >
- Falcone, J. A. and D. K. Pearson. 2006. *Land-cover and imperviousness data for regional areas near Denver, Colorado; Dallas-Fort Worth, Texas; and Milwaukee-Green Bay, Wisconsin-2001*: U.S. Geological Survey Data Series 221, 17 p. < <http://pubs.usgs.gov/ds/2006/221/> >.
- GeoLytics. 2003. *CensusCD 1970,1980,1990*. GeoLytics, Inc. East Brunswick, NJ. < <http://www.geolytics.com/USCensus,Census-1970-1980-1990,Categories.asp> >.
- Goetz, S. J., S. D. Prince, M. M. Thawley, A. J. Smith, and R. Wright. 2000. *The Mid-Atlantic Regional Earth Science Applications Center (RESAC): an overview*. Available at www.geog.umd.edu/resac and on ASPRS CD-ROM in American Society for Photogrammetry and Remote Sensing (ASPRS) Conference Proceedings, Washington DC.

Homer, C., C. Huang, L. Yang, B. Wylie, and M. Coan. 2004. Development of a 2001 National Landcover Database for the United States. *Photogrammetric Engineering and Remote Sensing* 70(7): 829-840.

Jarnagin, S. T. 2004. Regional and Global Patterns of Population, Land Use, and Land Cover Change: An Overview of Stressors and Impacts. *GIScience & Remote Sensing* 41(3): 207-227.

Jarnagin, S. T., D. B. Jennings, and D. W. Ebert. 2004. A Technique for Assessing the Accuracy of Sub-Pixel Estimates Extracted from Landsat TM Imagery. pp. 269-280 In: Lunetta, R. S., and J. G. Lyon (Editors). *Remote Sensing and GIS Accuracy Assessment*. CRC Press, Boca Raton, FL (320 p.).

Jarnagin, S. T., J. W. Jones, & S. G. Winters. 2006. Accuracy Assessment of the National Land Cover Database 2001 (NLCD2001) Imperviousness Data. Poster presentation at the EPA Science Forum 2006: Your Health, Your Environment, Your Future: Envisioning the Future. Washington DC. (5/06). Link to abstract: < http://www.epa.gov/scienceforum/2006/poster_abstracts/built_environment/BE_Jarnagin.pdf >. Link to poster: < http://www.epa.gov/ord/scienceforum/2006/pdfs/the_built_environment_final_posters/BE-17_Jarnagin.pdf >.

Jarnagin, S. T. 2007. Collaborative Research: Streamflow, Urban Riparian Zones, BMPs, and Impervious Surfaces. United States Environmental Protection Agency, Office of Research and Development, Environmental Photographic Interpretation Center, Reston, VA. < <http://www.epa.gov/esd/land-sci/epic/clarksburg01-05.htm> >.

Jennings, D. B. and S. T. Jarnagin. 2002. Changes in anthropogenic impervious surfaces, precipitation and daily streamflow discharge: a historical perspective in a mid-Atlantic subwatershed. *Landscape Ecology* 17(5): 471-489.

Jennings, D. B., S. T. Jarnagin, and D. W. Ebert. 2004. A modeling approach for estimating watershed impervious surface area from National Land Cover Data 92. *Photogrammetric Engineering & Remote Sensing* 70(11): 1295-1307.

Jennings, D. and S. T. Jarnagin. 2004. The derivation of impervious surface area from population and remotely sensed data and the application to projections of population growth in the Baltimore-Washington region. United States Environmental Protection Agency, Office of Research and Development, Washington, D.C., September 2004, EPA/600/X-04/111, 42p.

Jones, J. W., P. Claggett, S. T. Jarnagin, and D. B. Jennings. 2003. Shared assessment of USGS and NGO impervious surface datasets for the Chesapeake Bay Watershed. USGS funded PROSPECTUS PROPOSAL: 32p.

LandScan. 2003. LandScan 1998 - 450m intermediate LandScan product for conterminous USA. Oak Ridge National Laboratory, Oak Ridge TN. < <http://www.ornl.gov/sci/landscan/index.html> >.

Leopold, L. B. 1973. River channel change with time: an example. Geological Society of America Bulletin, 84(6): 1845-1860.

Mid-Atlantic RESAC. 2003. Land Cover Mapping of the Chesapeake Bay Watershed. Department of Geography, University of Maryland, College Park. College Park, MD. < <http://www.geog.umd.edu/resac/lc2.html> >.

National Climatic Data Center (NCDC). 1998. Cooperative Summary of the Day. TD3200. Web site: < <http://www4.ncdc.noaa.gov/cgi-win/wwcgi.dll?wwDI~StnSrch~StnID~20027267> >.

National Land Cover Dataset 1992 (NLCD1992): < <http://landcover.usgs.gov/natl/landcover.php> >

National Land Cover Dataset 2001 (NLCD2001): < http://www.mrlc.gov/mrlc2k_nlcd.asp >

Olden, J. D. and N. L. Poff. 2003. Redundancy and the choice of hydrologic indices for characterizing streamflow regimes. River Research and Applications 19(2): 101-121.

Sala, O. E., F. S. Chapin III, J. J. Armesto, E. Berlow, J. Bloomfield, R. Dirzo, E. Huber-Sanwald, L. F. Huenneke, R. B. Jackson, A. Kinzig, R. Leemans, D. M. Lodge, H. A. Mooney, M. Oesterheld, N. L. Poff, M. T. Sykes, B. H. Walker, M. Walker, and D. H. Wall. 2000. Global biodiversity scenarios for the year 2100. Science 287(5459): 1770-1774.

Schueler, T. 1994. The importance of imperviousness. Watershed Protection Techniques 1(3): 100-111.

Slonecker, E. T. and J. S. Tilley. 2004. An evaluation of the individual components and accuracies associated with the determination of impervious area. GIScience and Remote Sensing 41(2): 165-184.

University of Virginia Library Historical Census Browser (UVA). 2004. Historical Census Browser. Retrieved June 2006, from the University of Virginia, Geospatial and Statistical Data Center: < <http://fisher.lib.virginia.edu/collections/stats/histcensus/index.html> >.

U.S. Census. 2004. State and County QuickFacts browser. Department of Commerce, U.S. Census Bureau, Washington DC. < <http://quickfacts.census.gov/qfd/> >.

U.S. Environmental Protection Agency (USEPA). 1994. The quality of our nation's water: 1992. EPA/841/S/94/002. U.S. Environmental Protection Agency, Office of Water, Washington D.C.

U.S. Environmental Protection Agency (USEPA). 2006. National Land Cover Data (NLCD)/MRLC/US EPA. Multi-Resolution Land Characteristics Consortium (MRLC), U.S. Environmental Protection Agency (EPA), Office of Research and Development (ORD), National

Exposure Research Laboratory (NERL), Environmental Sciences Division (ESD), Landscape Ecology Branch (LEB),
RTP, NC. < <http://www.epa.gov/mrlc/nlcd.html> >.

USGS National Elevation Dataset (NED). 2002. National Elevation Dataset, U.S. Geological Survey, EROS Data Center, Sioux Falls, SD. < <http://ned.usgs.gov/> >.

USGS National Water Information System (NWIS). 2006. Water resources of the United States, National Water Information System NWISWeb Water Data, USGS Surface-Water Daily Data for the Nation, U.S. Geological Survey, Water Resources Discipline, Reston VA. < http://waterdata.usgs.gov/nwis/dv/?referred_module=sw >.

Vogelmann, J. E., S. M. Howard, L. Yang, C. R. Larson, B. K. Wylie, and N. Van Driel. 2000. Completion of the 1990s National Land Cover Dataset for the Conterminous United States from Landsat Thematic Mapper Data and Ancillary Data Sources. *Photogrammetric Engineering and Remote Sensing* 67(6): 650-661.

Wade, T. G. and D. W. Ebert. 2004. Analytical Tools Interface for Landscape Assessments (ATtILA). U.S. Environmental Protection Agency (EPA), Office of Research and Development (ORD), National Exposure Research Laboratory (NERL), Environmental Sciences Division (ESD), Landscape Ecology Branch (LEB), Las Vegas, NV. EPA/600/R-04/083. < <http://www.epa.gov/nerlesd1/land-sci/attila/index.htm> >.

Wilson, E. O. 2002. *The future of life*. Alfred A. Knopf, New York NY. 229 pp.

Appendix 1: County-Level Decadal Population Density for EPA Region 3.

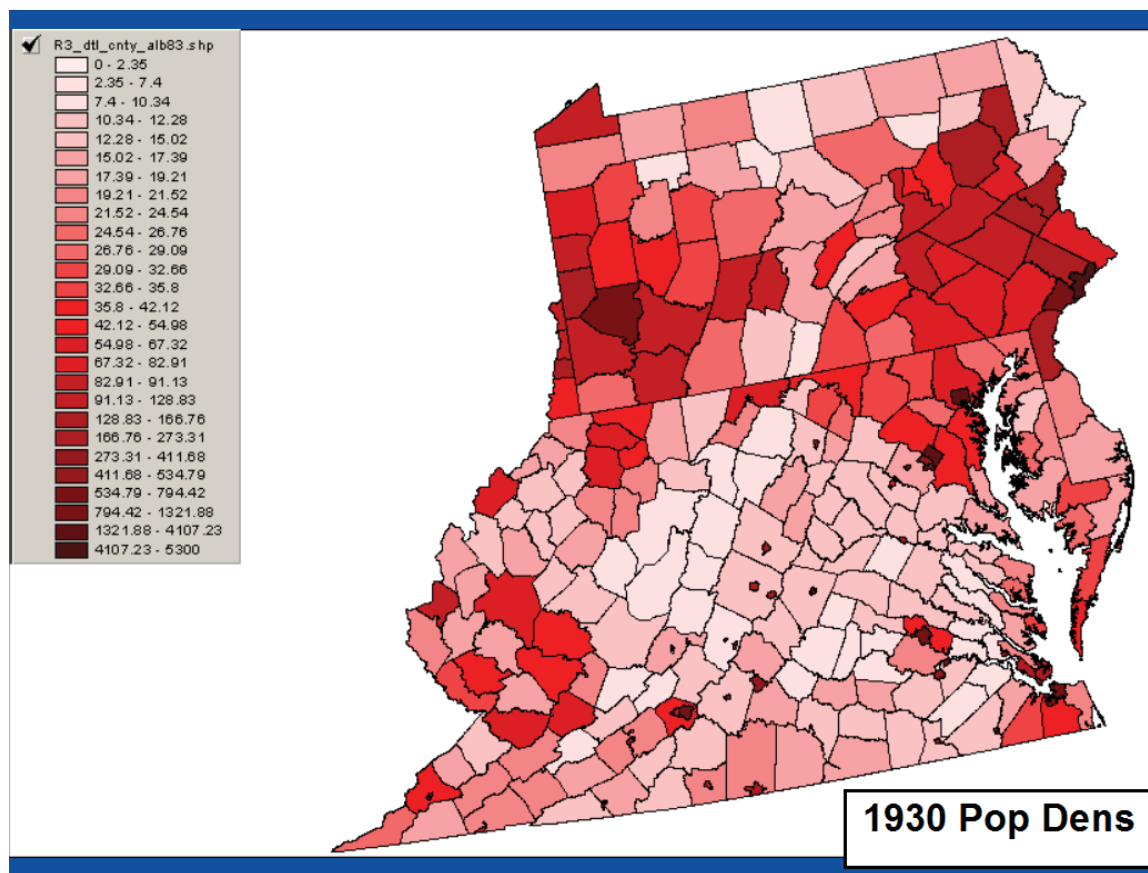


Figure A1: 1930 Population Density (people·km⁻¹). From 1930 - 2000 U.S. Census data for EPA Region 3: Delaware, District of Columbia, Maryland, Pennsylvania, Virginia, and West Virginia.

Appendix 1: County-Level Decadal Population Density for EPA Region 3.

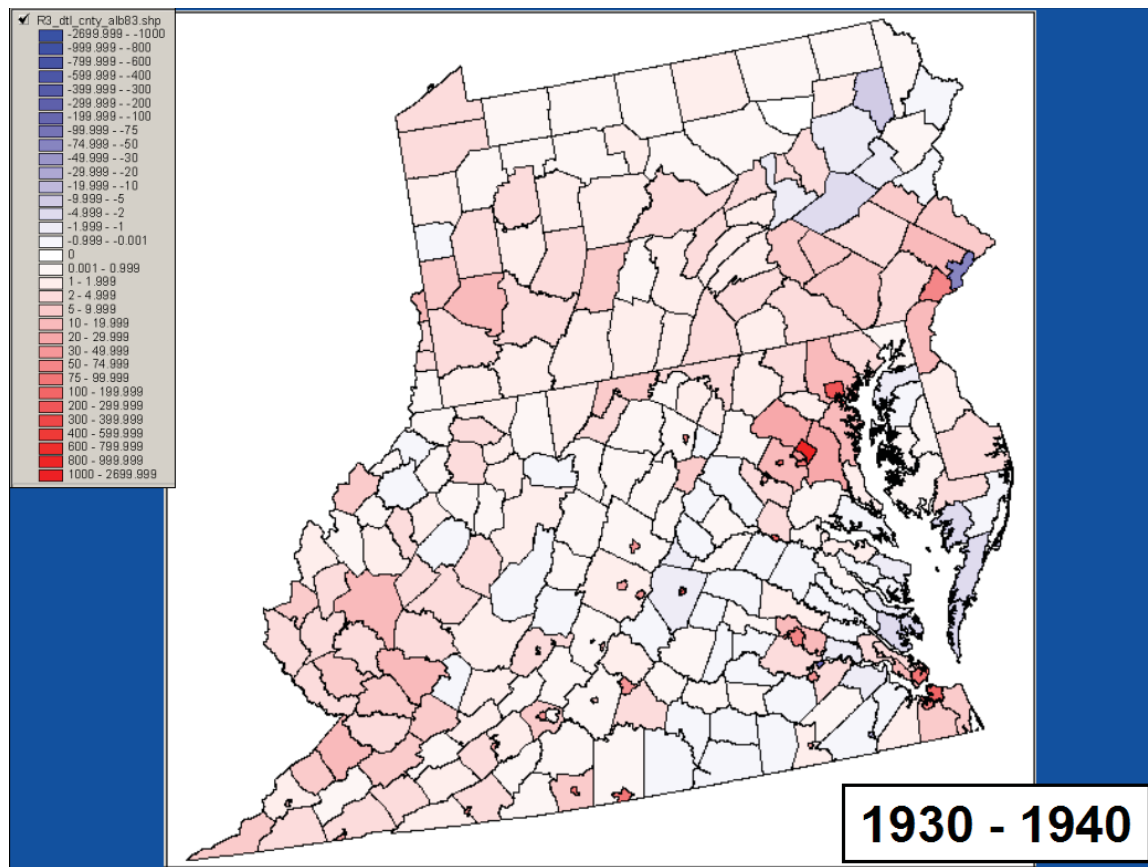


Figure A2: 1930-1940 Population Density Change (people·km⁻¹). From 1930 - 2000 U.S. Census data for EPA Region 3: Delaware, District of Columbia, Maryland, Pennsylvania, Virginia, and West Virginia.

Appendix 1: County-Level Decadal Population Density for EPA Region 3.

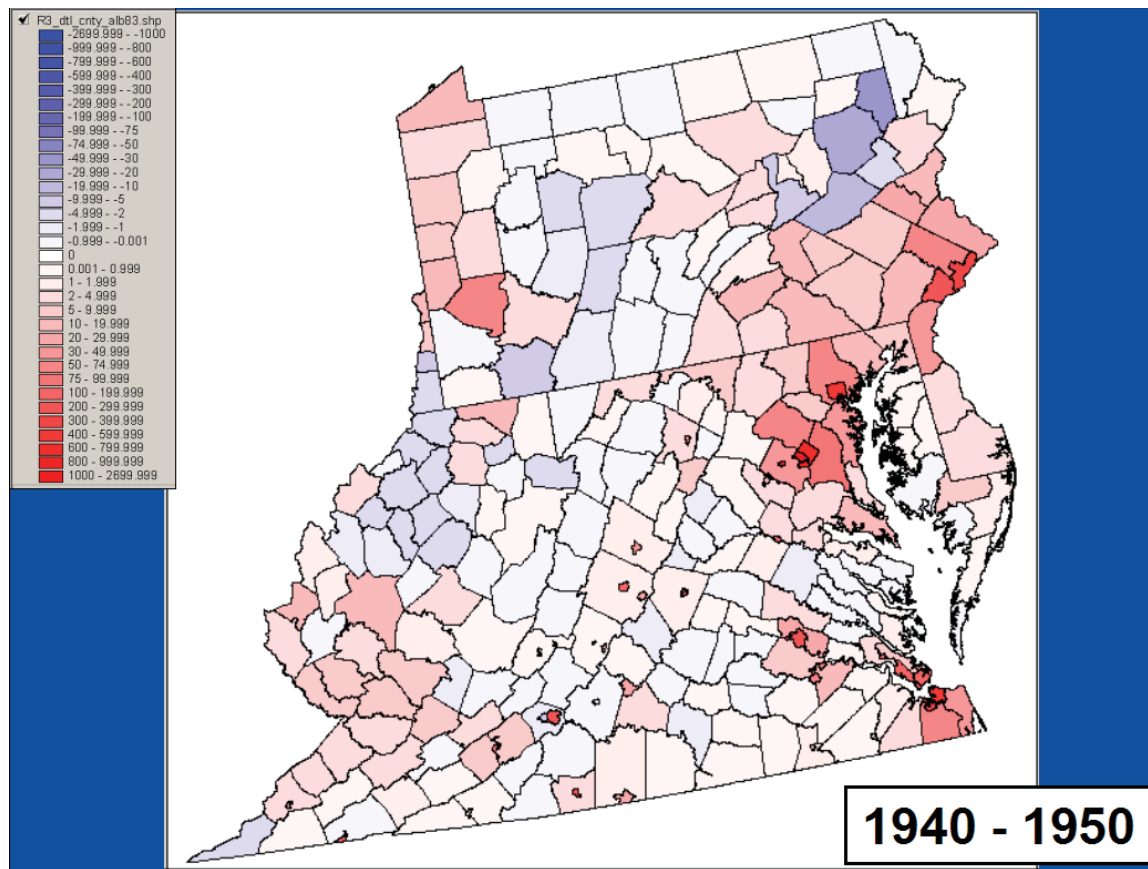


Figure A3: 1940-1950 Population Density Change (people·km⁻¹). From 1930 - 2000 U.S. Census data for EPA Region 3: Delaware, District of Columbia, Maryland, Pennsylvania, Virginia, and West Virginia.

Appendix 1: County-Level Decadal Population Density for EPA Region 3.

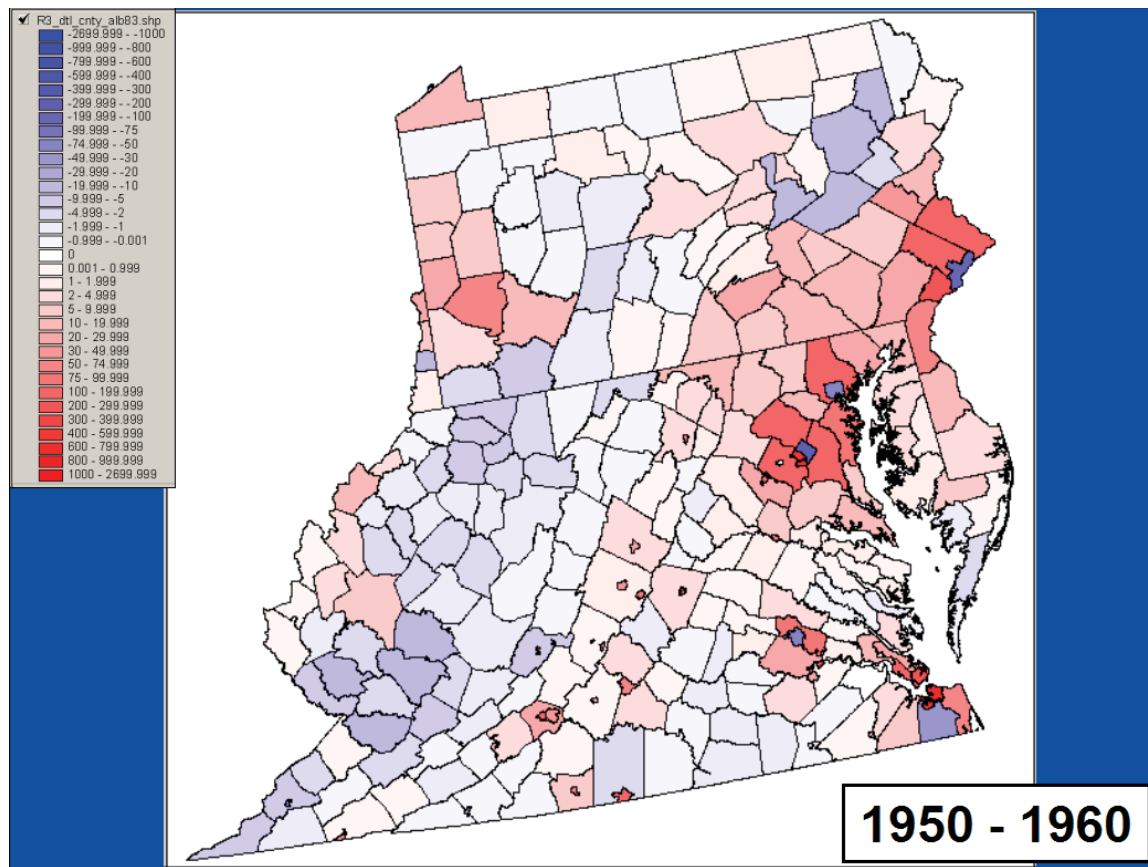


Figure A4: 1950-1960 Population Density Change (people·km⁻¹). From 1930 - 2000 U.S. Census data for EPA Region 3: Delaware, District of Columbia, Maryland, Pennsylvania, Virginia, and West Virginia.

Appendix 1: County-Level Decadal Population Density for EPA Region 3.

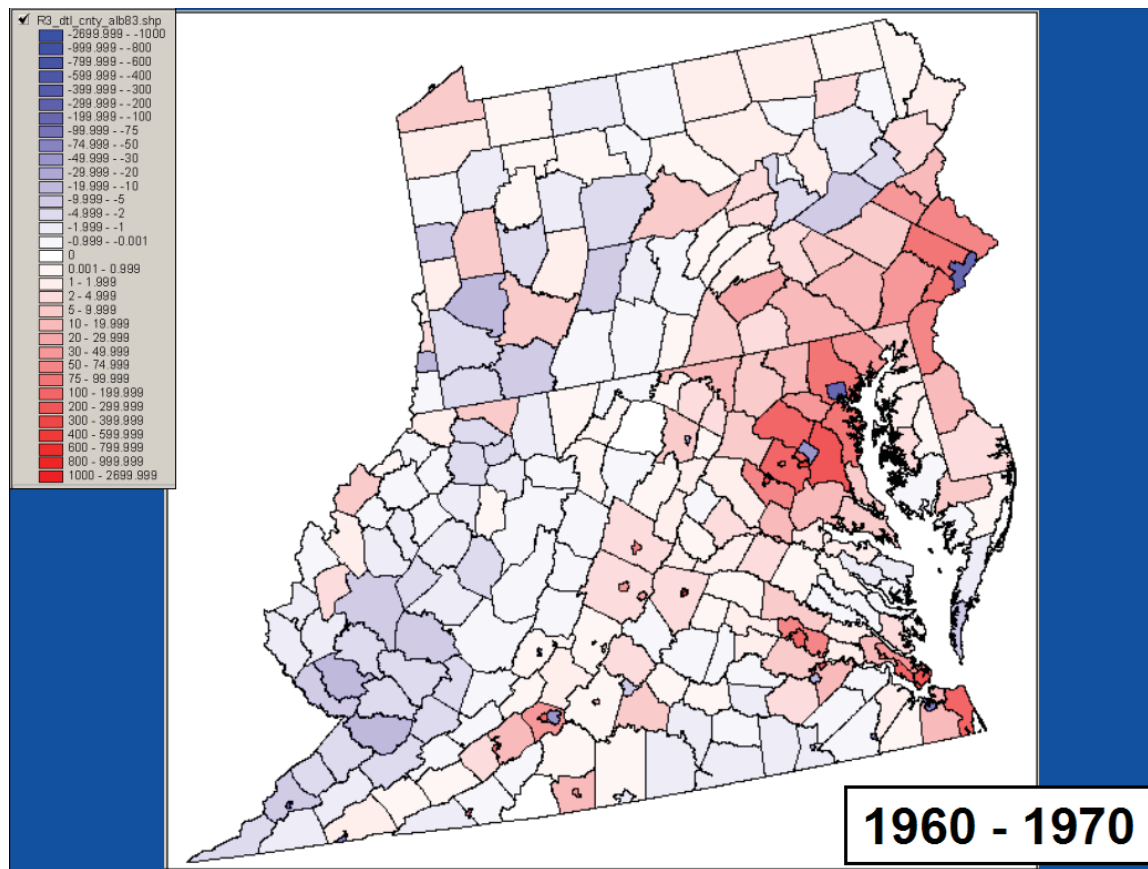


Figure A5: 1960-1970 Population Density Change (people·km⁻¹). From 1930 - 2000 U.S. Census data for EPA Region 3: Delaware, District of Columbia, Maryland, Pennsylvania, Virginia, and West Virginia.

Appendix 1: County-Level Decadal Population Density for EPA Region 3.

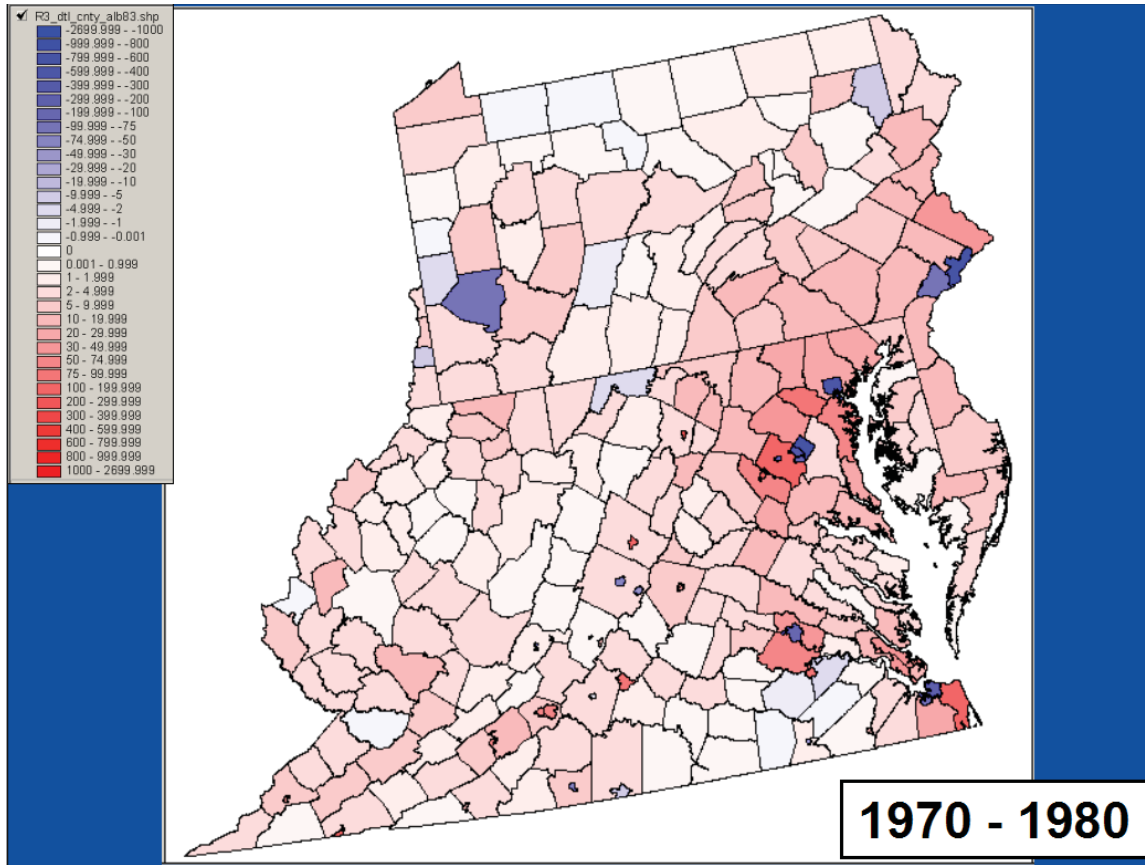


Figure A6: 1970-1980 Population Density Change (people·km⁻¹). From 1930 - 2000 U.S. Census data for EPA Region 3: Delaware, District of Columbia, Maryland, Pennsylvania, Virginia, and West Virginia.

Appendix 1: County-Level Decadal Population Density for EPA Region 3.

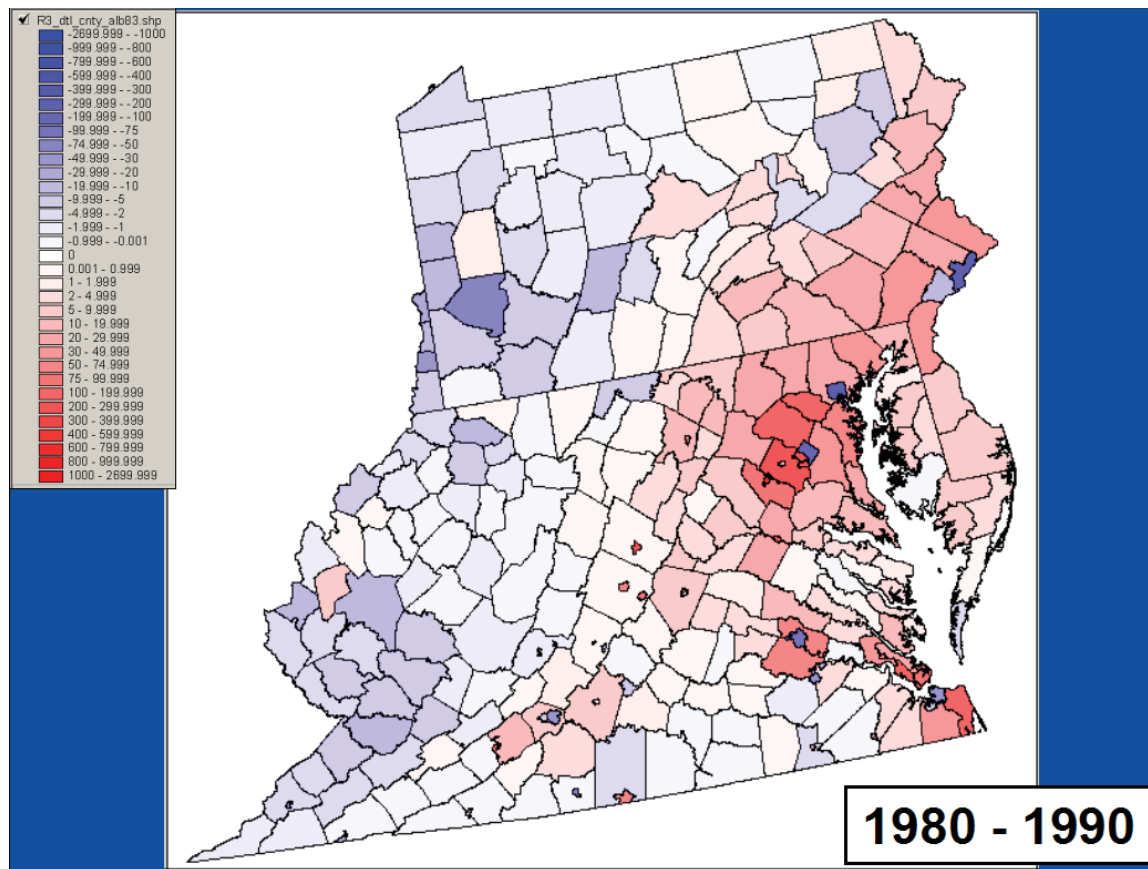


Figure A7: 1980-1990 Population Density Change (people·km⁻¹). From 1930 - 2000 U.S. Census data for EPA Region 3: Delaware, District of Columbia, Maryland, Pennsylvania, Virginia, and West Virginia.

Appendix 1: County-Level Decadal Population Density for EPA Region 3.

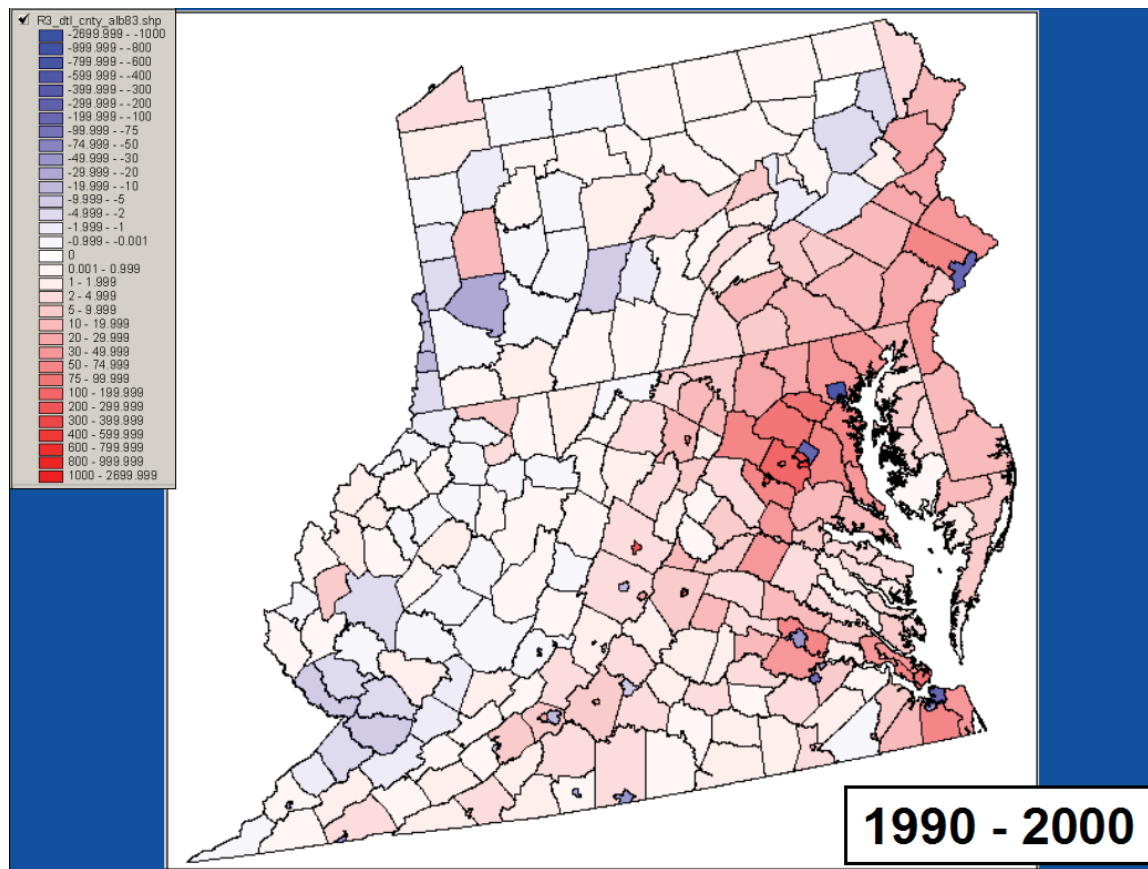


Figure A8: 1990-2000 Population Density Change (people·km⁻¹). From 1930 - 2000 U.S. Census data for EPA Region 3: Delaware, District of Columbia, Maryland, Pennsylvania, Virginia, and West Virginia.

Appendix 1: County-Level Decadal Population Density for EPA Region 3.

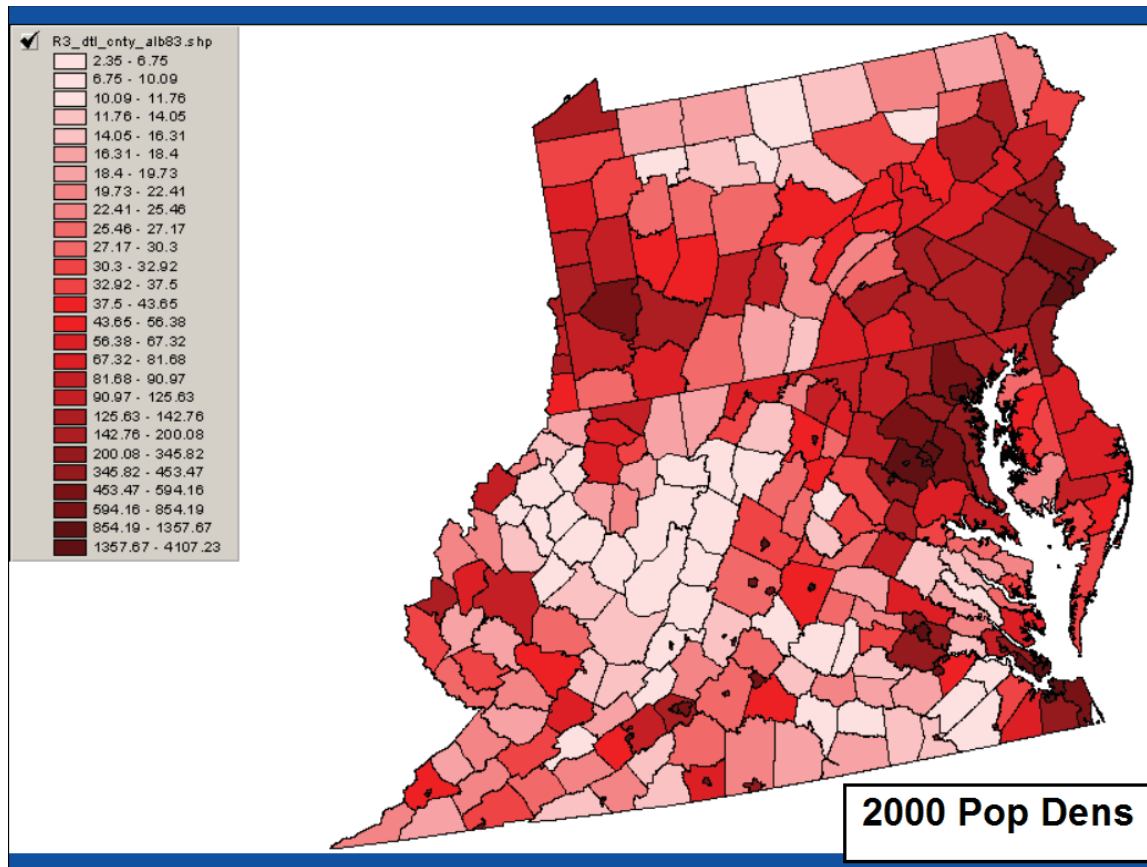


Figure A9: 2000 Population Density (people-km⁻¹). From 1930 - 2000 U.S. Census data for EPA Region 3: Delaware, District of Columbia, Maryland, Pennsylvania, Virginia, and West Virginia.

Appendix 1: County-Level Decadal Population Density for EPA Region 3.

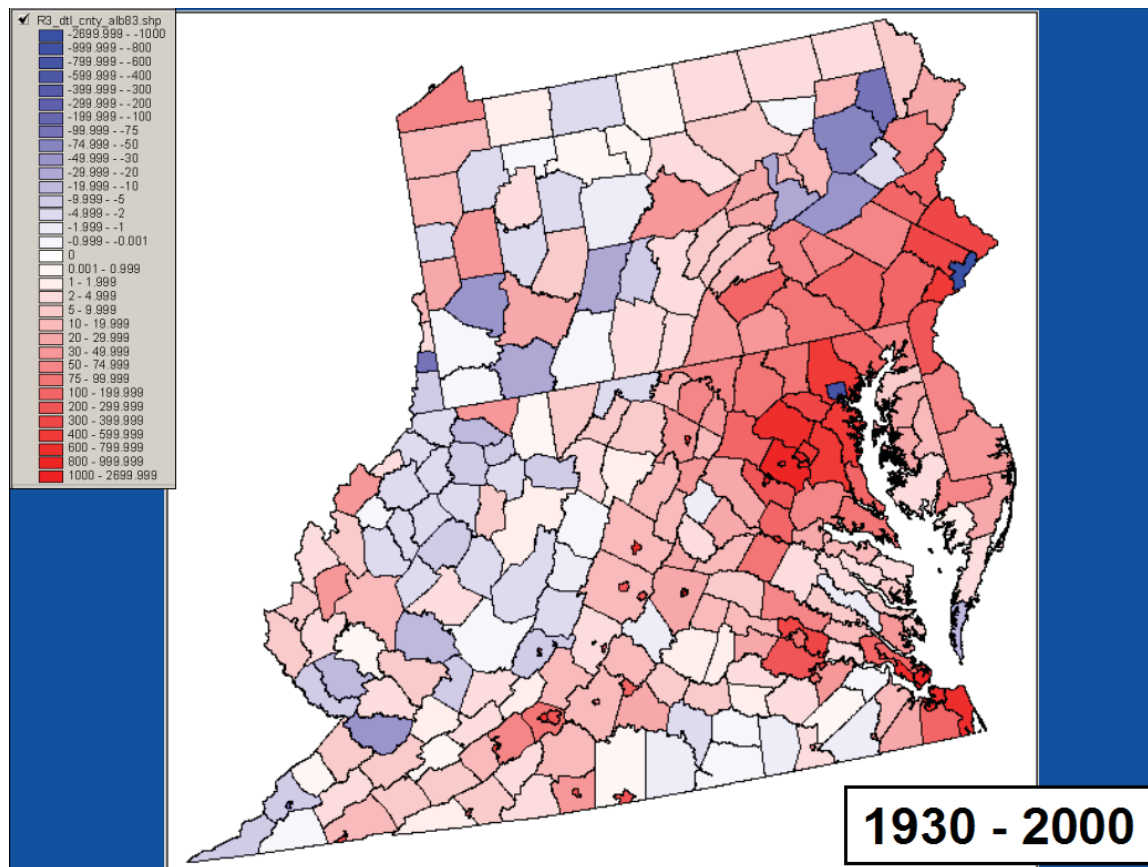


Figure A10: 1930-2000 Population Density Change (people·km⁻¹). From 1930 - 2000 U.S. Census data for EPA Region 3: Delaware, District of Columbia, Maryland, Pennsylvania, Virginia, and West Virginia.

Site ID Number	Station Name	State	Latitude	Longitude	Altitude (ft)	Drainage Area (mi. ²)	Start Date	End Date	Observations Count
01447680	Tunkhannock Creek near Long Pond	PA	41.0654	-75.5202	1805	18.0	4/1/1965	9/30/2000	12967
01448500	Dilldown Creek near Long Pond	PA	41.0357	-75.5432	1665	2.4	10/1/1948	9/30/1996	17532
01449360	Pohopoco Creek at Kresgeville	PA	40.8976	-75.5024	660	49.9	10/1/1966	9/30/2001	12784
01449500	Wild Creek at Hatchery	PA	40.9229	-75.5585	843	16.8	10/1/1940	9/30/1979	14244
01452500	Monocacy Creek at Bethlehem	PA	40.6412	-75.3793	247	44.5	10/1/1948	9/30/2001	19358
01465798	Poquessing Creek at Grant Ave. at Philadelphia	PA	40.0570	-74.9852	3	21.4	7/1/1965	9/30/2000	12876
01467048	Pennypack Cr at Lower Rhawn St Bdg Phila.	PA	40.0501	-75.0327	21	49.8	6/1/1965	9/30/2001	13271
01467086	Tacony Creek at County Line Philadelphia	PA	40.0465	-75.1107	61	16.6	10/1/1965	11/17/1988	8448
01469500	Little Schuylkill River at Tamaqua	PA	40.8070	-75.9718	817	42.9	10/1/1919	9/30/2001	29951
01475510	Darby Creek near Darby	PA	39.9290	-75.2724	19	37.4	2/1/1964	10/3/1990	9742
01475550	Cobbs Creek at Darby	PA	39.9173	-75.2474	12	22.0	1/1/1964	10/3/1990	9765
01476500	Ridley Creek at Moylan	PA	39.9029	-75.3927	87	31.9	10/1/1931	9/30/1954	8401
01477800	Shellpot Creek at Wilmington	DE	39.7608	-75.5194	15	7.5	12/1/1945	9/30/2000	20028
01478000	Christina River at Coochs Bridge	DE	39.6372	-75.7283	26	20.5	4/1/1943	9/30/2001	21368
01480000	Red Clay Creek at Wooddale	DE	39.7644	-75.6356	81	47.0	4/1/1943	9/30/2001	21368
01480300	West Branch Brandywine Creek near Honey Brook	PA	40.0729	-75.8608	591	18.7	6/1/1960	9/30/2000	14732
01480500	West Branch Brandywine Creek at Coatesville	PA	39.9857	-75.8275	306	45.8	10/1/1943	9/30/2001	14518
01480675	Marsh Creek near Glenmoore	PA	40.0979	-75.7416	450	8.6	8/1/1966	9/30/2000	12480

XI

Appendix 2 - Station Table: Streamflow Station ID codes, names, locations, etc.
Latitude and longitude are shown in decimal degrees north and west respectively.
Historical analysis of the relationship of streamflow flashiness
with population density, imperviousness,
and percent urban land cover in the Mid-Atlantic region

Site ID Number	Marsh Creek near Downingtown	PA	Latitude	Longitude	Altitude (ft)	Drainage Area (mi ²)	Start Date	End Date	Observations Count
01480685			40.0554	-75.7164	280	20.3	6/1/1973	9/30/2000	9984
01483200	Blackbird Creek at Blackbird	DE	39.3661	-75.6694	19	3.9	10/1/1956	9/30/2000	16071
01483700	St Jones River at Dover	DE	39.1636	-75.5194	1	31.9	1/1/1958	9/30/2001	15979
01484000	Murderkill River near Felton	DE	38.9759	-75.5671	22	13.6	7/1/1931	9/30/1999	11202
01484100	Beaverdam Branch at Houston	DE	38.9056	-75.5136	36	2.8	5/1/1958	9/30/2000	15494
01484300	Sowbridge Branch near Milton	DE	38.8143	-75.3271	3	7.1	10/1/1956	9/30/1978	8035
01484500	Stockley Branch at Stockley	DE	38.6386	-75.3419	25	5.2	4/1/1943	9/30/2001	21368
01484800	Guy Creek near Nassawadox	VA	37.5023	-75.8725	12	1.7	11/21/1963	10/22/1996	12025
01485500	Nassawango Creek near Snow Hill	MD	38.2289	-75.4719	12	44.9	12/1/1949	9/30/2001	18932
01486000	Manokin Branch near Princess Anne	MD	38.2139	-75.6717	15	4.8	5/1/1951	9/30/2000	16955
01486500	Beaverdam Creek near Salisbury	MD	38.3514	-75.5697	9	19.5	10/1/1929	9/30/1975	14610
01487500	Trap Pond Outlet near Laurel	DE	38.5278	-75.4828	20	16.7	7/1/1951	9/30/1971	7397
01488500	Marshyhope Creek near Adamsville	DE	38.8497	-75.6733	28	43.9	4/1/1943	9/30/2001	20455
01489000	Faulkner Branch at Federalsburg	MD	38.7123	-75.7925	17	7.1	8/1/1950	2/19/1992	15178
01490000	Chicamacomico River near Salem	MD	38.5125	-75.8806	10	15.0	5/1/1951	9/30/1980	10746
01492000	Beaverdam Branch at Matthews	MD	38.8115	-75.9705	2	5.9	8/1/1950	9/30/1981	11384
01493000	Unicorn Branch near Millington	MD	39.2497	-75.8611	4	19.7	1/1/1948	9/30/2001	19632
01493500	Morgan Creek near Kennedyville	MD	39.2800	-76.0150	15	12.7	5/31/1951	9/30/2001	18386

Appendix 2 - Station Table: Streamflow Station ID codes, names, locations, etc.
Latitude and longitude are shown in decimal degrees north and west respectively.
Historical analysis of the relationship of streamflow flashiness
with population density, imperviousness,
and percent urban land cover in the Mid-Atlantic region

01496000	Northeast Creek at Leslie	MD	39.6279	-75.9441	115	24.3	10/1/1948	9/30/1984	13149
01496200	Principio Creek near Principio Furnace	MD	39.6262	-76.0405	215	9.0	6/1/1967	4/2/1992	9073
01516500	Corey Creek near Mainesburg	PA	41.7909	-77.0147	1338	12.2	5/1/1954	9/30/2000	16955
Site ID Number	Station Name	State	Latitude	Longitude	Altitude (ft)	Drainage Area (mi ²)	Start Date	End Date	Observations Count
01517000	Elk Run near Mainesburg	PA	41.8151	-76.9650	1385	10.2	10/1/1954	9/30/1978	8766
01534300	Lackawanna River near Forest City	PA	41.6798	-75.4718	1551	38.8	10/1/1958	9/30/2001	15706
01537000	Toby Creek at Luzerne	PA	41.2809	-75.8957	575	32.4	10/1/1941	9/30/1993	18993
01537500	Solomon Creek at Wilkes-Barre	PA	41.2276	-75.9043	548	15.7	3/1/1940	9/30/1990	18476
01538000	Wapwallopen Creek near Wapwallopen	PA	41.0593	-76.0936	752	43.8	10/1/1919	9/30/2001	29951
01542810	Waldy Run near Emporium	PA	41.5790	-78.2925	1264	5.2	9/1/1964	9/30/2000	13179
01545600	Young Womans Creek near Renovo	PA	41.3895	-77.6908	780	46.2	12/1/1964	9/30/2001	13453
01547700	Marsh Creek at Blanchard	PA	41.0595	-77.6058	586	44.1	10/1/1955	9/30/2001	16802
01549500	Blockhouse Creek near English Center	PA	41.4737	-77.2308	1042	37.7	10/1/1940	9/30/2001	22280
01552500	Muncy Creek near Sonestown	PA	41.3570	-76.5347	1025	23.8	10/1/1940	9/30/2000	21915
01557500	Bald Eagle Creek at Tyrone	PA	40.6837	-78.2336	922	44.1	10/1/1944	9/30/2001	20819
01561000	Brush Creek at Gapsville	PA	39.9557	-78.2539	1122	36.8	12/1/1929	9/30/1958	10439
01567500	Bixler Run near Loysville	PA	40.3709	-77.4022	601	15.0	2/1/1954	9/30/2000	17044
01568500	Clark Creek near Carsonville	PA	40.4604	-76.7514	552	22.5	10/1/1937	12/31/1996	21642
01569800	Letort Spring Run near Carlisle	PA	40.2348	-77.1394	410	21.6	6/15/1976	9/30/2000	8874

Appendix 2 - Station Table: Streamflow Station ID codes, names, locations, etc.
Latitude and longitude are shown in decimal degrees north and west respectively.
Historical analysis of the relationship of streamflow flashiness
with population density, imperviousness,
and percent urban land cover in the Mid-Atlantic region

01581500	Bynum Run at Bel Air	MD	39.5417	-76.3306	252	8.5	6/1/1944	9/30/2000	8559
01581700	Winters Run near Benson	MD	39.5200	-76.3733	195	34.8	8/1/1967	9/30/2001	12480
01583000	Slade Run near Glyndon	MD	39.4945	-76.7955	425	2.1	10/1/1947	9/30/1981	12419
01584050	Long Green Creek at Glen Arm	MD	39.4547	-76.4792	230	9.4	10/1/1975	9/30/2000	9132
01584500	Little Gunpowder Falls at Laurel Brook	MD	39.5050	-76.4322	261	36.1	11/1/1926	9/30/2001	17136
Site ID Number	Station Name	State	Latitude	Longitude	Altitude (ft)	Drainage Area (mi ²)	Start Date	End Date	Observations Count
01585095	North Fork Whitemarsh Run near White Marsh	MD	39.3859	-76.4689	75	1.3	4/22/1992	9/30/2000	5605
01585100	Whitemarsh Run at White Marsh	MD	39.3708	-76.4461	39	7.6	2/1/1959	9/30/2000	14330
01585200	West Branch Herring Run at Idlewylde	MD	39.3736	-76.5931	285	2.1	7/1/1957	9/30/2000	12296
01585300	Stemmers Run at Rossville	MD	39.3412	-76.4878	22	4.5	12/1/1958	9/30/1989	10897
01585400	Brien Run at Stemmers Run	MD	39.3337	-76.4728	10	2.0	5/1/1958	9/30/1987	10745
01585500	Cranberry Branch near Westminster	MD	39.5931	-76.9681	670	3.3	10/1/1949	9/30/2000	18628
01588000	Piney Run near Sykesville	MD	39.3820	-76.9664	450	11.4	9/22/1931	9/30/1958	9871
01589100	East Branch Herbert Run at Arbutus	MD	39.2400	-76.6925	45	2.5	8/1/1957	9/30/2000	12480
01589300	Gwynns Falls at Villa Nova	MD	39.3458	-76.7336	361	32.5	2/1/1957	9/30/2001	13391
01589330	Dead Run at Franklintown	MD	39.3111	-76.7172	310	5.5	10/1/1959	9/30/2000	11042
01589440	Jones Falls at Sorrento	MD	39.3917	-76.6617	240	25.2	4/1/1966	9/30/2001	10045
01589500	Sawmill Creek at Glen Burnie	MD	39.1700	-76.6308	26	5.0	6/1/1944	9/30/2000	9265
01590000	North River near Annapolis	MD	38.9859	-76.6222	7	8.5	12/1/1931	9/30/1974	15645

Appendix 2 - Station Table: Streamflow Station ID codes, names, locations, etc.
Latitude and longitude are shown in decimal degrees north and west respectively.
Historical analysis of the relationship of streamflow flashiness
with population density, imperviousness,
and percent urban land cover in the Mid-Atlantic region

01590500	Bacon Ridge Branch at Chesterfield	MD	39.0020	-76.6144	15	6.9	10/1/1942	9/30/1990	9497
01591000	Patuxent River near Unity	MD	39.2383	-77.0564	365	34.8	7/20/1944	9/30/2001	20892
01591400	Cattail Creek near Glenwood	MD	39.2558	-77.0514	380	22.9	6/6/1978	9/30/2001	8512
01591700	Hawlings River near Sandy Spring	MD	39.1747	-77.0228	320	27.0	6/7/1978	9/30/2001	8517
01593500	Little Patuxent River at Guilford	MD	39.1678	-76.8519	259	38.0	4/1/1932	9/30/2001	25385
01594500	Western Branch near Largo	MD	38.8762	-76.7980	47	30.2	10/1/1949	9/30/1975	9494
01594930	Laurel Run at Dobbin Rd near Wilson	MD	39.2436	-79.4286	2600	8.2	5/1/1980	9/30/2000	7452
Site ID Number	Station Name	State	Latitude	Longitude	Altitude (ft)	Drainage Area (mi ²)	Start Date	End Date	Observations Count
01594936	North Fork Sand Run near Wilson	MD	39.2600	-79.4100	2515	1.9	5/1/1980	9/30/2000	7458
01595200	Stony River near Mount Storm	WV	39.2695	-79.2623	2555	48.7	10/1/1961	9/30/2000	14245
01595300	Abram Creek at Oakmont	WV	39.3668	-79.1790	834	42.6	8/14/1956	9/30/1982	9544
01596500	Savage River near Barton	MD	39.5681	-79.1028	1605	49.1	9/18/1948	9/30/2001	19371
01597000	Crabtree Creek near Swanton	MD	39.5001	-79.1595	1529	16.7	9/17/1948	9/30/1981	12067
01603500	Evitts Creek near Centerville	PA	39.7898	-78.6464	1028	30.2	9/3/1932	9/30/1982	18290
01613050	Tonoloway Creek near Needmore	PA	39.8984	-78.1322	689	10.7	10/1/1965	9/30/2000	12761
01613900	Hogue Creek near Hayfield	VA	39.2145	-78.2880	669	15.0	8/1/1960	9/30/2000	12587
01614090	Conococheague Creek near Fayetteville	PA	39.9301	-77.4394	1133	5.1	9/1/1960	3/31/1981	7517
01616000	Abrams Creek near Winchester	VA	39.1779	-78.0858	526	16.5	7/27/1949	11/14/1994	9711
01617000	Tuscarora Creek Above Martinsburg	WV	39.4695	-77.9714	446	11.3	10/1/1948	9/30/1977	9131

Appendix 2 - Station Table: Streamflow Station ID codes, names, locations, etc.
Latitude and longitude are shown in decimal degrees north and west respectively.
Historical analysis of the relationship of streamflow flashiness
with population density, imperviousness,
and percent urban land cover in the Mid-Atlantic region

01617800	Marsh Run at Grimes	MD	39.5147	-77.7772	355	18.9	10/1/1963	9/30/2001	13859
01620500	North River near Stokesville	VA	38.3376	-79.2401	2055	17.2	10/1/1946	9/30/2000	19724
01636210	Happy Creek at Front Royal	VA	38.9057	-78.1858	610	14.0	10/1/1948	10/19/1977	10611
01640500	Owens Creek at Lantz	MD	39.6768	-77.4636	965	5.9	10/1/1931	9/30/1984	19359
01641000	Hunting Creek at Jimtown	MD	39.5945	-77.3969	355	18.4	10/1/1949	2/18/1992	15481
01641500	Fishing Creek near Lewistown	MD	39.5265	-77.4664	735	7.3	10/1/1947	9/30/1984	13515
01645200	Watts Branch at Rockville	MD	39.0843	-77.1769	330	3.7	10/1/1957	9/30/1987	10957
01646550	Little Falls Branch near Bethesda	MD	38.9576	-77.1083	169	4.1	6/1/1944	1/17/1979	11857
01650500	Nw Branch Anacostia River near Colesville	MD	39.0653	-77.0300	265	21.1	10/1/1923	9/30/2001	23319
Site ID Number	Station Name	State	Latitude	Longitude	Altitude (ft)	Drainage Area (mi ²)	Start Date	End Date	Observations Count
01651000	Nw Branch Anacostia River near Hyattsville	MD	38.9525	-76.9667	17	49.4	7/1/1938	9/30/2001	23103
01652500	Fourmile Run at Alexandria	VA	38.8434	-77.0791	23	13.8	10/1/1951	9/30/1999	8936
01653000	Cameron Run at Alexandria	VA	38.8057	-77.1019	32	33.7	6/1/1955	9/30/2001	15244
01653500	Henson Creek at Oxon Hill	MD	38.7879	-76.9780	62	16.7	8/1/1948	9/30/1978	11018
01653600	Piscataway Creek at Piscataway	MD	38.7056	-76.9667	10	39.5	10/1/1965	9/30/2001	13149
01654000	Accotink Creek near Annandale	VA	38.8129	-77.2283	191	23.5	10/1/1947	9/30/2000	19359
01655500	Cedar Run near Warrenton	VA	38.7404	-77.7875	419	12.3	10/1/1950	1/6/1987	13247
01658500	S F Quantico Creek near Independent Hill	VA	38.5873	-77.4286	239	7.6	5/1/1951	9/30/2000	18051
01660400	Aquia Creek near Garrisonville	VA	38.4904	-77.4336	120	34.9	9/1/1971	9/30/2001	10239

Appendix 2 - Station Table: Streamflow Station ID codes, names, locations, etc.
Latitude and longitude are shown in decimal degrees north and west respectively.
Historical analysis of the relationship of streamflow flashiness
with population density, imperviousness,
and percent urban land cover in the Mid-Atlantic region

01661000	Chaptico Creek at Chaptico	MD	38.3793	-76.7819	15	10.4	6/20/1947	9/30/1972	9235
01661050	St Clement Creek near Clements	MD	38.3333	-76.7253	8	18.5	10/1/1968	9/30/2001	12053
01661500	St Marys River at Great Mills	MD	38.2433	-76.5036	10	24.0	6/21/1946	9/30/2001	20191
01661800	Bush Mill Stream near Heathsville	VA	37.8768	-76.4947	24	6.8	10/1/1963	1/13/1987	8323
01662500	Rush River at Washington	VA	38.7140	-78.1711	598	14.7	10/1/1953	9/30/1977	8766
01662800	Battle Run near Laurel Mills	VA	38.6557	-78.0739	375	27.6	5/1/1958	9/30/2001	15046
01665000	Mount Run near Culpeper	VA	38.4807	-78.0525	389	15.9	9/10/1949	9/29/1999	17568
01668500	Cat Point Creek near Montross	VA	38.0398	-76.8269	3	45.6	10/1/1943	9/30/1999	20454
01669000	Piscataway Creek near Tappahannock	VA	37.8770	-76.9005	3	28.0	10/1/1951	9/30/2001	18263
01670000	Beaverdam Swamp near Ark	VA	37.4707	-76.5630	36	6.6	10/1/1949	1/18/1989	14355
Site ID Number	Station Name	State	Latitude	Longitude	Altitude (ft)	Drainage Area (mi ²)	Start Date	End Date	Observations Count
01671500	Bunch Creek near Boswells Tavern	VA	38.0318	-78.1914	377	4.4	10/1/1948	9/30/1979	11322
01673500	Totopotomoy Creek near Atlee	VA	37.6693	-77.3825	116	5.9	10/1/1948	9/30/1977	10592
01673550	Totopotomoy Creek near Studley	VA	37.6626	-77.2578	38	26.2	10/1/1977	9/30/2001	8766
02017000	Meadow Creek at Newcastle	VA	37.4932	-80.1095	1337	13.8	10/1/1929	9/30/1952	8401
02018500	Catawba Creek near Catawba	VA	37.4682	-80.0054	1300	34.3	10/1/1943	9/30/2001	21185
02022500	Kerrs Creek near Lexington	VA	37.8257	-79.4431	980	35.0	4/1/1927	9/30/2001	27029
02027500	Piney River at Piney River	VA	37.7023	-79.0275	634	47.6	10/1/1949	9/30/2001	18993
02036500	Fine Creek at Fine Creek Mills	VA	37.5979	-77.8197	157	22.1	10/1/1944	9/30/2000	20454

Appendix 2 - Station Table: Streamflow Station ID codes, names, locations, etc.
Latitude and longitude are shown in decimal degrees north and west respectively.
Historical analysis of the relationship of streamflow flashiness
with population density, imperviousness,
and percent urban land cover in the Mid-Atlantic region

02038000	Falling Creek near Chesterfield	VA	37.4437	-77.5222	126	32.8	10/1/1955	12/7/1994	14313
02038850	Holiday Creek near Andersonville	VA	37.4154	-78.6358	473	8.5	4/27/1966	9/30/2000	12576
02043500	Cypress Swamp at Cypress Chapel	VA	36.6235	-76.6016	29	23.8	10/1/1953	10/3/1996	13346
02044000	Nottoway River near Burkeville	VA	37.0780	-78.1969	355	38.7	10/1/1946	1/13/1987	14715
02051600	Great Creek near Cochran	VA	36.8129	-77.9216	216	30.7	5/1/1958	1/7/1987	10479
02055100	Tinker Creek near Daleville	VA	37.4176	-79.9354	1217	11.7	5/1/1956	9/30/2000	16224
02076500	Georges Creek near Gretna	VA	36.9365	-79.3114	630	9.2	10/1/1949	10/8/1997	17540
03011800	Kinzua Creek near Guffey	PA	41.7665	-78.7187	1540	46.4	10/1/1965	9/30/2001	13149
03022540	Woodcock C at Blooming Valley	PA	41.6907	-80.0481	1200	31.1	9/4/1974	9/30/1995	7675
03026500	Sevenmile Run near Rasselas	PA	41.6312	-78.5766	1691	7.8	11/1/1951	9/30/2000	17867
03049800	Little Pine Creek near Etna	PA	40.5204	-79.9381	774	5.8	10/1/1962	9/30/2000	13880
03052500	Sand Run near Buckhannon	WV	38.9640	-80.1526	1530	14.3	10/1/1946	9/30/2000	19716
Site ID Number	Station Name	State	Latitude	Longitude	Altitude (ft)	Drainage Area (mi ²)	Start Date	End Date	Observations Count
03062400	Cobun Creek at Morgantown	WV	39.6082	-79.9551	890	11.0	4/1/1965	9/30/2000	11863
03076600	Bear Creek at Friendsville	MD	39.6561	-79.3947	1551	48.9	10/1/1964	9/30/2001	13514
03083000	Green Lick Run at Green Lick Reservoir	PA	40.1051	-79.5001	1255	3.1	10/1/1941	9/30/1979	13879
03084000	Abers Creek near Murrys ville	PA	40.4504	-79.7137	937	4.4	10/1/1948	9/30/1993	16436
03101000	Sugar Run at Pymatuning Dam	PA	41.4973	-80.4651	985	9.3	3/1/1934	9/30/1955	7884
03111150	Brush Run near Buffalo	PA	40.1984	-80.4076	954	10.3	10/1/1960	9/30/1985	7734

Appendix 2 - Station Table: Streamflow Station ID codes, names, locations, etc.
Latitude and longitude are shown in decimal degrees north and west respectively.
Historical analysis of the relationship of streamflow flashiness
with population density, imperviousness,
and percent urban land cover in the Mid-Atlantic region

03165000	Chestnut Creek at Galax	VA	36.6459	-80.9192	2344	39.4	10/1/1944	9/30/2001	20819
03178500	Camp Creek near Camp Creek	WV	37.5043	-81.1276	2218	32.0	10/1/1946	12/27/1971	9219
03206600	East Fork Twelvepole Creek near Dunlow	WV	38.0173	-82.2960	710	38.5	10/1/1964	9/30/2000	13149
03208700	N F Pound River at Pound	VA	37.1257	-82.6266	1500	18.5	10/1/1961	9/30/1987	9496
03213500	Panther Creek near Panther	WV	37.4451	-81.8706	1050	31.0	8/1/1946	9/30/1986	14671
03478400	Beaver Creek at Bristol	VA	36.6318	-82.1338	1781	27.7	10/1/1957	9/30/2001	16071
04213040	Raccoon Creek near West Springfield	PA	41.9451	-80.4473	715	2.5	10/1/1968	9/30/1995	9861

Appendix 2 - Station Table: Streamflow Station ID codes, names, locations, etc.
Latitude and longitude are shown in decimal degrees north and west respectively.
Historical analysis of the relationship of streamflow flashiness
with population density, imperviousness,
and percent urban land cover in the Mid-Atlantic region

Appendix 3: NLCD1992 and NLCD2001 Land Cover Class Definitions

< <http://landcover.usgs.gov/classes.php> >

The USGS Land Cover Institute (LCI)

NLCD Land Cover Class Definitions

The classification system used for NLCD is modified from the Anderson land-use and land-cover classification system. Many of the Anderson classes, especially the Level III classes, are best derived using aerial photography. It is not appropriate to attempt to derive some of these classes using Landsat TM data due to issues of spatial resolution and interpretability of data. Thus, no attempt was made to derive classes that were extremely difficult or “impractical” to obtain using Landsat TM data, such as the Level III urban classes. In addition, some Anderson Level II classes were consolidated into a single NLCD class.

Some similarities and differences between Anderson and NLCD systems:

< <http://landcover.usgs.gov/classes.php#similar> >.

Water

11 Open Water

12 Perennial Ice/Snow

Developed

21 Low Intensity Residential

22 High Intensity Residential

23 Commercial/Industrial/Transportation

Barren

31 Bare Rock/Sand/Clay

32 Quarries/Strip Mines/Gravel Pits

33 Transitional

Forested Upland

41 Deciduous Forest

42 Evergreen Forest

43 Mixed Forest

Shrubland

51 Shrubland

Non-Natural Woody

61 Orchards/Vineyards/Other

Herbaceous Upland Natural/Semi-natural Vegetation

71 Grasslands/Herbaceous

Herbaceous Planted/Cultivated

81 Pasture/Hay

82 Row Crops

83 Small Grains

84 Fallow

85 Urban/Recreational Grasses

Wetlands

91 Woody Wetlands

92 Emergent Herbaceous Wetlands

NLCD1992 Land Cover Class Definitions

Water - All areas of open water or permanent ice/snow cover.

11. Open Water - all areas of open water, generally with less than 25% cover of vegetation/land cover.

12. Perennial Ice/Snow - all areas characterized by year-long surface cover of ice and/or snow.

Developed Areas characterized by a high percentage (30 percent or greater) of constructed materials (e.g. asphalt, concrete, buildings, etc).

21. Low Intensity Residential - Includes areas with a mixture of constructed materials and vegetation. Constructed materials account for 30-80 percent of the cover. Vegetation may account for 20 to 70 percent of the cover. These areas most commonly include single-family housing units. Population densities will be lower than in high intensity residential areas.

22. High Intensity Residential - Includes highly developed areas where people reside in high numbers. Examples include apartment complexes and row houses. Vegetation accounts for less than 20 percent of the cover. Constructed materials account for 80 to 100 percent of the cover.

23. Commercial/Industrial/Transportation - Includes infrastructure (e.g. roads, railroads, etc.) and all highly developed areas not classified as High Intensity Residential.

Barren - Areas characterized by bare rock, gravel, sand, silt, clay, or other earthen material, with little or no "green" vegetation present regardless of its inherent ability to support life. Vegetation, if present, is more widely spaced and scrubby than that in the "green" vegetated categories; lichen cover may be extensive.

31. Bare Rock/Sand/Clay - Perennially barren areas of bedrock, desert pavement, scarps, talus, slides, volcanic material, glacial debris, beaches, and other accumulations of earthen material.

32. Quarries/Strip Mines/Gravel Pits - Areas of extractive mining activities with significant surface expression.

33. Transitional - Areas of sparse vegetative cover (less than 25 percent of cover) that are dynamically changing from one land cover to another, often because of land use activities. Examples include forest clearcuts, a transition phase between forest and agricultural land, the temporary clearing of vegetation, and changes due to natural causes (e.g. fire, flood, etc.).

Forested Upland - Areas characterized by tree cover (natural or semi-natural woody vegetation, generally greater than 6 meters tall); tree canopy accounts for 25-100 percent of the cover.

41. Deciduous Forest - Areas dominated by trees where 75 percent or more of the tree species shed foliage simultaneously in response to seasonal change.

42. Evergreen Forest - Areas dominated by trees where 75 percent or more of the tree species maintain their leaves all year. Canopy is never without green foliage.

43. Mixed Forest - Areas dominated by trees where neither deciduous nor evergreen species represent more than 75 percent of the cover present.

Shrubland - Areas characterized by natural or semi-natural woody vegetation with aerial stems, generally less than 6 meters tall, with individuals or clumps not touching to interlocking. Both evergreen and deciduous species of true shrubs, young trees, and trees or shrubs that are small or stunted because of environmental conditions are included.

51. Shrubland - Areas dominated by shrubs; shrub canopy accounts for 25-100 percent of the cover. Shrub cover is generally greater than 25 percent when tree cover is less than 25 percent. Shrub cover may be less than 25 percent in cases when the cover of other life forms (e.g. herbaceous or tree) is less than 25 percent and shrubs cover exceeds the cover of the other life forms.

Non-Natural Woody - Areas dominated by non-natural woody vegetation; non-natural woody vegetative canopy accounts for 25-100 percent of the cover. The non-natural woody classification is subject to the availability of sufficient ancillary data to differentiate non-natural woody vegetation from natural woody vegetation.

61. Orchards/Vineyards/Other - Orchards, vineyards, and other areas planted or maintained for the production of fruits, nuts, berries, or ornamentals.

Herbaceous Upland - Upland areas characterized by natural or semi-natural herbaceous vegetation; herbaceous vegetation accounts for 75-100 percent of the cover.

71. Grasslands/Herbaceous - Areas dominated by upland grasses and forbs. In rare cases, herbaceous cover is less than 25 percent, but exceeds the combined cover of the woody species present. These areas are not subject to intensive management, but they are often utilized for grazing.

Planted/Cultivated - Areas characterized by herbaceous vegetation that has been planted or is intensively managed for the production of food, feed, or fiber; or is maintained in developed settings for specific purposes. Herbaceous vegetation accounts for 75-100 percent of the cover.

81. Pasture/Hay - Areas of grasses, legumes, or grass-legume mixtures planted for livestock grazing or the production of seed or hay crops.

82. Row Crops - Areas used for the production of crops, such as corn, soybeans, vegetables, tobacco, and cotton.

83. Small Grains - Areas used for the production of graminoid crops such as wheat, barley, oats, and rice.

84. Fallow - Areas used for the production of crops that do not exhibit visible vegetation as a result of being tilled in a management practice that incorporates prescribed alternation between cropping and tillage.

85. Urban/Recreational Grasses - Vegetation (primarily grasses) planted in developed settings for recreation, erosion control, or aesthetic purposes. Examples include parks, lawns, golf courses, airport grasses, and industrial site grasses.

Wetlands - Areas where the soil or substrate is periodically saturated with or covered with water as defined by Cowardin et al.

91. Woody Wetlands - Areas where forest or shrubland vegetation accounts for 25-100 percent of the cover and the soil or substrate is periodically saturated with or covered with water.

92. Emergent Herbaceous Wetlands - Areas where perennial herbaceous vegetation accounts for 75-100 percent of the cover and the soil or substrate is periodically saturated with or covered with water.

Reference

Cowardin, L.M., V. Carter, F.C. Golet, and E.T. LaRoe, 1979. Classification of Wetlands and Deepwater Habitat of the United States, Fish and Wildlife Service, U.S. Department of the Interior, Washington, D.C.

< <http://landcover.usgs.gov/classes.php#similar> >

Similarities and differences between Anderson and NLCD systems are as follows:

Urban or built-up classes: Commercial, Industrial, Transportation, and Communications/Utilities (all separate Anderson Level II classes) were treated as one NLCD class (Commercial/Industrial/Transportation). No attempt was made to derive Anderson Level III classes in NLCD. "Recreational" grasses, such as those that occur in golf courses or parks (treated as an urban class by Anderson) are considered to be a non-urban class in NLCD (a subdivision of "Herbaceous Planted/Cultivated). Residential (an Anderson Level II class) was divided into Low and High Intensity classes in NLCD.

Water: Anderson Level II Water classes (Streams/Canals, Lakes/Ponds, Reservoirs, Bays, Open Marine) were classed as a single class (Open Water) in NLCD.

Agriculture: Agricultural areas that are herbaceous in nature (Cropland and Pasture; Anderson Level II) are subdivided into four NLCD classes: Pasture/Hay, Row Crops, Small Grains and Fallow.

Rangeland: No rangeland class (Anderson Level I) is identified by NLCD. Rather, "rangeland" is subdivided by NLCD into Grasslands/Herbaceous and Shrubland classes.

Forest land: Evergreen Forest, Deciduous Forest and Mixed Forest are the same in both Anderson and NLCD. Clearcut and burned areas are classed as "Transitional Bare" areas in NLCD.

Wetlands: Two classes are defined by NLCD. These are Woody wetlands and Emergent/Herbaceous wetlands. These are very analogous to the Anderson Level II wetland classes.

Bare: Three NLCD classes are recognized. These are: Bare Rock/Sand Clay, Quarries/Strip Mines/Gravel Pits and Transitional Bare. These represent a consolidation of Anderson Level II classes.

Tundra: While "tundra" is treated as a distinct Anderson Level I class, tundra (including arctic/alpine vegetation) is considered to be either "Grasslands/Herbaceous" or "Shrubland" classes by NLCD.

U.S. Department of the Interior | U.S. Geological Survey

URL: <http://landcover.usgs.gov>

Page Contact Information: LCI@usgs.gov

Page Last Modified: March 2007

< http://www.mrlc.gov/nlcd_definitions.asp >

NLCD 2001 Land Cover Class Definitions

11. Open Water - All areas of open water, generally with less than 25% cover of vegetation or soil.

12. Perennial Ice/Snow - All areas characterized by a perennial cover of ice and/or snow, generally greater than 25% of total cover.
21. Developed, Open Space - Includes areas with a mixture of some constructed materials, but mostly vegetation in the form of lawn grasses. Impervious surfaces account for less than 20 percent of total cover. These areas most commonly include large-lot single-family housing units, parks, golf courses, and vegetation planted in developed settings for recreation, erosion control, or aesthetic purposes
22. Developed, Low Intensity - Includes areas with a mixture of constructed materials and vegetation. Impervious surfaces account for 20-49 percent of total cover. These areas most commonly include single-family housing units.
23. Developed, Medium Intensity - Includes areas with a mixture of constructed materials and vegetation. Impervious surfaces account for 50-79 percent of the total cover. These areas most commonly include single-family housing units.
24. Developed, High Intensity - Includes highly developed areas where people reside or work in high numbers. Examples include apartment complexes, row houses and commercial/industrial. Impervious surfaces account for 80 to 100 percent of the total cover.
31. Barren Land (Rock/Sand/Clay) - Barren areas of bedrock, desert pavement, scarps, talus, slides, volcanic material, glacial debris, sand dunes, strip mines, gravel pits and other accumulations of earthen material. Generally, vegetation accounts for less than 15% of total cover.
32. Unconsolidated Shore* - Unconsolidated material such as silt, sand, or gravel that is subject to inundation and redistribution due to the action of water. Characterized by substrates lacking vegetation except for pioneering plants that become established during brief periods when growing conditions are favorable. Erosion and deposition by waves and currents produce a number of landforms representing this class.
41. Deciduous Forest - Areas dominated by trees generally greater than 5 meters tall, and greater than 20% of total vegetation cover. More than 75 percent of the tree species shed foliage simultaneously in response to seasonal change.
42. Evergreen Forest - Areas dominated by trees generally greater than 5 meters tall, and greater than 20% of total vegetation cover. More than 75 percent of the tree species maintain their leaves all year. Canopy is never without green foliage.
43. Mixed Forest - Areas dominated by trees generally greater than 5 meters tall, and greater than 20% of total vegetation cover. Neither deciduous nor evergreen species are greater than 75 percent of total tree cover.
51. Dwarf Scrub - Alaska only areas dominated by shrubs less than 20 centimeters tall with shrub canopy typically greater than 20% of total vegetation. This type is often co-associated with grasses, sedges, herbs, and non-vascular vegetation.

52. Shrub/Scrub - Areas dominated by shrubs; less than 5 meters tall with shrub canopy typically greater than 20% of total vegetation. This class includes true shrubs, young trees in an early successional stage or trees stunted from environmental conditions.
71. Grassland/Herbaceous - Areas dominated by grammanoid or herbaceous vegetation, generally greater than 80% of total vegetation. These areas are not subject to intensive management such as tilling, but can be utilized for grazing.
72. Sedge/Herbaceous - Alaska only areas dominated by sedges and forbs, generally greater than 80% of total vegetation. This type can occur with significant other grasses or other grass like plants, and includes sedge tundra, and sedge tussock tundra.
73. Lichens - Alaska only areas dominated by fruticose or foliose lichens generally greater than 80% of total vegetation.
74. Moss - Alaska only areas dominated by mosses, generally greater than 80% of total vegetation.
81. Pasture/Hay - Areas of grasses, legumes, or grass-legume mixtures planted for livestock grazing or the production of seed or hay crops, typically on a perennial cycle. Pasture/hay vegetation accounts for greater than 20 percent of total vegetation.
82. Cultivated Crops - Areas used for the production of annual crops, such as corn, soybeans, vegetables, tobacco, and cotton, and also perennial woody crops such as orchards and vineyards. Crop vegetation accounts for greater than 20 percent of total vegetation. This class also includes all land being actively tilled.
90. Woody Wetlands - Areas where forest or shrubland vegetation accounts for greater than 20 percent of vegetative cover and the soil or substrate is periodically saturated with or covered with water.
91. Palustrine Forested Wetland* -Includes all tidal and non-tidal wetlands dominated by woody vegetation greater than or equal to 5 meters in height and all such wetlands that occur in tidal areas in which salinity due to ocean-derived salts is below 0.5 percent. Total vegetation coverage is greater than 20 percent.
92. Palustrine Scrub/Shrub Wetland* - Includes all tidal and non-tidal wetlands dominated by woody vegetation less than 5 meters in height, and all such wetlands that occur in tidal areas in which salinity due to ocean-derived salts is below 0.5 percent. Total vegetation coverage is greater than 20 percent. The species present could be true shrubs, young trees and shrubs or trees that are small or stunted due to environmental conditions.
93. Estuarine Forested Wetland* - Includes all tidal wetlands dominated by woody vegetation greater than or equal to 5 meters in height, and all such wetlands that occur in tidal areas in which salinity due to ocean-derived salts is equal to or greater than 0.5 percent. Total vegetation coverage is greater than 20 percent.

94. Estuarine Scrub/Shrub Wetland* - Includes all tidal wetlands dominated by woody vegetation less than 5 meters in height, and all such wetlands that occur in tidal areas in which salinity due to ocean-derived salts is equal to or greater than 0.5 percent. Total vegetation coverage is greater than 20 percent.

95. Emergent Herbaceous Wetlands - Areas where perennial herbaceous vegetation accounts for greater than 80 percent of vegetative cover and the soil or substrate is periodically saturated with or covered with water.

96. Palustrine Emergent Wetland (Persistent)* - Includes all tidal and non-tidal wetlands dominated by persistent emergent vascular plants, emergent mosses or lichens, and all such wetlands that occur in tidal areas in which salinity due to ocean-derived salts is below 0.5 percent. Plants generally remain standing until the next growing season.

97. Estuarine Emergent Wetland* - Includes all tidal wetlands dominated by erect, rooted, herbaceous hydrophytes (excluding mosses and lichens) and all such wetlands that occur in tidal areas in which salinity due to ocean-derived salts is equal to or greater than 0.5 percent and that are present for most of the growing season in most years. Perennial plants usually dominate these wetlands.

98. Palustrine Aquatic Bed* - The Palustrine Aquatic Bed class includes tidal and nontidal wetlands and deepwater habitats in which salinity due to ocean-derived salts is below 0.5 percent and which are dominated by plants that grow and form a continuous cover principally on or at the surface of the water. These include algal mats, detached floating mats, and rooted vascular plant assemblages.

99. Estuarine Aquatic Bed* - Includes tidal wetlands and deepwater habitats in which salinity due to ocean-derived salts is equal to or greater than 0.5 percent and which are dominated by plants that grow and form a continuous cover principally on or at the surface of the water. These include algal mats, kelp beds, and rooted vascular plant assemblages.

* Coastal NLCD class only

U.S. Department of the Interior
U.S. Geological Survey
USGS: Privacy Statement, Disclaimer, Accessibility, FOIA
DOI: Privacy Statement, Privacy Disclaimer, No FEAR Act, FOIA,
Performance Plan, Children's Privacy
URL: http://www.mrlc.gov/nlcd_definitions.asp
Maintainer: erosweb@usgs.gov
Last Update: Thursday, March 16, 2006

Site ID Number	Station Name	State	Linear p-value and direction of slope	Kendall p-value and direction of slope
01661000	Chaptico Creek at Chaptico	MD	-0.9939	0.9604
01583000	Slade Run near Glyndon	MD	-0.9812	0.9014
01517000	Elk Run near Mainesburg	PA	-0.9242	-0.5792
01590000	North River near Annapolis	MD	-0.9192	0.9223
01660400	Aquia Creek near Garrisonville	VA	-0.8920	-0.6920
01591400	Cattail Creek near Glenwood	MD	-0.8912	-0.8879
01449360	Pohopoco Creek at Kresgeville	PA	-0.8866	-0.6673
01452500	Monocacy Creek at Bethlehem	PA	-0.8727	0.8006
01538000	Wapwallopen Creek near Wapwallopen	PA	-0.8510	-0.6774
01585400	Brien Run at Stemmers Run	MD	-0.8198	-0.8434
01584050	Long Green Creek at Glen Arm	MD	-0.8148	-0.8153
01661500	St Marys River at Great Mills	MD	-0.8128	0.7825
01646550	Little Falls Branch near Bethesda	MD	-0.7951	-0.6959
03101000	Sugar Run at Pymatuning Dam	PA	-0.7888	-0.8562
01487500	Trap Pond Outlet near Laurel	DE	-0.7464	-0.7529
01617000	Tuscarora Creek Above Martinsburg	WV	-0.7407	0.8949
01476500	Ridley Creek at Moylan	PA	-0.6826	-0.5921
02038850	Holiday Creek near Andersonville	VA	-0.6687	-0.8753
01591000	Patuxent River near Unity	MD	-0.6191	0.9887

XXVIII

Appendix 4: Flashiness Results Table: Flashiness results for gages ($n = 151$).

P-values show the significance and direction of the slope of the trend line.

Station ID number and associated p-value are shaded light green for either a linear and/or a

Mann-Kendall τ test result at $\alpha = 0.05$. Stations are ranked in ascending order of linear regression p-value.

Historical analysis of the relationship of streamflow flashiness

with population density, imperviousness,

and percent urban land cover in the Mid-Atlantic region

Site ID Number	Station Name	State	Linear p-value and direction of slope	Kendall p-value and direction of slope
01596500	Savage River near Barton	MD	-0.5700	-0.5593
01591700	Hawlings River near Sandy Spring	MD	-0.5378	-0.7564
02044000	Nottoway River near Burkeville	VA	-0.5084	0.9814
01636210	Happy Creek at Front Royal	VA	-0.5066	0.7928
03026500	Sevenmile Run near Rasselas	PA	-0.4835	-0.6187
01449500	Wild Creek at Hatchery	PA	-0.4795	-0.1554
01568500	Clark Creek near Carsonville	PA	-0.4714	-0.7486
03478400	Beaver Creek at Bristol	VA	-0.4714	-0.7141
02036500	Fine Creek at Fine Creek Mills	VA	-0.4630	-0.8988
03206600	East Fork Twelvepole Creek near Dunlow	WV	-0.4621	-0.3133
01561000	Brush Creek at Gapsville	PA	-0.4451	-0.5455
01588000	Piney Run near Sykesville	MD	-0.4237	-0.3432
03083000	Green Lick Run at Green Lick Reservoir	PA	-0.3940	-0.1999
01669000	Piscataway Creek near Tappahannock	VA	-0.3779	-0.4481
01641000	Hunting Creek at Jimtown	MD	-0.3115	-0.4289
03022540	Woodcock C at Blooming Valley	PA	-0.3105	-0.2700
03111150	Brush Run near Buffalo	PA	-0.2859	-0.2992
01549500	Blockhouse Creek near English Center	PA	-0.2604	-0.1805
02043500	Cypress Swamp at Cypress Chapel	VA	-0.2211	-0.3404
01662500	Rush River at Washington	VA	-0.2016	-0.4758

Appendix 4: Flashiness Results Table: Flashiness results for gages ($n = 151$).

P-values show the significance and direction of the slope of the trend line.

Station ID number and associated p-value are shaded light green for either a linear and/or a

Mann-Kendall τ test result at $\alpha = 0.05$. Stations are ranked in ascending order of linear regression p-value.

Historical analysis of the relationship of streamflow flashiness

with population density, imperviousness,

and percent urban land cover in the Mid-Atlantic region

Site ID Number	Station Name	State	Linear p-value and direction of slope	Kendall p-value and direction of slope
01496200	Principio Creek near Principio Furnace	MD	-0.1915	-0.1971
03062400	Cobun Creek at Morgantown	WV	-0.1658	-0.0125
03178500	Camp Creek near Camp Creek	WV	-0.1656	-0.0317
01516500	Corey Creek near Mainesburg	PA	-0.1525	-0.3377
01557500	Bald Eagle Creek at Tyrone	PA	-0.1453	-0.1378
01597000	Crabtree Creek near Swanton	MD	-0.1244	-0.1444
02022500	Kerrs Creek near Lexington	VA	-0.1203	-0.1450
01552500	Muncy Creek near Sonestown	PA	-0.1125	-0.1150
03213500	Panther Creek near Panther	WV	-0.1002	-0.1433
01584500	Little Gunpowder Falls at Laurel Brook	MD	-0.0518	-0.0419
01486000	Manokin Branch near Princess Anne	MD	-0.0441	-0.0604
01668500	Cat Point Creek near Montross	VA	-0.0289	-0.0311
01467086	Tacony Creek at County Line Philadelphia	PA	-0.0111	-0.0121
04213040	Raccoon Creek near West Springfield	PA	-0.0030	-0.0039
01475550	Cobbs Creek at Darby	PA	-0.0010	-0.0081
01469500	Little Schuylkill River at Tamaqua	PA	-0.0009	-0.0016
01665000	Mount Run near Culpeper	VA	-0.0006	-0.0047
01537000	Toby Creek at Luzerne	PA	-0.0003	-0.0007
03208700	N F Pound River at Pound	VA	-0.0002	-0.0002
01670000	Beaverdam Swamp near Ark	VA	-0.0001	-0.0001

Appendix 4: Flashiness Results Table: Flashiness results for gages ($n = 151$).

P-values show the significance and direction of the slope of the trend line.

Station ID number and associated p-value are shaded light green for either a linear and/or a

Mann-Kendall τ test result at $\alpha = 0.05$. Stations are ranked in ascending order of linear regression p-value.

Historical analysis of the relationship of streamflow flashiness

with population density, imperviousness,

and percent urban land cover in the Mid-Atlantic region

Site ID Number	Station Name	State	Linear p-value and direction of slope	Kendall p-value and direction of slope
01654000	Accotink Creek near Annandale	VA	0.0000	0.0000
01585500	Cranberry Branch near Westminster	MD	0.0000	0.0000
01477800	Shellpot Creek at Wilmington	DE	0.0000	0.0000
01589100	East Branch Herbert Run at Arbutus	MD	0.0000	0.0000
01585100	Whitemarsh Run at White Marsh	MD	0.0000	0.0000
01593500	Little Patuxent River at Guilford	MD	0.0000	0.0000
01653500	Henson Creek at Oxon Hill	MD	0.0000	0.0001
01585200	West Branch Herring Run at Idlewylde	MD	0.0000	0.0002
02038000	Falling Creek near Chesterfield	VA	0.0001	0.0006
01486500	Beaverdam Creek near Salisbury	MD	0.0001	0.0002
01484500	Stockley Branch at Stockley	DE	0.0001	0.0006
01594500	Western Branch near Largo	MD	0.0001	0.0008
01645200	Watts Branch at Rockville	MD	0.0001	0.0021
01652500	Fourmile Run at Alexandria	VA	0.0003	0.0006
01485500	Nassawango Creek near Snow Hill	MD	0.0004	0.0010
01589300	Gwynns Falls at Villa Nova	MD	0.0007	0.0006
01595200	Stony River near Mount Storm	WV	0.0016	0.0064
01475510	Darby Creek near Darby	PA	0.0028	0.0131
01480685	Marsh Creek near Downingtown	PA	0.0037	0.0034
01478000	Christina River at Coochs Bridge	DE	0.0039	0.0071

Appendix 4: Flashiness Results Table: Flashiness results for gages ($n = 151$).

P-values show the significance and direction of the slope of the trend line.

Station ID number and associated p-value are shaded light green for either a linear and/or a

Mann-Kendall τ test result at $\alpha = 0.05$. Stations are ranked in ascending order of linear regression p-value.

Historical analysis of the relationship of streamflow flashiness

with population density, imperviousness,

and percent urban land cover in the Mid-Atlantic region

Site ID Number	Station Name	State	Linear p-value and direction of slope	Kendall p-value and direction of slope
01613050	Tonoloway Creek near Needmore	PA	0.0041	0.0067
01650500	Nw Branch Anacostia River near Colesville	MD	0.0048	0.0035
01467048	Pennypack Cr at Lower Rhawn St Bdg Phila.	PA	0.0095	0.0140
01490000	Chicamacomico River near Salem	MD	0.0116	0.0243
01662800	Battle Run near Laurel Mills	VA	0.0129	0.0115
01653000	Cameron Run at Alexandria	VA	0.0143	0.0358
03084000	Abers Creek near Murrysville	PA	0.0225	0.0152
01673550	Totopotomoy Creek near Studley	VA	0.0307	0.0369
02017000	Meadow Creek at Newcastle	VA	0.0331	0.0589
01585300	Stemmers Run at Rossville	MD	0.0338	0.0329
01581500	Bynum Run at Bel Air	MD	0.0395	0.0217
02076500	Georges Creek near Gretna	VA	0.0415	0.0755
01616000	Abrams Creek near Winchester	VA	0.0469	0.0685
01651000	Nw Branch Anacostia River near Hyattsville	MD	0.0505	0.0512
01614090	Conococheague Creek near Fayetteville	PA	0.0562	0.0692
01590500	Bacon Ridge Branch at Chesterfield	MD	0.0576	0.0741
01484100	Beaverdam Branch at Houston	DE	0.0580	0.0973
01447680	Tunkhannock Creek near Long Pond	PA	0.0717	0.0423
03165000	Chestnut Creek at Galax	VA	0.0953	0.0821
01613900	Hogue Creek near Hayfield	VA	0.0991	0.1127

Appendix 4: Flashiness Results Table: Flashiness results for gages ($n = 151$).

P-values show the significance and direction of the slope of the trend line.

Station ID number and associated p-value are shaded light green for either a linear and/or a

Mann-Kendall τ test result at $\alpha = 0.05$. Stations are ranked in ascending order of linear regression p-value.

Historical analysis of the relationship of streamflow flashiness

with population density, imperviousness,

and percent urban land cover in the Mid-Atlantic region

Site ID Number	Station Name	State	Linear p-value and direction of slope	Kendall p-value and direction of slope
01620500	North River near Stokesville	VA	0.1017	0.0418
01465798	Poquessing Creek at Grant Ave. at Philadelphia	PA	0.1024	0.1629
01671500	Bunch Creek near Boswells Tavern	VA	0.1127	0.1587
01589500	Sawmill Creek at Glen Burnie	MD	0.1165	0.0594
01595300	Abram Creek at Oakmont	WV	0.1210	0.2072
01594936	North Fork Sand Run near Wilson	MD	0.1231	0.2145
01483700	St Jones River at Dover	DE	0.1234	0.1140
01484300	Sowbridge Branch near Milton	DE	0.1383	0.2512
01480675	Marsh Creek near Glenmoore	PA	0.1934	0.1727
01569800	Letort Spring Run near Carlisle	PA	0.2120	0.1124
01483200	Blackbird Creek at Blackbird	DE	0.2287	0.3417
01534300	Lackawanna River near Forest City	PA	0.2484	0.3919
01448500	Dilldown Creek near Long Pond	PA	0.2528	0.3265
01489000	Faulkner Branch at Federalsburg	MD	0.2662	0.2614
01547700	Marsh Creek at Blanchard	PA	0.2755	0.4002
02051600	Great Creek near Cochran	VA	0.3331	0.0970
01617800	Marsh Run at Grimes	MD	0.3444	0.3464
01484000	Murderkill River near Felton	DE	0.3589	0.5534
01589440	Jones Falls at Sorrento	MD	0.3693	0.4944
01480500	West Branch Brandywine Creek at Coatesville	PA	0.3813	0.3588

XXXXIII

Appendix 4: Flashiness Results Table: Flashiness results for gages ($n = 151$).

P-values show the significance and direction of the slope of the trend line.

Station ID number and associated p-value are shaded light green for either a linear and/or a

Mann-Kendall τ test result at $\alpha = 0.05$. Stations are ranked in ascending order of linear regression p-value.

Historical analysis of the relationship of streamflow flashiness

with population density, imperviousness,

and percent urban land cover in the Mid-Atlantic region

Site ID Number	Station Name	State	Linear p-value and direction of slope	Kendall p-value and direction of slope
01493500	Morgan Creek near Kennedyville	MD	0.4143	0.9176
01496000	Northeast Creek at Leslie	MD	0.4242	0.3863
01655500	Cedar Run near Warrenton	VA	0.4302	0.3543
03076600	Bear Creek at Friendsville	MD	0.4481	0.4138
01658500	S F Quantico Creek near Independent Hill	VA	0.4629	0.4582
01585095	North Fork Whitmarsh Run near White Marsh	MD	0.4632	0.4579
01641500	Fishing Creek near Lewistown	MD	0.4756	0.4788
01661800	Bush Mill Stream near Heathsville	VA	0.4784	0.3521
01484800	Guy Creek near Nassawadox	VA	0.4938	0.2781
01492000	Beaverdam Branch at Matthews	MD	0.4955	0.6300
01581700	Winters Run near Benson	MD	0.5257	0.4570
01589330	Dead Run at Franklinton	MD	0.5259	0.5736
03052500	Sand Run near Buckhannon	WV	0.5374	0.8180
01594930	Laurel Run at Dobbin Rd near Wilson	MD	0.5843	0.5592
01640500	Owens Creek at Lantz	MD	0.5869	0.3683
02027500	Piney River at Piney River	VA	0.5976	0.6434
02018500	Catawba Creek near Catawba	VA	0.6146	0.7620
01567500	Bixler Run near Loysville	PA	0.6249	0.5258
01673500	Totopotomoy Creek near Atlee	VA	0.6281	0.2206
01537500	Solomon Creek at Wilkes-Barre	PA	0.6289	0.6216

XXXIV

Appendix 4: Flashiness Results Table: Flashiness results for gages ($n = 151$).

P-values show the significance and direction of the slope of the trend line.

Station ID number and associated p-value are shaded light green for either a linear and/or a

Mann-Kendall τ test result at $\alpha = 0.05$. Stations are ranked in ascending order of linear regression p-value.

Historical analysis of the relationship of streamflow flashiness

with population density, imperviousness,

and percent urban land cover in the Mid-Atlantic region

Site ID Number	Station Name	State	Linear p-value and direction of slope	Kendall p-value and direction of slope
03049800	Little Pine Creek near Etna	PA	0.6972	0.5650
03011800	Kinzua Creek near Guffey	PA	0.7840	0.6598
01480300	West Branch Brandywine Creek near Honey Brook	PA	0.7851	-0.9133
01488500	Marshyhope Creek near Adamsville	DE	0.7906	-0.8560
02055100	Tinker Creek near Daleville	VA	0.7944	0.6858
01603500	Evitts Creek near Centerville	PA	0.8272	0.5348
01653600	Piscataway Creek at Piscataway	MD	0.8424	-0.7873
01661050	St Clement Creek near Clements	MD	0.8756	-0.8457
01545600	Young Womans Creek near Renovo	PA	0.9064	0.8917
01542810	Waldy Run near Emporium	PA	0.9182	-0.6805
01480000	Red Clay Creek at Wooddale	DE	0.9279	-0.8248
01493000	Unicorn Branch near Millington	MD	0.9853	-0.7127

Appendix 4: Flashiness Results Table: Flashiness results for gages ($n = 151$).

P-values show the significance and direction of the slope of the trend line.

Station ID number and associated p-value are shaded light green for either a linear and/or a

Mann-Kendall τ test result at $\alpha = 0.05$. Stations are ranked in ascending order of linear regression p-value.

Historical analysis of the relationship of streamflow flashiness

with population density, imperviousness,

and percent urban land cover in the Mid-Atlantic region



Printed on 100% recycled/recyclable paper
with a minimum 50% post-consumer
fiber using vegetable-based ink.



Office of Research and Development (8101R)
Washington, DC 20460

Official Business
Penalty for Private Use
\$300

PRESORTED STANDARD
POSTAGE & FEES PAID
EPA
PERMIT NO. G-35